

Review

Zeolite Membranes in Catalysis—From Separate Units to Particle Coatings

Radostina Dragomirova [†] and Sebastian Wohlrab ^{†,*}

Leibniz Institute for Catalysis, University of Rostock (LIKAT Rostock), Albert-Einstein-Str. 29a, D-18059 Rostock, Germany; E-Mail: radostina.dragomirova@catalysis.de

[†] These authors contributed equally to this work.

* Author to whom correspondence should be addressed; E-Mail: sebastian.wohlab@catalysis.de; Tel.: +49-381-128-1328; Fax: +49-3811-2815-1328.

Academic Editors: Andreas Martin and Keith Hohn

Received: 31 October 2015 / Accepted: 4 December 2015 / Published: 16 December 2015

Abstract: Literature on zeolite membranes in catalytic reactions is reviewed and categorized according to membrane location. From this perspective, the classification is as follows: (i) membranes spatially decoupled from the reaction zone; (ii) packed bed membrane reactors; (iii) catalytic membrane reactors and (iv) zeolite capsuled catalyst particles. Each of the resulting four chapters is subdivided by the kind of reactions performed. Over the whole sum of references, the advantage of zeolite membranes in catalytic reactions in terms of conversion, selectivity or yield is evident. Furthermore, zeolite membrane preparation, separation principles as well as basic considerations on membrane reactors are discussed.

Keywords: membrane reactor; permselectivity; permselective zeolite membrane; zeolite membrane reactor; packed bed membrane reactor; catalytic membrane reactor; zeolite membrane coating; zeolite capsuled catalyst; equilibrium shift

1. Introduction

It is not possible to imagine industrial catalysis without zeolites. Over the years, zeolites gained that importance owing to their outstanding properties which are (i) high surface area; (ii) pore sizes in the molecular range; (iii) adsorption capacity; (iv) controllable adsorption properties; (v) inherent active

sites; (vi) shape selectivity and (vii) stability [1,2]. Certainly, due to these unique features the application of zeolites is not only restricted to catalysis. Their potential to serve as highly selective sorption materials make zeolites also indispensable for industrial separation tasks [3]. Highlighting, separation and purification of gases [4], especially swing adsorption techniques [5–7], as well as water and waste water treatment [8,9] are also not imaginable without zeolitic materials.

To run separation processes continuously and without recurring regeneration steps zeolite membranes have been developed and studied over the last decades [10–20]. With this development, the utilization of zeolite membranes was progressively investigated for catalytic reactions [21–32]. The special interest in membranes for catalysis science lies in the possibilities of equilibrium shifts, improved yields and selectivities as well as more compact operations compared to conventional processes. Nevertheless, no industrial commercialization of zeolite membrane reactors has been occurring until now. However, recent pioneering developments towards sub- μm membranes [33–38] or the reduction of defects [39–41] promise a revival of zeolite membrane applications. Furthermore, novel cost reduction concepts [42] will make zeolite membranes more attractive for industry.

However, a first application of zeolite membranes in industry already exists. It is the use of hydrophilic zeolite membranes in the dehydration of organic solvents. In detail, NaA membranes have been used in a large-scale pervaporation plant mainly for alcohols by BNRI (Mitsui Holding) [43], and further progress on LTA membranes in the pervaporation separation of water was achieved over the years [44–47]. An important consideration on the way for industrial application might be the availability of membranes characterized by suitable performances at reasonable prices. On the one hand, a 10,000 m^2/year production line for LTA membranes was established [48]. In this context, the further up-scaling also of other membrane types will be of significant importance whether zeolite membranes will be applied in industrial catalysis or not. On the other hand, over the last years, membrane coatings on catalyst particles have been successfully developed and applied as micro membrane reactors [24]. Perhaps, these zeolite capsuled catalysts will be the final breakthrough for zeolite membrane reactors in industry?

A review of the state of the art of permselective zeolite membranes in reaction processing is given in the following for anyone who is already engaged with the matter and for those who want to start with. In particular, the application of zeolite membranes for a bunch of different possible reactions is presented. In the first part, a short overview on zeolite membrane synthesis will be given, followed by discussion on the transport mechanisms in a zeolite membrane. Afterwards, the application of zeolite membrane reactors in diverse configurations will be presented and discussed for the different reaction types. Starting with zeolite membranes apart from the reaction zone over packed bed membrane reactors and catalytic membrane reactors, zeolite coatings on catalyst particles are finally covered.

2. Separation by Zeolite Membranes

2.1. Synthesis of Zeolite Membranes

Over the last decades a great research effort is allocated in the preparation of zeolite membranes applying different synthesis techniques. Generally, for the synthesis of zeolite membranes two procedure routes are followed. On the one hand, one-step techniques referred to as direct *in situ* crystallization are

applied. Thereby, the surface of the untreated either tubular or disc support is brought in a direct contact with an aluminosilicate precursor solution and the membrane crystallization is performed under hydrothermal conditions as shown exemplarily in the following references [49–55]. Alternatively, Caro *et al.* proposed a seeding-free synthesis strategy for the preparation of dense and phase-pure zeolite LTA and FAU membranes using 3-aminopropyltriethoxysilane (APTES) as covalent linker between the zeolite layer and the alumina support [56,57]. Moreover, considerable effort has been directed towards controlled crystal orientation of MFI by *in situ* crystallization [58–61].

On the other hand, two-step syntheses referred to as secondary growth are applied for zeolite membrane preparation. Therefore, a seeding layer is deposited on the membrane support at first and the membrane layer is grown in a second step via hydrothermal synthesis [62–67]. Seeds can be prepared either by bottom-up approaches [15] or by top-down techniques *ex situ*. The latter include template assisted nanoscale zeolite syntheses [68,69], exfoliation of zeolite sheets [34,70,71] or simply crushing. The nature of the obtained zeolite membrane depends strongly on the seeding and the subsequent secondary growth technique applied. Figure 1 displays two examples of MFI membranes obtained by the two-step hydrothermal preparation procedure. Figure 1a illustrates the outcome of a recent development resulting in the most probable thinnest membrane ever reported [34]. In detail, MFI-nanosheets were prepared by exfoliation of multilamellar MFI. After purification, these sheets were supported onto either Stöber silica supports or novel highflux, high-strength porous silica fibre supports. Secondary intergrowth of the film was performed using the so called gel-less growth technique first described by Pham *et al.* [35]. This approach could be a more powerful strategy for the preparation of sub- μm membranes compared to the alternative Langmuir through assembly [36,72].

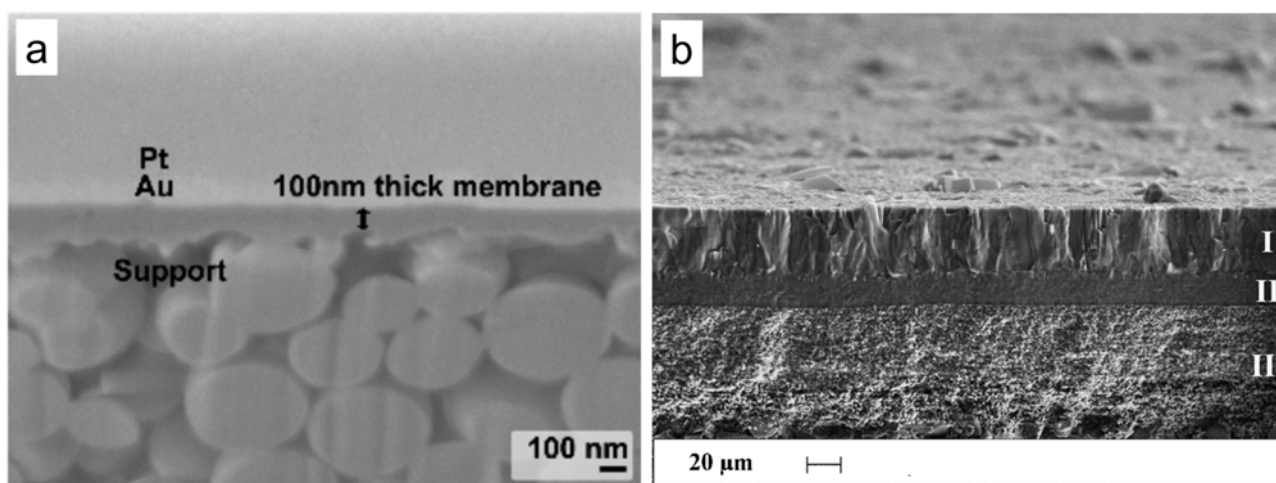


Figure 1. Scanning electron micrographs of (a) MFI film prepared by gel-less growth of MFI-nanosheets on a Stöber silica support (Reprinted with permission from [34]. Copyright (2015) John Wiley and Sons.); and (b) MFI membrane from ball milled MFI seeds and subsequent secondary growth (I) MFI membrane; (II) MFI seed layer; and (III) alumina microfiltration layer on a macroporous alumina support. (Reprinted from [67]. Copyright (2011) Elsevier).

Figure 1b shows a MFI membrane obtained by seeding of ball milled silicalite used for the functionalization of an inert alumina microfiltration layer (denoted as III in Figure 1b) located on a

macroporous Al₂O₃ support. Thus, the resulting MFI seed layer (denoted as II in Figure 1b) acts both as heterogeneous nucleation site and as flexible distance holder between support and MFI membrane, suppressing defect formations during thermal template removal. Onto the MFI seed layer the MFI membrane layer (denoted as I in Figure 1b) was formed by hydrothermal synthesis [67]. Of course, both archetypes provide different properties. The thin membrane from Figure 1a offers high flux whereas the membrane in Figure 1b possesses high pressure stability.

Parasitic twin crystals were identified as defect-forming during the thermal removal of the structure directing agent (SDA) and should be prevented. By using a low SDA/Si reactant ratio (≤ 0.05) it was found, the formation of twin crystals can be reduced [40]. Alternatively, SDA-free zeolite syntheses are available [39,41], and a template-free secondary growth synthesis of MFI type zeolite membranes [73] is known for nearly 15 years.

On the search of the most efficient synthesis technique, several more methods were reported. A secondary growth method with vacuum seeding for the preparation of A-type zeolite membranes [74] and diverse techniques for crystal orientation in zeolite membranes [75–82] were proposed. A vapor-phase transport (VPT) method was first reported by Xu *et al.* as an alternative approach to the hydrothermal synthesis for the preparation of ZSM-5 zeolite [83]. The VPT method was extensively studied by Matsukata *et al.* for the synthesis of defect-free zeolite-alumina composite membranes [84], MFI-type zeolitic membrane [85] as well as preferentially oriented MFI layers [86], compact ferrierite (FER)-alumina composite layer [87,88], where a dry aluminosilicate gel layer was deposited on the support and then further crystallized under vapors of amines and water. Besides, the achieved progress in microwave assisted syntheses of zeolite membrane has been outlined by Li *et al.* [89]. Gascon and coworkers debated on the limitations of the existing preparation techniques and evaluated future perspectives of zeolite and zeolite-type materials for membrane production [19].

For further reading on the progress in the seeding and secondary growth techniques used for the preparation of zeolite membranes two recent reviews are recommended [42,48].

2.2. Permeation in Zeolite Membranes

According to Weisz, classical catalytic reactors should work in a certain “window of reality” in order to run efficiently. Consequently, the optimal space time yield of a conventional membrane reactor should be centered around $STY = 10^{-6}$ – 10^{-5} mol·cm⁻³·s⁻¹ [90]. Weisz explained this window with time limitations at the lower border and issues on mass flow, diffusion and heat transfer at the upper limit. Years later, in 1997, Boudart suggested membrane reactors should be classified analogously [91]. When an industrial reactor should have its STY around 10^{-6} – 10^{-5} mol·cm⁻³·s⁻¹, a membrane reactor should be located in the same window—defined by its areal time yield (ATY). Boudart referred to a Pd/Al₂O₃ membrane and its ability to permeate hydrogen at a permeability P of at least 10^{-5} mol·cm⁻²·s⁻¹ [92]. By assuming a cylindrical reactor of diameter d , ATY can be calculated from the STY by multiplying with the surface to volume ratio, $d/4$. As an example, a reactor tube of 40 cm in diameter would fit in a “window of reality” of a membrane reactor matching P , or ATY ($40/4 \times 10^{-6}$ mol·cm⁻²·s⁻¹). By simply adjusting the diameter of the membrane tube, the “window of reality” can be reached in the case of high permeation rates. What about zeolite membranes?

Van de Graaf *et al.* compared the volume ratio of the catalytic reactor derived from the productivity per unit volume (defined as STY) to the permeation per membrane area (defined as permeation flux), or in other words the ATY [93,94]. By dividing STY through ATY, the area to volume ratio (A/V) of the catalytic membrane reactor is obtained as a simple measure of the industrial feasibility of membrane reactors. However, the authors calculated A/V values between 20 and 5000 m^{-1} for porous inorganic membranes, whereas the example referred by Boudart ($\text{Pd}/\text{Al}_2\text{O}_3$ [92]) shows a much better performance of $A/V = 10$. It is clear, the smaller the A/V ratio the more realistic becomes an industrial transfer.

Deeper insights between catalytic reaction and permeation can be obtained by comparison of catalytic performance and permeation rate—which are the two limiting factors of a membrane reactor. The catalytic performance can be understood as ratio between reaction rate and convective transport rate of the feed, given as Damkohler number (Da). The ratio of convective transport to permeation rate through the membrane is the so called Peclet number (Pe). The product of both numbers defines the efficiency of a given membrane reactor [95–97]. Hence, a catalytic membrane reactor can be optimized either by catalyst activity adjustment or by manipulating the permeability of the membrane. For industrial applications the focus should be on the latter: (i) diameters of membrane supports can be reduced up to a certain value (e.g., as hollow support fibres); and (ii) permeability can be increased. Recent developments in the fabrication of ultrathin membranes (see Section 2.1.) are promising enough to overcome barriers. Since permeation is inversely proportional to membrane thickness [98] a novel generation of fast permeating zeolite membranes can be directed towards industrial applications.

Generally, the transport of molecules through zeolite membranes depends strongly on the membrane pore size and the interaction of the permeating species with the zeolite structure and can be modelled mainly as combined effect between adsorption and diffusion. This surface diffusion of adsorbed species from multi-component mixtures can be described by the aid of the Maxwell-Stefan model as Krishna and co-workers impressively have been demonstrated over the past years [99–103]. For further reading on modelling the permeation through zeolite membranes a recent review by Rangnekar *et al.* is recommended [42].

The permeation through the zeolite membrane is controlled by either shape selectivity, diffusion or adsorption properties [12]. Considering shape selectivity, the separation ability of a membrane is based on retaining components larger in size than the zeolite membrane pores and permeation of only the smaller components [65,104–106]. For mixtures having components with similar adsorption properties the gas transport is determined by the mobility of molecules inside the zeolite pores. Exemplarily, the diffusion controlled permeation was demonstrated for *n*-butane/*i*-butane mixtures in MFI membranes [107–109]. In detail, both components show strong adsorption in the zeolite so that the permeation is mainly governed by the diffusion mobilities of the components. For mixtures comprising components with different adsorption and diffusion properties the selective gas transport is predominantly controlled by adsorption. So for example, for hydrogen/*n*-butane and methane/*n*-butane mixtures the permeation fluxes of the less adsorbing components, in these cases hydrogen and methane, respectively, are significantly suppressed by the strongly adsorbing component *n*-butane. Thereby, the arising higher occupancy of *n*-butane leads to a higher driving force for its diffusion [99,110]. Similarly, for mixtures of ethane and *i*-butane the passage of ethane through the membrane was retained by pore blocking effect caused by the stronger adsorption of *i*-butane on the MFI zeolite [111]. For sorption-driven separation processes the transport through porous single-crystal membranes [112] further adopted for zeolite

membrane [113] was described by a five-step transport model, including: (1) molecule adsorption from the gas phase at the external surface of the zeolite; (2) transport from the external surface into the pores; (3) intracrystalline transport; (4) transport from the pores to the external surface and (5) desorption from the external surface to the gas phase. For mixtures comprising strongly and weakly adsorbing components, the membrane performance is significantly affected by the operating parameters—pressure and temperature. In this regard, by employing experimental configurations with varying operating conditions the significance of adsorption and diffusion [67,114], desorption [115] as well as condensation [116] was recently demonstrated by our group for the separation of methane/*n*-butane mixtures by MFI membranes.

As shown until now, zeolite membranes could offer diverse separation properties. According to the specific needs of a process, the type of membranes but also their localization to the reaction zone has to be well-chosen. In the following subchapter the advantages of implementing zeolite membranes in catalytic reactions are reviewed for spatially decoupled processes before we proceed with arrays of membranes and catalysts in close contact with each other in the following main chapters.

2.3. Zeolite Membrane Separation Spatially Decoupled from the Catalytic Unit

Zeolite membrane modules could be applied apart from the reaction zone as alternatives to the complex conventional separation processes. Figure 2 reveals two application possibilities of zeolite membranes where the separation process is either for (i) feed treatment (Figure 2A) or (ii) product treatment (Figure 2B) with optional retentate stream recycle. The current chapter briefly discusses only examples where the catalytic process is spatially decoupled from the membrane unit.

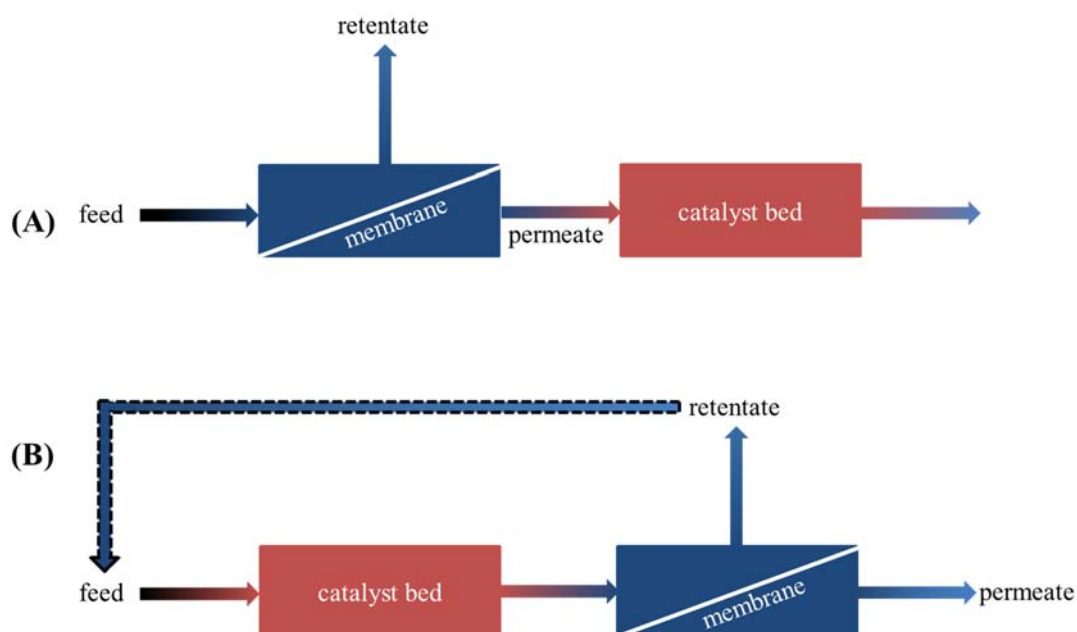


Figure 2. Schematic drawing of different set-ups of zeolite membranes apart from the reaction zone; (A) feed treatment; and (B) product treatment with optional retentate recycle.

Starting with the feed treatment configuration, the membrane module could be used to adjust the feed stream in order to intensify processes. Beside polymer membranes [117], MFI zeolite membranes can

be applied for the conditioning of natural gas [118]. Simplified natural gas model mixtures comprising methane and *n*-butane were separated with high efficiency under permeate vacuum [115]. Well-pronounced loading gradients across the membrane, decreased coverages of the adsorbed *n*-butane molecules at the permeate side as well as decreased diffusion resistances were registered. The resulting permeate streams, highly enriched with *n*-butane, were converted with steam at low (450 °C) and high (750 °C) temperatures over 1 wt. % Rh/ γ -Al₂O₃ for syngas production [119]. The positive influence of the membrane upstream on the steam reforming was demonstrated. For example, at a temperature of only 450 °C a H₂ volume content of 57 vol. % at a H₂/CO ratio of 3.6 could be obtained from a methane/*n*-butane mixture with $\phi_{C_4H_{10}}$ 70.4 vol. % underlining the potential for natural gas processing and conversion.

Considering product treatment, the membrane module is placed downstream to the catalytic reactor in order to purify the product stream, thus allowing membrane process conduction at operating conditions different from those of the catalytic unit. In this context, the applicability of zeolite membranes for the separation of hydrogen from reforming streams during syngas production has been recently reviewed [31,120]. Interestingly, during the evaluation of as-prepared and ion-exchanged zeolite LTA membranes for the separation of hydrogen from a simulated gas reformer mixtures, Cs-exchanged LTA membrane demonstrated stable H₂ permeance in the presence of water [121]. Nenoff *et al.* evaluated theoretically the hydrogen separation selectivities of silicalite and ETS-10 membranes [122] as well as of zeolite NaA and zinc phosphate molecular sieve Na₃ZnO(PO₄)₃ [123] using Grand Canonical Monte Carlo techniques. The same working group modified the internal surface of MFI-type zeolite membranes by silane precursors and obtained a H₂/CO₂ permselectivity of 141 combined with high hydrogen permeance [124].

On the other hand, the well-established capability of hydrophilic NaA zeolite membranes for selective water separation has entailed the first industrial implementation of zeolite membranes for de-watering of ethanol and *i*-propanol [43]. The high separation efficiency of this kind of membrane in pervaporation processes (see for instance reviews [13,125]) has motivated further research effort coupling water releasing reactions and water separations in equilibrium limited reactions. As an alternative to reactive distillation, different reactor configurations including pervaporation membranes could be applied in the esterification reactions [126], where the water permeation through the membrane is assisted by the mean of applied vacuum or sweep gas and then further condensed in a cold trap. In the last decades, membranes coupled to esterification processes have been investigated considering different zeolite structures, including zeolite A [127], sodalite (SOD) [128], chabazite CHA [129].

So for instance, Jafar *et al.* [127] investigated the homogeneously catalyzed esterification of lactic acid and ethanol by *p*-toluene sulphonic acid as catalyst, using a zeolite A membrane supported on carbon/zirconia tube for the separation of the produced water. Despite the superior performance of the zeolite A membrane in terms of water flux and selectivity [130,131], its low stability in acidic media [132] imposed the need of performing the process under vapor permeation conditions in order to avoid the direct contact of the membrane with the acidic reaction environment. Not surprisingly, high separation selectivities were achieved during the experiments resulting in significantly improved yields above the equilibrium limit. Similarly, Hasegawa *et al.* [129] adopted CHA-type zeolite membrane in the vapor phase during the esterification of adipic acid with isopropyl alcohol using sulfuric acid as catalyst. Thus, the profit from the effective water removal by the membrane was revealed since the yield

of diisopropyl adipate reached 98%. In comparison an equilibrium yield of 56% was obtained during the operation without membrane. After 10 runs the permeation fluxes of water were reduced, however the reaction maintained stable performance showing 99% esterification conversion and 97% yield. On the other hand, acid-resistant hydrophilic merlionite (MER), phillipsite (PHI) and chabazite (CHA) zeolite membranes [133] have been also applied in pervaporation-aided ester condensation reactions with alcohols in order to extract water and so shift the equilibrium position. The authors recorded more than 20% increased yield compared to the equilibrium conversion demonstrating the profit of using zeolite membranes for selective water removal.

Hydroxy sodalite (SOD) zeolite membranes combine excellent separation of water from various organic alcohol streams and good resistance to the acidic medium in esterification reactions as shown by Khajavi *et al.* [128,134]. For this reason, SOD zeolite membranes were applied in the pervaporation-aided esterification of acetic acid with either ethanol or 1-butanol. The membrane exhibited absolute water selectivity, thereby. Moreover, the membrane was able to permeate water in rates comparable to its formation rate giving rise to enhanced yield and almost complete conversion. Importantly, the membrane demonstrated stable water permeation under mild acidic conditions for long period of operation. This behavior was ascribed by the authors mainly to low aluminum leaching out of the zeolite structure due the narrow window openings of the SOD zeolite.

Very recently, kinetic modeling of pervaporation-aided esterification of propionic acid and ethanol with T-type zeolite membranes has been performed and compared with the experimental data obtained in order to provide further insights on the effect of the operating parameters temperature, ethanol/acid molar ration, as well as ratio of membrane area to amount of initial reaction liquid [135]. As a result, more effective water removal and thus improved esterification conversion could be ensured by the use of membranes with larger area, however to the disadvantages of higher equipment costs. Further example of process intensification by incorporation of NaA zeolite membrane tubes into a reactive distillation column for the etherification of tert-amyl alcohol with ethanol was given by Aiouache *et al.* [136]. The hybrid configuration was found to be effective for the removal of water and consequently for the surpassing of the thermodynamic limitations leading to increased tert-amyl ethyl ether yield.

However, the special implementation of zeolite membranes in membrane reactors, where catalysis and selective separation are combined in the same unit, could offer several advantages in comparison to the conventional reactor (CR) configuration and is considered a promising concept to overcome limitations in the performance of catalytic reactors [22,30,137–140].

3. Membrane Reactor Concepts

According to the IUPAC definition, a membrane reactor couples a chemical reaction and a membrane-based separation process in the same unit so as to intensify the whole process [141]. Generally, for this purpose permselective and non-permselective membranes can be employed in different membrane reactor configurations as show in Figure 3.

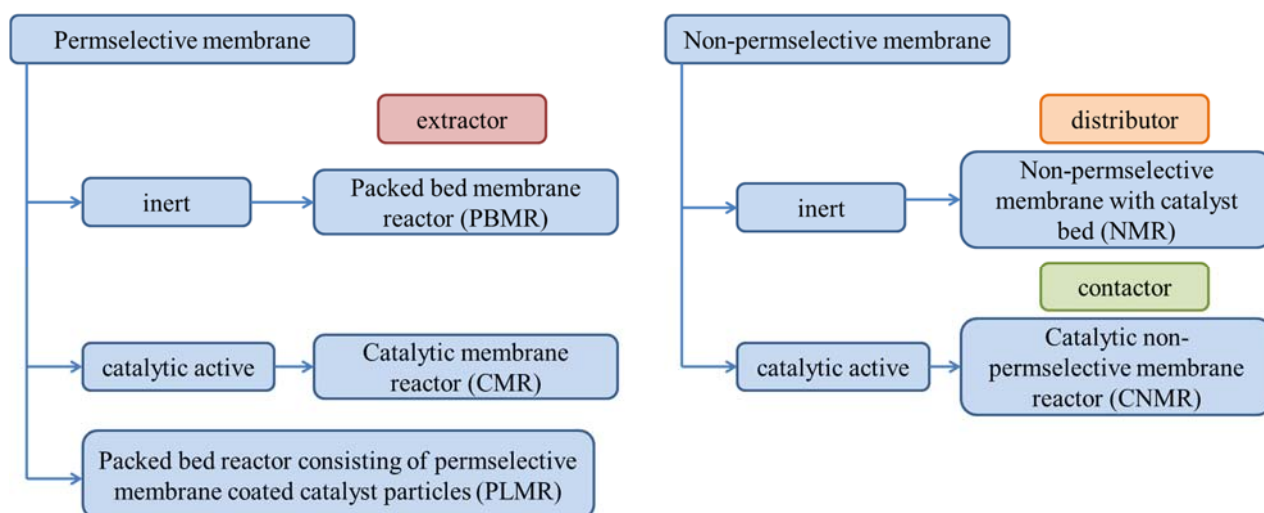


Figure 3. Classification of membrane reactor configurations according to membrane function, after conventional classifications [23,26,29,142,143].

On the one hand, depending on how permselective membranes are combined with catalysts in the reactor unit, membrane reactors can be divided generally into packed bed membrane reactors (PBMR) and catalytic membrane reactors (CMR). On the other hand, the membrane utilized in the membrane reactor can also be non-permselective so that further membrane reactor configurations are possible, namely non-permselective membrane reactors (NMR) with direct contact to a catalyst bed and catalytic (active) non-permselective membrane reactors (CNMR). Another membrane reactor configuration is represented by reactors packed with permselective membrane-coated catalyst particles (PLMR). These capsuled particles can be also understood as microscopic structured membrane reactors.

In the following, we want to discuss the classification of zeolite membranes on the basis of their function either as extractor, distributor or contactor.

3.1. Extractor Type Zeolite Membrane Reactors

As extractors either catalytic or inert permselective membranes can be applied so that here the CMR and PBMR configurations are included. The membrane has thereby the function to remove selectively one or more products from the reaction zone, thus improving the conversion/selectivity/yield in equilibrium limited reactions. Alternatively, the membrane could be employed to supply selective reactants from the feed mixture in order to enhance the selectivity. Possible applications of extractors with either catalytic active permselective membranes in CMR or inert permselective membranes in PBMR configurations are listed in Table 1 and will be discussed in further details in Sections 4 and 5.

Although the main focus of this review is laid on permselective membranes some examples considering the application of non-permselective membranes in membrane reactor should be given in the following paragraphs for completeness.

Table 1. Overview of the application of permselective inert or catalytic active zeolite membranes in membrane reactor configurations for different processes reported in the literature.

Reaction	Reactor Type	Feed	Operating Conditions	Catalyst	Membrane	X _{CR} (%)	X _{MR} (%)	References
						S _{CR} (%)	S _{MR} (%)	
Dehydrogenation of ethylbenzene to styrene	CMR	water, ethyl-benzene	600 °C sweep gas: nitrogen	Fe-MFI/ α -Al ₂ O ₃ tube		X _{ethylbenzene} = 45.1 S _{styrene} = 92.8 Y _{styrene} = 41.9	X _{ethylbenzene} = 60.1 S _{styrene} = 96.9 Y _{styrene} = 58.6	[144]
Dehydrogenation of <i>i</i> -butane	PBMR	<i>i</i> -butane, hydrogen, balance nitrogen	730 K $p = 100$ – 170 kPa sweep gas: nitrogen	PtIn/MFI 0.8 wt. % In 0.5 wt. % Pt	MFI/ α -Al ₂ O ₃ tube	n.r.	n.r.	[145]
Dehydrogenation of <i>i</i> -butane	PBMR	pure <i>i</i> -butane	510 °C WHSV = 0.5 – 1.6 h ⁻¹ sweep gas: nitrogen	Cr ₂ O ₃ /Al ₂ O ₃	MFI/ α -Al ₂ O ₃ tube	X _{<i>i</i>-butane} = 29.1 S _{<i>i</i>-butene} = ~90	X _{<i>i</i>-butane} = 41.7–48.6 S _{<i>i</i>-butene} = 96	[146]
Dehydrogenation of <i>i</i> -butane	PBMR	pure <i>i</i> -butane	712–762 K $p_{\text{feed}} = 101$ kPa sweep gas: nitrogen	Cr ₂ O ₃ /Al ₂ O ₃	DD3R/ α -Al ₂ O ₃ tube	Y _{<i>i</i>-butene} = 0.28 at 762 °C	Y _{<i>i</i>-butene} = 0.41 at 762 °C	[147]
Dehydrogenation of cyclohexane	PBMR	cyclo-hexane diluted in argon	423–523 K $p = 101.3$ kPa Sweep gas: argon	Pt/Al ₂ O ₃ 1 wt. % Pt	FAU/ α -Al ₂ O ₃ tube	X _{cyclohexane} = 32.2	X _{cyclohexane} = 72.1	[148,149]
Dehydrogenation of ethylbenzene to styrene	PBMR	water and ethyl-benzene	580–640 °C $\Delta p = 0.8$ atm sweep gas: nitrogen	Fe ₂ O ₃	silicalite-1/ stainless steel tube	X _{ethylbenzene} = 67.5 at 610 °C	X _{ethylbenzene} = 74.8 at 610 °C	[150]
Dehydrogenation of ethane	PBMR	pure ethane	500–550 °C $p_{\text{feed}} = 104$ kPa $p_{\text{perm}} = 101.3$ kPa sweep gas: argon	Pt-Sn/Al ₂ O ₃ 1 wt. % Pt, 0.3 wt. % Sn	natural mordenite disk	X _{ethane} = 9.7 S _{ethylene} = 92.2 Y _{ethylene} = 9 at 550 °C	X _{ethane} = 10.5 S _{ethylene} = 93.7 Y _{ethylene} = 9.8 at 550 °C	[151]

Table 1. Cont.

Reaction	Reactor Type	Feed	Operating Conditions	Catalyst	Membrane	X_{CR} (%)	X_{MR} (%)	References	
						S_{CR} (%)	S_{MR} (%)		
						Y_{CR} (%)	Y_{MR} (%)		
High-temperature water gas shift reaction	PBMR	carbon monoxide, water steam	400–550 °C $H_2O/CO = 1.0–3.5$ sweep gas: nitrogen	Fe/Ce	MFI/ α - Al_2O_3 tube	$X_{CO} = 62.5$	$X_{CO} = 81.7$	[152]	
Low-temperature water gas shift reaction	PBMR	carbon monoxide and water steam diluted in nitrogen	220–290 °C $p = 6$ bar GHSV = 1000–7500 L _N /kg _{cat} sweep gas: nitrogen	CuO-ZnO/ Al_2O_3	MFI/ α - Al_2O_3 disc	$X_{CO} = 89.1$	$X_{CO} = 95.4$	[153]	
High-temperature water gas shift reaction	PBMR	carbon monoxide, water steam and nitrogen	400–550 °C $H_2O/CO = 1.0–3.5$ WHSV = 7500–60,000 h ⁻¹ $p = 2–6$ atm sweep gas: nitrogen	Fe/Ce	MFI/ α - Al_2O_3 disc	$X_{CO} = \sim 90$	$X_{CO} > 95$	[154,155]	
Water gas shift reaction	PBMR	carbon monoxide, water steam	500 °C $p = 5$ atm $H_2O/CO = 3.0$ GHSV = 72,000 h ⁻¹ sweep gas: argon	Fe-Cr-Cu	ZSM-5/ silicalite bilayer/ α - Al_2O_3	n.r.	$X_{CO} = 89.8$	[156]	
High-temperature water gas shift reaction	PBMR	carbon monoxide, hydrogen, preheated steam	300–450 °C $p_{feed} = 0.1–0.15$ MPa $p_{perm} = 0.1$ MPa sweep gas: steam	$Fe_2O_3/Cr_2O_3/Al_2O_3$	MFI/ α - Al_2O_3 hollow fibre	$X_{CO} = 63.4$	$X_{CO} = 73.6$	[157]	

Table 1. Cont.

Reaction	Reactor Type	Feed	Operating Conditions	Catalyst	Membrane	X _{CR} (%) S _{CR} (%) Y _{CR} (%)	X _{MR} (%) S _{MR} (%) Y _{MR} (%)	References
Xylene isomerization	PBMR	<i>m</i> -xylene diluted in nitrogen	577 K sweep gas: nitrogen in counter-current mode	Pt on zeolite	MFI/ α -Al ₂ O ₃ tube	<i>S</i> _{<i>p</i>-xylene} = 58 <i>Y</i> _{<i>p</i>-xylene} = 21	<i>S</i> _{perm. only} = 100 <i>S</i> _{perm.+Ret.} = 65 <i>Y</i> _{<i>p</i>-xylene} = 23	[158]
Xylene isomerization	CMR	pure <i>m</i> -xylene; carrier gas: nitrogen	300–400 °C sweep gas: nitrogen	H-ZSM-5/316L stainless steel disc		<i>X</i> _{<i>m</i>-xylene} = 5.87 <i>S</i> _{<i>p</i>-xylene} = 55.6 <i>S</i> _{<i>o</i>-xylene} = 44.4	<i>X</i> _{<i>m</i>-xylene} = 6.9 <i>S</i> _{<i>p</i>-xylene} = 66.7 <i>S</i> _{<i>o</i>-xylene} = 33.3	[159]
Xylene isomerization	CMR	<i>m</i> -xylene diluted in helium	370 °C sweep gas: nitrogen	Pt/H-ZSM-5/stainless steel tube		n.r.	<i>S</i> _{<i>p</i>-xylene} = 67	[160]
Xylene isomerization	PBMR	mixture of <i>m</i> -, <i>p</i> - and <i>o</i> -xylene carrier gas: hydrogen	340–390 °C WHSV = 550 h ⁻¹	Pt/H-ZSM-5	Ba-ZSM-5/ Stainless steel	<i>S</i> _{<i>p</i>-xylene} = 52	<i>S</i> _{<i>p</i>-xylene} = 69	[160]
<i>m</i> -xylene isomerization	PBMR	<i>m</i> -xylene diluted in helium	270–390 °C sweep gas: helium diverse packing configurations	HZSM-5	silicalite-1/ α -Al ₂ O ₃ disc	GHSV = 1574 h ⁻¹ <i>X</i> _{<i>m</i>-xylene} = 51.9 <i>S</i> _{<i>p</i>-xylene} = 35.7 GHSV = 4722 h ⁻¹ <i>X</i> _{<i>m</i>-xylene} = 36.5 <i>S</i> _{<i>p</i>-xylene} = 47.3	- <i>X</i> _{<i>m</i>-xylene} = 47.8 <i>S</i> _{<i>p</i>-xylene} = 44.6 - <i>X</i> _{<i>m</i>-xylene} = 36.1 <i>S</i> _{<i>p</i>-xylene} = 49.6	[161]
<i>m</i> -xylene isomerization	PBMR	<i>m</i> -xylene, carrier gas: nitrogen	473–573 K sweep gas: nitrogen	Pt-HZSM-5	MFI/ α -Al ₂ O ₃ tube	<i>S</i> _{<i>p</i>-xylene} = 42 <i>Y</i> _{<i>p</i>-xylene} = 27	<i>S</i> _{<i>p</i>-xylene} = 49 <i>Y</i> _{<i>p</i>-xylene} = 23	[162,163]
xylene isomerization	CMR	<i>m</i> -xylene diluted in hydrogen	355–450 °C <i>p</i> = 101 kPa sweep gas: nitrogen	acid-functionalized silicalite-1/ α -Al ₂ O ₃ disc propylsulfonic and arenesulfonic acid sites		n.r.	<i>X</i> _{<i>m</i>-xylene} = 52 <i>Y</i> _{<i>p</i>-xylene} = 32 at 450 °C	[164]
<i>m</i> -xylene isomerization	CMR	<i>m</i> -xylene diluted in helium	270 °C weep gas: helium	H-MFI/ α -Al ₂ O ₃ disc		n.r.	<i>X</i> _{<i>m</i>-xylene} = 6.5 <i>S</i> _{<i>p</i>-xylene} = 92.1	[165]

Table 1. Cont.

Reaction	Reactor Type	Feed	Operating Conditions	Catalyst	Membrane	X _{CR} (%) S _{CR} (%) Y _{CR} (%)	X _{MR} (%) S _{MR} (%) Y _{MR} (%)	References
Double-bond isomerization of 1-butene	CMR	1-butene diluted in nitrogen	120–250 °C $p = 1$ bar sweep gas: nitrogen	[B]MFI/ α -Al ₂ O ₃ tube		n.r.	$X = 44.5$ ratio <i>trans/cis</i> = 2.2 at 250 °C	[166]
Esterification of ethanol with acetic acid	CMR	ethanol, acetic acid	333–363 K $\Delta p = 0$ –1 bar sweep gas: He	H-ZSM-5/ α -Al ₂ O ₃ or stainless steel tubes		$X = 49.4$	$X = 63.1$	[167]
Esterification of acetic acid with ethanol	PBMR	ethanol, acetic acid	358 K $p_{\text{ret}} = 1.3$ bar $p_{\text{perm}} = 2$ mbar	Amberlyst 15	modernite/ α -Al ₂ O ₃ zeolite A/ α -Al ₂ O ₃	$X = 66.9$	$X = \sim 90$	[168]
Catalytic dehydration of methanol	PBMR	methanol	150–250 °C WHSV = 0.5–2.6 h ⁻¹ $p_{\text{feed}} = 1$ –1.7 bar $p_{\text{perm}} = 1$ mbar	γ -alumina	NaA/stainless steel wire mesh	$X_{\text{CH}_3\text{OH}} = 61$ at 230 °C	$X_{\text{CH}_3\text{OH}} = 85$ at 230 °C	[169]
CO ₂ hydrogenation into methanol	PBMR	carbon dioxide, hydrogen	200–263 °C $p = 20$ –24 bar H ₂ /CO ₂ = 3–7	Cu/ZnO/Al ₂ O ₃	NaA/ α -Al ₂ O ₃ tube	$X_{\text{CO}_2} = 5$ $S_{\text{CH}_3\text{OH}} = 48$ $Y_{\text{CH}_3\text{OH}} = 2.4$	$X_{\text{CO}_2} = 11.6$ $S_{\text{CH}_3\text{OH}} = 75$ $Y_{\text{CH}_3\text{OH}} = 8.7$	[170]
Metathesis of propene and geometrical isomerization of <i>cis</i> -2-butene	PBMR	pure propene	296 K sweep gas: helium	Re ₂ O ₇ / γ -Al ₂ O ₃	silicalite-1/ stainless steel disc	$X_{\text{propene}} = 33.4$ $X_{\text{cis-2-butene}} = 76.1$	$X_{\text{propene}} = 38.4$ $X_{\text{cis-2-butene}} = 79.4$ $Y_{\text{trans-2-butene}} = 79$	[93,94]
Hydro-isomerization of C ₆	PBMR	<i>n</i> -hexane, 2-methyl-pentane (MP); carrier gas: helium	393 K WHSV = 0.21 gHC/(g _{cat} h) sweep gas: hydrogen	Pt-chlorinated alumina (AT-2G)	silicalite-1/ TiO ₂ /stainless steel tube	n.r.	$X_{\text{n-hexane}} = 71.8$ at 393 K	[171]

3.2. Distributor Type Zeolite Membrane Reactors

The distributor type membrane reactor configuration is characterized by controlled permeation/dosing of reactants via a non-permselective membrane. Especially for oxidation reactions, such a configuration could offer diverse benefits compared to conventional reactors, namely precise distribution of the reactant along the catalyst bed, thus minimizing the local appearance of dangerous conditions. Mota *et al.* [172] carried out the selective oxidation of butane to maleic anhydride in membrane reactors of the distributor type combining zeolite MFI membranes used to distribute oxygen and vanadium phosphorus mixed oxides-based catalysts known for their high selectivity and conversion of alkanes [173]. Even though, the obtained results were in fact quite similar with those of the conventional co-feed configuration, the authors pointed out, that the separated O₂ feeding could be beneficial to avoid flammability problems. Nevertheless, employing non-permselective mesoporous ceramic membranes to distribute the oxygen allows an operation with higher *n*-butane concentrations leading to higher maleic anhydride yields [174,175]. Moreover, Mallada *et al.* [174] reversed the butane flow in the inner volume of the membrane reactor in order to overcome the problem with observed heterogeneity of the oxidation state of the catalyst bed. As a result, maleic anhydride yields above those obtained in the conventional reactor mode were recorded. In a later work from the same working group, zeolite membranes were combined with cobalt-doped vanadium phosphorus mixed oxides-based catalysts in membrane reactors operating at high butane concentrations in the feed [176]. Due to the O₂ distribution, the studied membrane reactors were able to eliminate the formation of critical concentrations and allowed the operation at the flammability zone, giving rise to three times higher maleic anhydride productivity.

Micro- and mesoporous zeolite membranes enclosing V-Mg-O catalyst beds have been employed to control the oxygen partial pressure in order to enhance the selectivity towards propene in the oxidative dehydrogenation of propane [177]. The microporous zeolite membrane evinced to be an effective gas barrier since only small amounts of the reactant propane diffused through the membrane and all the oxygen permeating was consumed in the dehydrogenation reaction causing remarkable increase in the propene yields at low C₃H₈/O₂ ratios under separate feeding configuration. Julbe *et al.* [178] studied MFI and vanadium-loaded MFI membranes for the same reaction using them in two configurations either as oxygen distributors or as flow-through contactors. The V-MFI membrane outperformed the MFI and in the flow-through configuration a propene yield of nearly 8% at selectivity of 40%–50% was obtained.

As an alternative to the conventional fixed-bed reactors, methanol oxidative dehydrogenation to yield formaldehyde was studied in a NMR with either methanol or oxygen as permeating species [179]. The non-permselective stainless steel membrane was packed with Fe-Mo oxide catalyst. The configuration with oxygen feeding though the membrane outperformed the membrane reactor with methanol as permeating component and that of the traditional reactor, assuring lower oxygen concentration and thus selectivity improvement and higher formaldehyde yields. Later on, the same authors optimized the oxygen feed distribution on the basis of productivity of the desired product formaldehyde [180].

Modified MFI membranes were utilized in membrane reactors of the distributor type to run butadiene hydrogenation in the vapor phase [181]. By the use of the zeolite membrane to distribute hydrogen in a controlled manner along the catalyst bed, it was possible to overcome the selectivity drawback, and to greatly improve the butadiene conversion.

3.3. Contactor Type Membrane Reactors

The last membrane reactor principle considering the membrane function is the contactor type, where catalytic active and non-permselective membranes can be employed. The use of contactors is usually announced when a reaction front should be set in order to intensify the contact between the catalyst and the reactants.

Torres *et al.* reported on *i*-butene oligomerization with catalytic BEA zeolite membranes in the temperature range from 373 to 423 K [182,183]. The non-permselective membrane was used as a contact medium demonstrating high activity towards *i*-butene dimers. Furthermore, Pt-ZSM-5 membranes prepared on tubular supports were applied for the combustion of volatile organic compounds (VOCs) at low concentrations [184]. The authors fed hexane as representative for VOC at the one side of the membrane and O₂ at the other side. Interestingly, a membrane with intermediate concentration of defects performed better due to improved contact between the reactants and the catalytic material leading to nearly complete combustion of *n*-hexane at 210 °C.

4. Applications in Packed Bed Membrane Reactors (PBMR)

The utilization of permselective zeolite membranes in a direct contact to the catalyst bed, as shown in Figure 4, could offer several advantages over alternative reactor concepts. On the one hand, zeolite membranes can remove products, catalyst poisons or inhibiting products from the reaction zone in order to enhance the conversion of a given reaction. On the other hand, zeolite membranes might provide selective reactant supply from the feed mixture as well as control of the reactant traffic or residence time, thus contributing to selectivity enhancement.

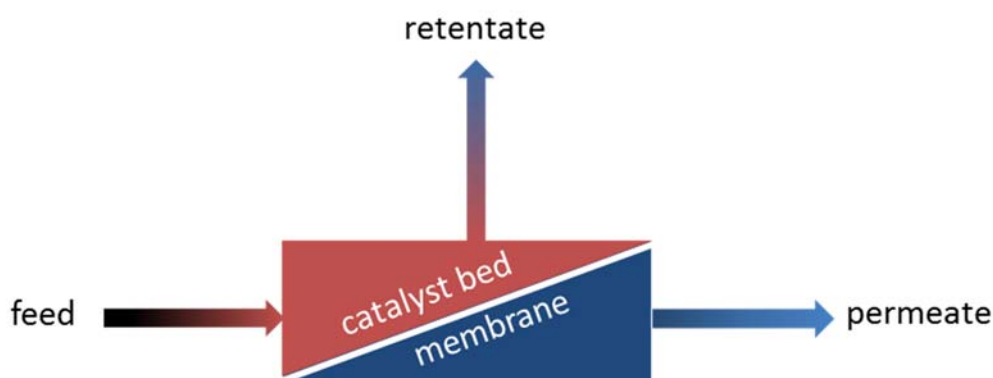


Figure 4. Schematic drawing of a packed bed membrane reactor (PBMR).

4.1. Product Removal: Enhanced Conversions by Shifting the Chemical Equilibrium

Zeolite membranes being able to preferentially transport one or more products from the reaction zone are intimately located to the catalyst bed. The so called extractor type membrane reactor unit is often utilized in equilibrium limited reactions in order to break this limitation and improve the yield of the desired products. However, sufficient permeation and sharp separation, as well as mechanical, thermal and chemical stabilities are considered as crucial membrane requirements for successful application in this membrane reactor mode. Contrarily, by employing membranes with poor selectivity, the reaction will

suffer from significant reactant loss. Similarly, low permeation rates will demand increased membrane area that will lead to discrepancies in regard to catalyst volume and higher investment costs.

4.1.1. Equilibrium Shift by Water Removal

As already discussed in Section 2.2. esterification is an equilibrium limited reaction, where water separation is required to increase conversion. Tanaka *et al.* [185,186] proposed zeolite T membranes for the pervaporation-aided esterification of acetic acid or lactic acid with ethanol, catalyzed by an exchange resin (Amberlyst 15, Organo) in batch reactor at 343 K. The membrane displayed good stability even being submerged in the acidic media and was able to selectively remove the produced water, thus exceeding the equilibrium limit. In such a way, nearly 100% conversion within 8 h of operation was reached. In this context, de la Iglesia *et al.* [168] employed modernite and zeolite A membranes in a continuous membrane reactor packed with Amberlyst™ as catalyst and evaluated their joint performance during esterification of ethanol and acetic acid. The used membranes exceeded the equilibrium conversion towards the esterification products in less than 1 day of operation, however displayed different resistance to the acidic reaction conditions affecting their long term stability. The modernite membrane leveled at a conversion of nearly 90% for 5 days of experiment attributed to its stability under the conditions applied, whereas the instability of zeolite A caused tremendous conversion loss. Interestingly, in the case of the modernite membrane significant rise in the separation factors of H₂O/Ethanol and H₂O/acetic acid from 55 and 25, respectively, at the beginning of the experiment towards 200 and 95 at the third day was observed associated with the increasing production of water in the catalyst zone. On the contrary, the initial higher separation factors of H₂O/Ethanol (315) and H₂O/acetic acid (89) for the zeolite A membrane declined sharply to 32 and 18, respectively, leading to reactants loss and conversion decreasing from 72% at the beginning of the experiment to 53% after two days of operation.

Beside esterification, further water releasing reactions can be enhanced using zeolite membranes for equilibrium shift. For instance, modernite or NaA zeolite membranes together with Amberlyst™ were implemented in membrane reactors for the gas-phase synthesis of methyl-*tert*-butyl ether (MTBE) from *tert*-butanol (TBA) and methanol (MeOH) [187]. In the first step, the membranes were characterized by separation experiments of multicomponent mixtures containing water, MeOH, TBA, MTBE and *i*-butene (IB) displaying the following selectivity trend: $S_{H_2O/IB} > S_{H_2O/MTBE} > S_{H_2O/TBA} > S_{H_2O/MeOH}$. The selective permeation of water across the zeolite membranes was attributed to their high polarities resulting in preferential adsorption and pore blocking for the other components. Then, during the reaction experiments the water removal in the membrane reactor operation contributed to 67.5% MTBE yield showing 6.7% absolute increase in the MTBE yield compared to the conventional configuration without water removal. Very recently, NaA zeolite membranes were also used as water extractors in the methanol dehydration to dimethyl ether (DME) [169]. The γ -Al₂O₃ catalyst was located between two disc membranes giving a ratio of membrane area to reactor volume of 200 m⁻¹, whereas 10–100 m⁻¹ is said being reasonable for industrial application [94]. For comparison, the authors performed the same reaction in a conventional fixed-bed reactor operated under the same conditions. Water and DME were the only products of the catalytic experiments. Increased temperature in the range of 150–250 °C and decreased weight hourly space velocity (WHSV) from 2.6 to 0.5 h⁻¹ evinced to be more beneficial for

the membrane reactor configuration, resulting in more than 20% absolute improvement of the methanol conversion. However, the limiting factor in course of the experimental study turned out to be on the one hand the reactor design and on the other hand the membrane selectivity since the separation of methanol and water is mainly based on competitive adsorption being so dependent on the process parameter temperature, pressure and composition.

Apart from overcoming equilibrium limited reactions, hydrophilic zeolite membranes can be employed in reactions where the water removal will contribute to decreased catalyst deactivation. So, the feasibility of NaA zeolite membranes for water liquid-phase etherification of *n*-pentanol to di-*n*-pentyl ether (DNPE) catalyzed by ion-exchange sulfonated resins has been evaluated [188]. In this reaction, the formed water has a strong deactivating effect on the catalyst. However, due to the excellent dehydration performance of the membrane an enhancement of the *n*-pentanol conversion (64% conversion compared to 35% in the fixed bed-reactor) was possible. Moreover, the authors analyzed the economic aspects of the membrane-based reactor configuration for DNPE production and estimated by assuming a 35,000 tm DNPE/year production about 30% of the investment costs for the membrane reactor. According to analysis of operational costs (OPEX) for 1 L of DNPE it would be related to 1.6 US\$ of unit costs.

Meanwhile, the carbon dioxide utilization is one of the most challenging tasks in chemistry [189,190]. Here, zeolite membranes might be used for the direct dimethyl ether synthesis from a mixture of syngas and carbon dioxide [191]. However, in the multistep reaction via methanol water is being released [192,193]. The advantageous performance of a packed bed zeolite membrane reactor was theoretically demonstrated for *in situ* water removal. However, based on mathematical models, the authors concluded that the dimethyl ether yield is highly dependent on the membrane water permselectivity. For instance, for membranes with low permselectivity, the dimethyl ether yield was nearly 50% lower due to reactant loss than that obtained in a conventional reactor (7.0% yield in the PBMR vs. 14.8% yield in the CR). Therefore, in further studies, the same authors analyzed and optimized theoretically the operating conditions leading to enhanced dimethyl ether yield and CO₂ recovery [194]. Thereby, the authors found an increase in CO₂ conversion up to 85% by using high sweep gas stream. Moreover, approximately 30% yield of DME could be obtained in the PBMR at high recirculation factors of the sweep gas stream due to reduction in the methanol loss across the membrane.

In addition, the application of hydrophilic membrane reactors for the selective *in situ* removal of water has been considered for Fischer–Tropsch synthesis in three directions: (i) improvement of the catalyst lifetime; (ii) rise of the reactor productivity; and (iii) displacement of the water gas shift equilibrium in favor of CO [195,196]. The use of hydrophilic zeolite membranes and their positive effect on the conversion in the Fischer-Tropsch process was earlier discussed by Espinoza *et al.* [197]. Later, Rohde *et al.* [196] evaluated thoroughly different membranes. The authors concluded that membranes with proper fluxes for the selective removal of water from mixtures comprising H₂, CO, CO₂ and hydrocarbons are still required for industrial application. For such applications H₂O permeances of over 1×10^{-7} mol/(s m² Pa) and ratios of H₂O permeance to that of respective reactants greater than 75 were defined. In this context, the literature study showed that zeolite membranes outperform both amorphous membranes and polymer membranes in regard to H₂O permeance (in the range of 1×10^{-7} and 10^{-6} mol/(s m² Pa)) and H₂O/H₂ permselectivity (>10), being however far from meeting the defined requirements for technical application. Hence, the authors suggested hydroxy sodalite zeolite membranes

with a layer thickness of 2 μm as auspicious candidate for the *in situ* water removal due to their extraordinary separation and permeation performance demonstrated as well earlier by Khajavi *et al.* [198]. Recently, a novel reactor configuration denoted as fixed-bed membrane reactor followed by fluidized-bed membrane reactor (FMFMDR) has been proposed for high temperature Fischer-Tropsch synthesis, in particular gasoline production from syngas [199,200]. This configuration combines a fixed-bed water permselective membrane reactor equipped with H-SOD zeolite membrane coated on $\alpha\text{-Al}_2\text{O}_3$ substrate and a fluidized-bed hydrogen permselective membrane reactor equipped with Pd-Ag membrane. By means of theoretical modeling, the authors stated the benefits of the studied reactor configuration in respect to improved gasoline yield and reduced CO_2 yield.

4.1.2. Hydrogen Permeation in Dehydrogenation Reactions

The dehydrogenation of alkanes to olefins is a strongly endothermic and thermodynamically equilibrium limited reaction [201]. By removing products from the reaction zone the reaction equilibrium will be displaced towards the product side, thus increasing the overall conversion. The performance of hydrogen selective zeolite membranes in terms of H_2 (product) removal and its effect on the reaction efficiency has been studied in dehydrogenation of alkanes by several groups. For instance, MFI zeolite membranes were applied in a PBMR configuration and extensively investigated in dehydrogenation of *i*-butane by the group of Dalmon *et al.* [145,202–204]. Either commercial Pt-Sn/ $\gamma\text{-Al}_2\text{O}_3$ [202], Pt-In/silicalite [145,203] or MFI supported Pt-In-Ge [204] catalysts placed in the core of the membrane tube were used. The effectiveness of the membrane reactor to improve dehydrogenation yields compared to the conventional reactor was up to four times higher [145]. When comparing mesoporous membranes with microporous zeolite membranes, the authors found hydrogen selectivity only for the latter, while the usage of larger-pored membranes led just to gas mixing at both sides of the membrane [202]. Moreover, the authors pointed on the importance of the precise control/selection of the operating parameters such as feed flow and sweep gas flow, as well as sweep gas configuration and found correlations between membrane reactor performance and membrane permeability or catalyst activity depending on the applied conditions [145,203]. In this regard, the reactor performance was limited by the catalyst activity under counter-current sweep flow conditions so that the catalyst was not active enough to follow the high membrane permeability. On the other side, choosing the co-current sweep configuration, the reactor performance was controlled by the membrane permeation efficiency and insufficient selectivity resulted thereby in reactants (*i*-butane) loss. Van Dyk *et al.* [204] confirmed these observations conducting a comparative study with microporous MFI and dense Pd membranes in membrane reactors packed with Pt-In-Ge/MFI catalyst. Generally, better yields were obtained with the membrane reactor configurations than with the conventional reactor. Nevertheless, the two membranes reached almost equal yields despite their different separation efficiencies so that the authors concluded that the membrane reactor performance was limited by the catalyst activity. At this point the fundamental work of Gokhale *et al.* [205] has to be mentioned. The authors presented insights on the relationship between permeation rates as function of separation selectivity and residence time. They focused on the possible operating conditions under which reactant loss controls conversion in dehydrogenation reactions. However, Illgen *et al.* [146] commented a feed dilution effect should always be considered during product analysis. It was stated that despite the high separation efficiency of the

MFI zeolite membranes, e.g. a H₂/*i*-butane mixture separation factor of 70 and a permeance of 1 m³/m² h bar at the reaction temperature of 510 °C, the increased conversion up to 49% obtained in the PBMR at WHSV of 0.5 h⁻¹, where the conversion of the conventional reactor was 29.1% was due to a great extent to the dilution of the reactant feed by the sweep gas and less to the removal of H₂ from the reaction zone.

Consequently, van den Bergh *et al.* [147] revealed the benefit of using small-pore zeolite DD3R membranes coupled to Cr₂O₃/Al₂O₃ catalysts in PBMR for the dehydrogenation of *i*-butane. The DD3R membrane is believed to be quite attractive for the present application since it is able to separate H₂ and *i*-butane by molecular sieving effects. Accordingly, only H₂ could pass the membrane and *i*-butane will be retained due to its bigger size. In this context, the membrane exhibited outstanding H₂/*i*-butane ideal selectivity (based on the single gas permeation fluxes) of over 500 at 773 K. However, slightly lower mixture selectivity was recorded since the driving force for permeation of H₂ in the mixture was reduced by the increased partial pressure of H₂ in the permeate and its decreased partial pressure in the feed. About 50% increase in yield compared to the equilibrium value was recorded mainly due to the effective removal of H₂ from the reaction zone. On the other hand, the studies provided evidence of a minor decrease in the catalyst activity compared to the conventional reactor. Moreover, a slightly increased coke formation, however with selectivity towards coke being still low than 5% was observed attributed by the authors to the lower H₂ partial pressure at the reaction side. Despite the fact that the catalyst activity and the H₂ removal hold a good balance, the authors concluded that both parameters limit to some extent the overall performance. Such being the case, further improvements in the catalyst activity and stability as well as in the permeation fluxes of the membrane are necessitated for successful application in dehydrogenation reactions at industrial scale.

The performance of large-pore FAU type zeolite membranes prepared on porous α -Al₂O₃ support tubes in the catalytic dehydrogenation of cyclohexane conducted in membrane reactors was evaluated experimentally [148] and theoretically [149] by the group of Kusakabe. The membranes were able to simultaneously remove hydrogen and benzene from the reaction zone filled with a Pt/Al₂O₃ catalyst. Moreover, higher sweep or lower feed flow rates affected positively the cyclohexane conversion. The authors evaluated mathematically the trade-off effect of membrane permeance and separation factor on the conversion and concluded that in terms of industrial practice high membrane permeability accompanied with reasonable selectivity might be the more favorable option than a high selectivity at the expense of low permeability. Furthermore, it was highlighted that the H₂ addition to the cyclohexane feed compensates the reduced H₂ partial pressure on the reaction side, caused by its continuous extraction, hence preventing the catalyst from coking [149].

Defect-free silicalite-1 zeolite membranes were used for the catalytic dehydrogenation of ethylbenzene to styrene in membrane reactors packed with Fe₂O₃ exposing their advantages (74.8% at 610 °C) over a conventional reactor (67.5% at the same temperature) in regard to conversion due to the instant extraction of the produced H₂ across the membrane [150]. However, the benefit of the membrane reactor diminished with increasing space velocities ranging from 0.5 to 1.5 and approached the performance of the conventional reactor configuration. On the contrary, rising the ratios of sweep gas to reactant feed from 0.5 to 2 contributed to increase in the ethylbenzene conversion (from 70.5% to 74.8%) since higher ratios induce generally larger driving force for permeation resulting in higher H₂ permeation rates. Further rise in the sweep/feed ratio from 2 to 6 resulted in a nearly constant conversion pointing out that

ratio of 2 was sufficient in order to remove the desorbing hydrogen from the permeate side of the membrane. The authors stressed once again the benefit of the zeolite membrane reactor operation in terms of reduced partial pressure of H₂ contributing to higher reaction rates.

Alternatively, small-pore size SOD membranes have been recently considered as an attractive candidate for the selective removal of H₂ in catalytic dehydrogenation of ethylbenzene to styrene [206]. The performance of a membrane reactor and a conventional plug flow reactor (PFR) was predicted, confirming the benefit of the membrane reactor with regard to an absolute ethylbenzene conversion increase of 3.45% and yield increase of 8.99% ascribed to the effective H₂ extraction from the reaction side. Due to the dynamic limitations, the PFR reached 80% conversion and 44.5% yield.

Very recent results promise the potential application of cost-effective natural mordenite membranes. Indeed, the mordenite membranes were fabricated by using rock material (Paradise Quarry Limited, Whangarei, New Zealand) processed by a diamond saw. In membrane reactors, packed with Pt/Al₂O₃ beads for the dehydrogenation reaction of ethane [151], the membrane was able to shift the reaction equilibrium at the studied temperature range of 500–550 °C due to its hydrogen-selective properties. Based on evaluation of the membrane reactor effectiveness in terms of permeation area to reactor volume ratio (*A/V* ratio), the authors demonstrated that increasing the ratio from 0.04 m⁻¹ to 0.16 m⁻¹ gives rise to additional reduction of the H₂ content in the reaction zone in relation with its formation rate and consequent increase in the reaction rate contributing to more enhanced ethane conversion compared to the PBMR with the smaller permeation area.

4.1.3. Hydrogen Permeation in Water Gas Shift Reaction

The water gas shift (WGS) reaction represents another equilibrium limited reaction for which the application of extractor type membrane reactors has been reported. The reversible and mildly exothermic WGS reaction is a subsequent step for the increased production of H₂ from initially produced CO gained from fossil fuel reforming. Generally, in order to overcome the thermodynamic and kinetic limitations, the WGS reaction is performed in two steps including high temperature shift favoring higher space time yields followed by low temperature shift to obtain high CO conversion [207]. However, coupling the reaction with a H₂-selective membrane can break the equilibrium constraints and facilitate the CO conversion, thus intensifying the process and resulting in economically beneficial application. Besides Pd- or Pd-Ag alloys membranes [208–211] and silica-based membranes [212,213], zeolite membranes are subject of intensive research interest for the present problem.

Considering the application of MFI zeolite membrane, several methods for modification of zeolite membranes prior to application in PBMR for WGS reaction are proposed. For instance, Tang *et al.* modified the pores of MFI zeolite membranes by a so called *in-situ* catalytic cracking deposition (CCD) of silane precursors [124,152,214]. The formed deposits reduce the effective pore size to below 0.36 nm hindering the entry of CO₂ into the pore channels. The idea behind this modification was the need to obtain controlled mass transport of H₂ over CO₂ since thought the unmodified MFI the transport of H₂ and CO₂, respectively, is controlled by gaseous diffusion resulting in separation factors slightly below the Knudsen factor. Accordingly, thanks to the the deposition of molecular silica species in the zeolite channels, the access of the slightly bigger CO₂ molecules (kinetic diameters of H₂ and CO₂ are 0.289 and 0.33 nm, respectively) was restrained giving rise to H₂/CO₂ permselectivity of 68.3 and equimolar

mixture separation factors of nearly 38 at 550 °C [152]. The modified zeolite MFI membrane packed with a $\text{Fe}_{1.82}\text{Ce}_{0.18}\text{O}_3$ catalyst was tested in WGS reaction at temperatures between 400 and 550 °C and near atmospheric pressure. At a reaction temperature of 550 °C ($\text{WHSV} = 60,000 \text{ h}^{-1}$, $\text{H}_2\text{O}/\text{CO} = 1$) the membrane reactor configuration exhibited CO conversion (81.7%) exceeding the equilibrium limit (65%) and the performance of the traditional packed-bed reactor (62.5%). However, decreasing the reaction temperatures below 500 °C caused a conversion drop due to kinetic resistance. With regard to the WGS reaction, low $\text{H}_2\text{O}/\text{CO}$ ratios are preferred since the hydrogen partial pressure is large and the driving force for permeation as a result, too. The same group evaluated the impact of elevated pressure (2–6 atm) on the efficiency of modified MFI disc membranes in high temperature (400–550 °C) WGS reaction and demonstrated its positive effect on the CO conversion. Furthermore, the authors pointed towards to the larger driving force for H_2 permeation at increased feed pressure and constant permeate pressure [154]. Figure 5 depicts the influence of reaction pressure and temperature on CO conversion (χ_{CO}), hydrogen recovery (R_{H_2}), and permeate side H_2 concentration ($\gamma_{\text{H}_2,p}$). As shown in Figure 5 (left) a higher driving force for hydrogen permeation is achieved by increasing the feed pressure leading to higher R_{H_2} . At the applied temperatures the separation factor $\alpha_{\text{H}_2\text{CO}_2}$ is not influenced by adsorption and the gases exhibit ideal gas behavior. The authors ascribed the decrease in $\gamma_{\text{H}_2,p}$ with increasing R_{H_2} and χ_{CO} at high pressure to the decreased value of $(\gamma_{\text{H}_2}/\gamma_{\text{CO}_2})_{\text{permeate}}$ ($=\alpha_{\text{H}_2\text{CO}_2}/(\gamma_{\text{H}_2}/\gamma_{\text{CO}_2})_{\text{feed}}$) when reducing $(\gamma_{\text{H}_2}/\gamma_{\text{CO}_2})_{\text{feed}}$. Furthermore, it is shown (Figure 5 (right)) that an increased feed pressure could be used to overcome the equilibrium CO conversion ($\chi_{\text{CO},e}$) using the PBMR. Generally, the findings indicate that even membranes with moderate selectivity could be powerful tool for conversion enhancement. Particularly, it was emphasized that the prepared MFI membrane showed good resistance against H_2S and was stable at the applied high temperatures and pressures. Recently, the same authors applied the model of one-dimensional plug-flow reactors (PFR) and related the results with data from MFI-type zeolite membranes. Simulations proved the potential of the membrane reactor, combining a modified MFI membrane and cerium-doped ferrite catalysts, to reach CO conversion above 99.5% at 550 °C and ~50 atm at a ratio of $\text{H}_2\text{O}/\text{CO} \sim 5.0$ [155]. Similarly, Lin *et al.* [156] evaluated the performance of ZSM-5/silicalite bilayer membranes packed with Fe-Cr-Cu catalysts combining experimental and theoretical studies and defined the optimal conditions under which CO conversion of over 95% together with H_2 recovery of over 90% could be achieved.

For low-temperature WGS reactions, Zhang *et al.* [153] illustrated the benefit of PBMRs coupling a H_2 -permselective MFI membrane modified by CCD of methyl-diethoxysilane and $\text{CuO}/\text{ZnO}/\text{Al}_2\text{O}_3$ catalyst over the conventional packed bed reactor. CO conversion exceeding the equilibrium was obtained at 300 °C attributed to the enhanced permeation of H_2 at the applied temperature on the one hand and the catalyst activity on the other hand. Very recently, the authors proposed the idea of using steam as sweep gas instead of inert gas in order to avoid subsequent separation to obtain pure hydrogen [157]. Figure 6 illustrates schematically this membrane reactor configuration with modified hollow fibre MFI zeolite membranes where the steam is applied in a counter-diffusion towards the reactions side in order to remove H_2 . The authors stated that sweeping with pure steam contributes to enhanced conversion combined with direct acquisition of the pure H_2 . Moreover, despite the fact that the membrane was characterized by high H_2 permeate flow, sweeping by N_2 -steam mixed gas resulted in lower conversion if compared to the experiments where pure steam was applied as sweep. The observed phenomenon was

attributed to the dilution of the steam by N_2 leading to reduced H_2O counter-diffusion effect due to the lower driving force through the membrane. Operating under low sweep steam flow rate as well as low feed pressure and H_2O/CO ratio contributed to highly pure H_2 permeate streams.

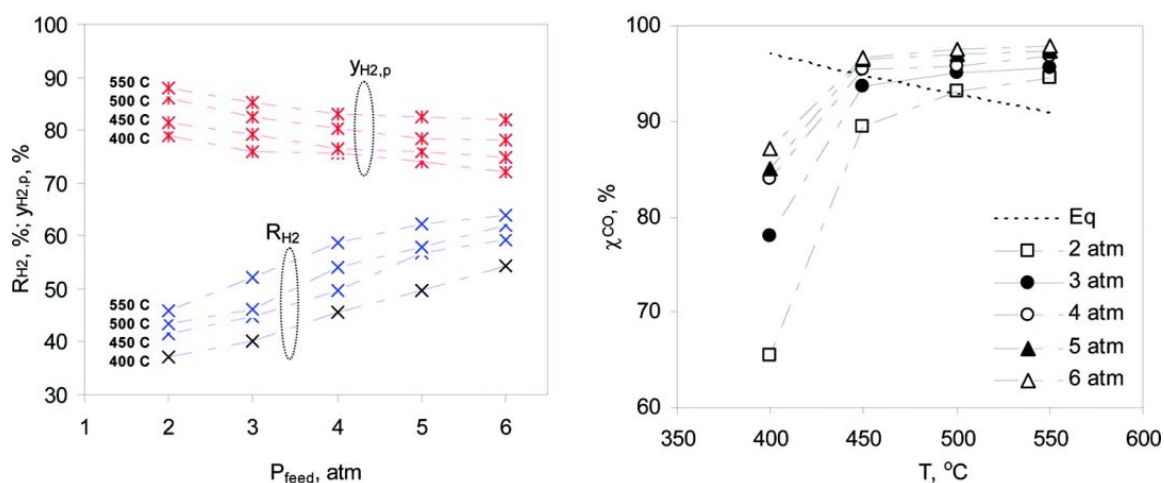


Figure 5. Water gas shift (WGS) reaction in a MFI zeolite membrane reactor (sweep: N_2 , at atmospheric pressure, WHSV at 7500 h^{-1} and ratio of $H_2O/CO = 3.5$): Influence of reaction pressure and temperature on CO conversion (χ_{CO}), hydrogen recovery (R_{H_2}) and permeate side H_2 concentration ($y_{H_2,p}$). Reprinted with permission from [154].



Figure 6. Schematic illustration of a WGS membrane reactor with modified hollow fibre MFI zeolite membrane swept by steam applied in a counter-diffusion towards the reaction side. Reprinted with permission from [157]. Copyright (2015) John Wiley and Sons.

4.1.4. Hydrogen Permeation in Syngas Production

The benefit of using zeolitic PBMRs over the traditional fixed-bed reactor has also been reported by Liu *et al.* [215,216] for selective product permeation in CO_2 reforming of methane for syngas production. The authors employed a combination of catalytic composite zeolite membranes either

$\text{La}_2\text{NiO}_4/\text{NaA}$ or $\text{La}_2\text{NiO}_4/\text{NaY}$ prepared on $\gamma\text{-Al}_2\text{O}_3/\alpha\text{-Al}_2\text{O}_3$ support packed with $\text{NiO-La}_2\text{O}_3/\gamma\text{-Al}_2\text{O}_3$ as catalyst. The idea behind this mixed configuration was the significantly low separation efficiency of the as-prepared inert zeolite membranes for the H_2/CH_4 mixture (binary mixture separation factor of 4.2 at room temperature decreasing to below 2 at temperature over 600 °C) and the arising diffusion of methane through the membranes during reforming. Therefore, the authors introduced the use of the catalytic active zeolite membranes packed with catalyst and managed so further methane reforming to syngas during its permeation through the membrane. The permselective permeation of CO and H_2 across the membrane contributed to enhanced CH_4 and CO_2 conversion of 73.6 and 82.4 mol % at 700 °C vs. 45 and 52 mol % over the fixed-bed reactor, respectively. Moreover, the coke deposition and thus the catalyst deactivation were remarkably reduced in the membrane reactor.

4.1.5. Hydrogenation

One of the most significant current discussions as previously mentioned is the need to reduce the CO_2 concentration in the atmosphere and so mitigate the greenhouse effect. Thereby, the CO_2 utilization as a useful chemical, e.g., through hydrogenation reactions to yield methanol used as fuel or basic chemical, is considered as a promising alternative [190]. Zeolite membrane reactors could be applied in order to assure removal of the condensable products (CH_3OH and H_2O) and to improve the methanol yield in the equilibrium limited reaction. The principle was first theoretically discussed by Barbieri *et al.* [217]. The authors confirmed the benefit of using either hydrophilic or hydrophobic zeolite membranes in terms of improved conversion, methanol selectivity and yield by operating at lower reaction volumes and residence times as well as higher temperatures and lower pressures compared to the conventional tubular reactor. The CO_2 conversion into methanol was later experimentally studied by Gallucci *et al.* in a membrane reactor with a zeolite NaA membrane enclosing a fixed bed of $\text{CuO-ZnO/Al}_2\text{O}_3$ catalyst [170]. Generally, the membrane reactor was able to display higher CO_2 conversion and selectivity than the traditional reactor mainly attributed to the selective removal of CH_3OH via the zeolite membrane. Moreover, the authors stressed the positive aspect of the reduced energy demand since the membrane reactor was able to reach the CO_2 conversions of the traditional reactor at milder conditions (e.g., PBMR operating at $\text{H}_2/\text{CO}_2 = 3$ and temperature of 225 °C could reach the conversion of conventional reactor operating at 265 °C). Furthermore, as stated by the authors the temperature seems to be the important process parameter in the PBMR operation since the methanol separation is mainly due to its capillary condensation inside the pores so that exceeding the critical temperature of methanol will sharply reduce the separation efficiency.

4.1.6. Metathesis of Propene

The selective product removal in the equilibrium limited metathesis of propene to ethene and 2-butene as well as from the simultaneous occurring geometrical isomerization of *cis*-2-butene into *trans*-2-butene was evaluated by the mean of a membrane reactor equipped with a silicalite-1 zeolite membrane supported on stainless steel and 16.4 wt. % $\text{Re}_2\text{O}_7/\gamma\text{-Al}_2\text{O}_3$ as catalyst [93,94]. The studied reactor benefited from the use of the membrane twice since (i) 13% absolute improvement of the propene conversion compared to the equilibrium value (25.4%) and (ii) 32% increase in the *trans*-2-butene/*cis*-2-butane ratio compared to the equilibrium ratio being 3.2 due to the preferential permeation of *trans*-2-butene were achieved.

However, even though the membrane did not show an absolute separation selectivity for *trans*-2-butene over *cis*-2-butene, it still displayed a balanced performance between sufficient product removal and reactant loss since the preferentially adsorbing *trans*-2-butane was able to block the pores for the permeation of propene. In addition, the use of a supplementary reactor for equilibration of the feed mixture before feeding the zeolite membrane reactor reduced the reactant loss. Furthermore, the authors evaluated the perspectives for industrial applications [93]. It was stated for high permeating silicalite-1 membranes this requirement was fulfilled. However, to the best of our knowledge no such industrial plant has ever been built up to now.

4.2. Product Removal: Enhanced Selectivity by Displacing the Chemical Equilibrium

Xylene isomers with a typical composition 18% *p*-xylene, 40% *m*-xylene, 22% *o*-xylene, and 20% ethylbenzene are generally produced from petroleum reformat streams [218]. However, the further use of the obtained isomers requires their separation. Due to the close boiling points of *p*- and *m*-xylene the use of distillation for their separation is not effective so that industrially crystallization and adsorption techniques have been developed, e.g., by using ZSM-5 [219]. The *o*- and *m*-xylenes can be isomerized to obtain more *p*-xylene.

As an energy-efficient alternative to the conventional techniques, membrane reactors coupling xylene isomerization and simultaneous selective recovery represent a research topic gaining in importance in the last years due to the increasing demand of xylenes estimated at approximately 22 Mtonnes in 2003 [220]. Applying this concept *p*-xylene, the raw material for production of polyester resins could be obtained as product at the permeate side. In a search of an appropriate membrane type, one should consider that *p*-xylene possesses a kinetic diameter of 5.8 Å which is significantly smaller than those of the *m*- and *o*- isomers being about 6.8 Å [221]. Due to the specific pore structure of the MFI-zeolite combining straight, circular pores (0.54 nm × 0.56 nm) and sinusoidal, elliptic pores (0.51 nm × 0.54 nm) [222] it became the membrane material of choice for xylene isomer separation as well as for the application in membrane reactors.

Several groups have studied the separation of xylenes with MFI zeolite membranes demonstrating high permselectivity for *p*-xylene over the other isomers, attributed mainly to the preferential permeation of *p*-xylene, since the zeolite pores expose sterical hindrance for the permeation of the bulkier *m*- and *o*-xylene isomer molecules [104,221,223–225]. In an outstanding study, Lai *et al.* [226] reported on dramatic improvement of the *p*-/*o*-xylene separation by *b*-oriented silicalite-1 membranes. In Figure 7 a comparison of achievable permeances as well as separation factors (SP) as a function of the operating temperature using (a) *c*-oriented; (b) [h0h]-oriented; (c) *a*- and *b*-oriented; and (d) *b*-oriented MFI films is given. It is clearly evidenced that the oriented membrane possesses the best properties for xylene isomer separation, demonstrating the strong impact of the crystal orientation on the membrane performance for certain separation task and for future applications in membrane reactors as well.

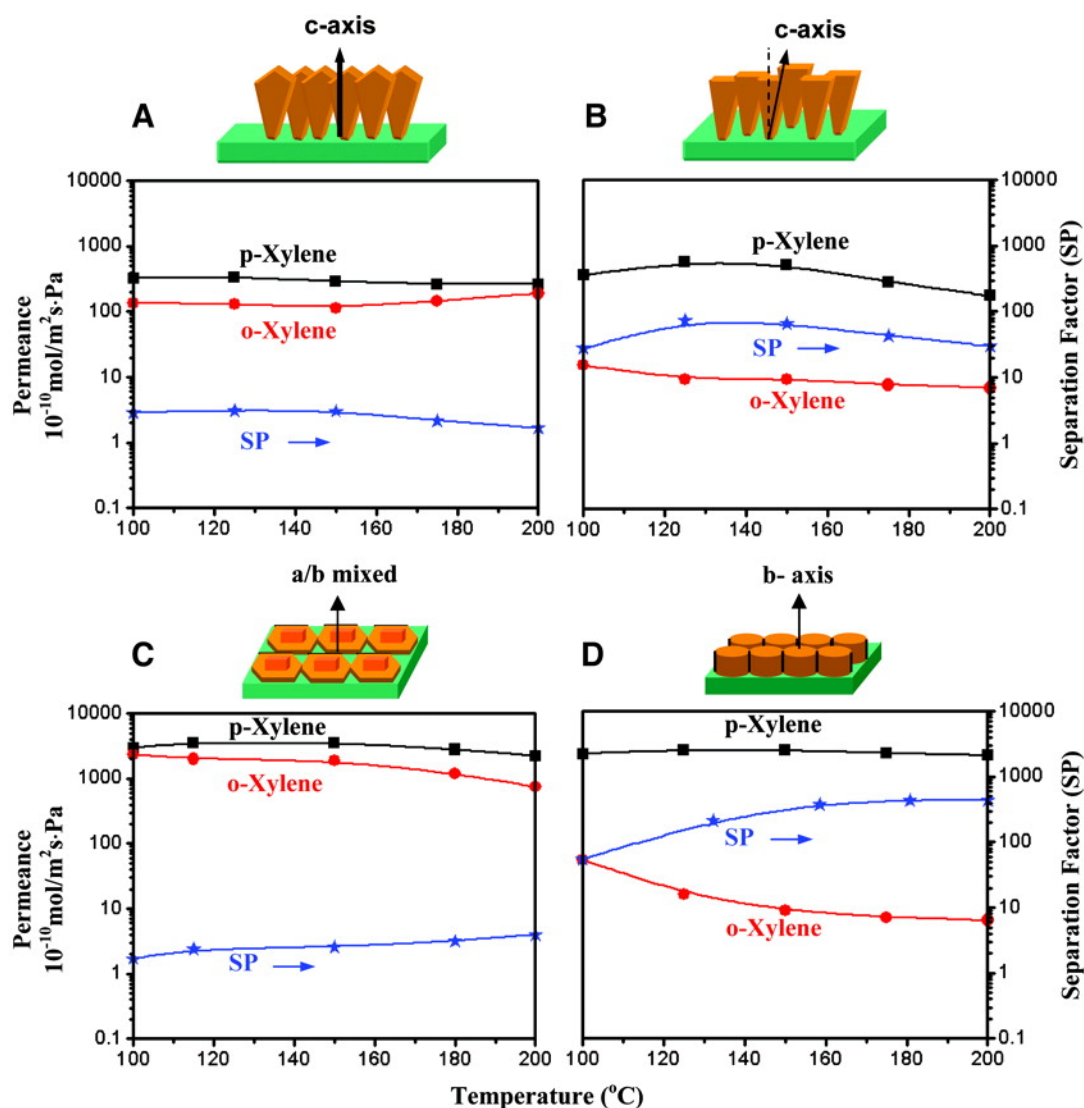


Figure 7. ZSM-5 membrane performance in xylene isomer separation (feed partial pressure of *p*-xylene and *o*-xylene are 0.45 kPa and 0.35 kPa, respectively): *p*-xylene, *o*-xylene permeance, and mixture separation factor (SP) in dependence on temperature for (A) *c*-oriented; (B) [h0h]-oriented; (C) *a*- and *b*-oriented; and (D) *b*-oriented film [226]. Reprinted with permission from AAAS.

Considering xylene isomerization in PBMRs, the extraction of the produced *p*-xylene from the reaction zone via zeolite membrane will shift the equilibrium and ensure selectivity enhancement and higher *p*-xylene yields.

In this context, Zhang *et al.* [161] tested silicalite-1/ α -Al₂O₃ zeolite membranes packed together with HZSM-5 catalysts in the isomerization of *m*-xylene to *p*-xylene, applying different packing methods: (i) by depositing the catalyst on the Al₂O₃ support on the opposite side of the membrane; and (ii) by packing it in the tube in contact with the membrane layer. The latter packing method turned out to be more effective for the studied reaction since it gave rise to higher *p*-xylene yield and selectivity than in conventional reactor ascribed to the immediate removal of *p*-xylene from the reaction zone due to molecular sieving effects. However, since the observed enhancement was found to be strongly dependent on the membrane flux, the authors pointed out the need of membranes exhibiting higher permeation

fluxes as a crucial requirement for the desired improvement of the membrane reactor efficiency. Moreover, in order to overcome the resistance diffusion through the catalytic bed, thus enhancing the permeation and intensifying the xylene isomerization, the authors suggested the use of catalytic membranes combining high-catalytic and separation efficiency. The performance of such catalytically active zeolite membranes will be discussed in more details in Section 5.

However, already with the intention to overcome the drawbacks of the supported zeolite films typically suffering from defects occurred during thermal stress causing diminished selectivity, van Dyk *et al.* [158] used a zeolite/alumina nanocomposite membrane of the pore-plugging type (zeolite crystals grown as film inside the pores of the porous tubular support) for the *m*-xylene isomerization in an extractor type zeolite membrane reactor. The tubular membrane used was equipped with the commercial xylene isomerization Pt catalyst, ISOXYL. The selectivity and the *p*-xylene yield of the conventional reactor were 58% and 21% respectively, demonstrating higher selectivity than the equilibrium value of 46% at the expense of the lower yield in comparison to the equilibrium yield of 24.9%. In contrast, by combining the retentate and permeate fractions para-selectivity of 65% and *p*-xylene yield of 23% were reported for the membrane reactor. More interestingly, operating in permeate-only mode, the authors managed to obtain *p*-xylene selectivity of 100%, however at the expense of low productivity. Recently, Daramola *et al.* [162,163] attempted to further reveal the advantages of the nanocomposite architecture over the “film-like” zeolite membranes, applying nanocomposite MFI-alumina membrane tubes prepared via pore-plugging synthesis packed with Pt-HZSM-5 catalyst for *m*-xylene isomerization. The effect of different reactor configurations, namely membrane reactor with catalyst bed packed either in the membrane lumen of the tube or between the membrane tube and the module shell, all operating in the temperature range of 523–673 K was evaluated [162]. Decreasing the operating temperature resulted in linear increase in the *p*-xylene yield for the PBMR configuration due to the effective extraction of *p*-xylene from the reaction zone. On the contrary, packing the catalyst bed outside the membrane layer reduced the effect of the membrane separation resulting in *p*-xylene yield leveling off with temperature decrease, due to diffusion limitations in the membrane substrate. Moreover, 100% selectivity to *p*-xylene was reported in the permeate-only mode, whereas the selectivity declined to nearly 48% when considering the retentate and permeate amounts. In a parallel study [163], the authors managed to synthesize higher quality membranes in terms of selectivity (*p*-xylene/*o*-xylene > 400). Accordingly, the membrane reactor outperformed the conventional one at the applied reaction temperature of 473 K. Furthermore, the same authors employed nanocomposite MFI-ceramic hollow fibre membranes for the xylene isomer separation, demonstrating nearly 30% *p*-xylene flux increase and reasonable selectivity [227]. Finally, the utilization of hollow fibre membranes in zeolite membrane reactors for the isomerization of xylene could offer the essential increase in the *p*-xylene permeation flux in order to overcome one of the considerable limitations of this reactor configuration in the competition with the existing technologies.

4.3. Selectivity Enhancement through Selective Distribution of Reactants or Removal of Intermediate Products

As reviewed in the previous section, the performance of zeolite membranes packed with catalysts is widely evaluated in membrane reactor configurations either for the selective extraction of products in equilibrium limited reactions or for extraction of products inhibiting the catalyst activity. All the efforts were to improve the conversion of the reactions studied. Besides, zeolite membranes could play a further role which is based on upstream separation of a component from the feed mixture or removal of intermediate products.

In this context, the principle of controlling reactants traffic from a feed mixture was demonstrated by Gora *et al.* [171]. In detail, the hydroisomerization of *n*-hexane was studied in single-pass operation with a membrane reactor combining silicalite-1/TiO₂/stainless steel tubular membrane and Pt-chlorinated catalyst. The silicalite-1 membrane was able to selectively permeate *n*-hexane due to its preferential adsorption from a feed mixture comprising *n*-hexane and 2-methyl-pentane with a purity of ~99% to the reaction zone, thus revealing to some extent the advantages of this reactor configuration. The same working group proposed a concept for industrial scale heptane hydroisomerization process combining two reactors and a zeolite membrane. According to the simulation data a total feed amount of 907 metric ton per day (existing C₅/C₆ isomerization technologies operate between 600 and 1200 metric ton per day) is processed forming 220 metric ton per day product with improved research octane number from 57 up to 92 [228]. After economical evaluation, the authors concluded a total investment cost of 40 million euros being significantly higher than the state of the art C₅/C₆ hydroisomerization process of UOP Penex/Molex plant with an investment of about 23 million euros. Approximately 42% of the total equipment cost belongs to the zeolite membrane.

Further example in this section is the application of membranes with sufficient selectivity for the permeation of valuable intermediate products for yield increase. In this context, the removal of the intermediate products from the reaction before consecutive reactions could be also considered as an example of residence time control. The concept was demonstrated by Piera *et al.* [229] based on zeolitic PBMRs in the oligomerization of *i*-butene, where MFI membranes packed with resin catalysts were used for the selective removal of the formed *i*-octene. In such a way, the formation of the undesired C₁₂ and C₁₆ hydrocarbons was decreased and at approximately 20 °C significant selectivity increase was obtained resulting in higher *i*-octene yields. Moreover, the authors explained the observed permselectivity to *i*-octene in a mixture of *i*-butene/*i*-octene by the preferential adsorption of *i*-octene and the thereby arising pore-blocking effect for the *i*-butane passage. Increasing the temperature contributed to higher *i*-butane conversion over 90%, however decreased the *i*-octene adsorption and thus the separation selectivity. As a result, the PBMR showed nearly the same conversion as the traditional reactor. Nevertheless, the yield in the PBMR still displayed an absolute enhancement between 20% and 30%.

5. Reaction Processing Using Permselective Catalytic Membrane Reactors (CMR)

So far, in the membrane-assisted reactor applications discussed up to now, the membrane used was inert. To put it differently, the membrane did not display any catalytic function, it showed only permselective properties depending on the dominant transport mechanism (see Section 2.1.) and the catalyst bed was a discrete part of the set-ups tested. The latter was either separated (see Section 2.3.) or packed in a direct contact to the zeolite membrane (PBMR, see Section 4.). In the majority of the applications of PBMRs the zeolite membranes were utilized either for selective product removal or for selective reactant supply. Similarly, in catalytic membrane reactors (CMR), where the zeolite membranes used display both catalytic activity and permselectivity, as shown schematically in Figure 8, e.g., dehydrogenation reactions [144], isomerization [159,160,164,165] and esterification reactions [167,230,231] have been investigated. However, it is the nature of the beast that not all the aforementioned reactions can be carried out in CMRs since zeolites simply are not the candidates of choice for all reactions.

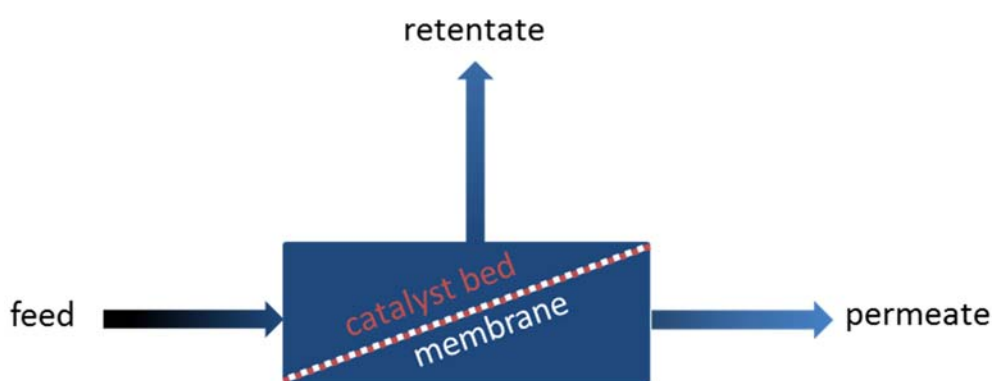


Figure 8. Schematic drawing of a catalytic membrane reactor (CMR).

Xiongfú and coworkers [144] studied the dehydrogenation of ethylbenzene to styrene using either Fe-ZSM-5 or Al-ZSM-5 zeolite membranes synthesized on porous α -Al₂O₃ tubes in CMRs. Generally, improved conversion compared to the conventional reactor configuration was obtained. However, the MFI membrane with incorporated Fe species showed better conversion compared to the Al-ZSM-5. The authors ascribed the observed effect on the one side to the better adsorption of ethylbenzene on the Fe-ZSM-5 membrane than on its counterpart Al-ZSM-5. On the other hand, the styrene adsorption on the Fe-ZSM-5 membrane was lower than on the Al-ZSM-5 membrane, thus ensuring lower carbon deposition on the membrane and higher ethylbenzene conversion.

The combination of catalytic and separation properties provided by the zeolite membranes has been also evaluated in isomerization reactions. Haag *et al.* [159] proposed the use of H-ZSM-5 zeolite membranes synthesized on top of stainless steel disks. Because of their intrinsic acidic properties, catalytically active sites for the isomerization of xylene were provided. The formed *p*-xylene was selectively separated from the other isomers due to the shape selective properties of the membrane. In contrast to conventional reactors packed with H-ZSM-5 catalyst, slightly enhanced conversions and selectivities were obtained with the membrane reactor configuration. However, the authors pointed out, that difficulties arise, when experimental data obtained in the two reactor configurations is compared

since the kinetic properties of the two catalytic materials are dissimilar. On the other hand, Tarditi *et al.* [160] carried isomerization reactions in a membrane reactor with an ion-exchanged Pt/H-ZSM-5 catalytic active membrane and in a membrane reactor equipped with a Ba-ZSM-5 zeolite membrane. Taken as a whole, the two membranes demonstrated reasonably enhanced *p*-xylene selectivity and yield compared to the conventional fixed-bed reactor packed with Pt/silica-alumina commercial catalyst. The *p*-xylene yield increased approximately 28% with the help of the Ba-ZSM-5 membrane, while the Pt-exchanged membrane achieved a bit lower *p*-xylene relative yield increase of 22% at 370 °C by feeding *m*-xylene. The *p*-xylene flux through the Ba-ZSM-5 membrane was found to be quite dependent on the Ba²⁺ concentration, where an increase in the ion concentration ensured higher *p*-xylene fluxes leading to better extraction from the reaction zone. Moreover, a ternary mixture (65% *m*-xylene, 14.5% *p*-xylene and 20.5% *o*-xylene) isomerization reaction in the fixed bed reactor as well as in the CMR with the fully exchanged Ba-ZSM-5 resulted in $2.86 \times 10^{-8} \text{ mol}\cdot\text{s}^{-1}$ and $3.74 \times 10^{-8} \text{ mol}\cdot\text{s}^{-1}$ *p*-xylene production, respectively confirming an increase of 31% in favor of the CMR at 370 °C. Due to experimental limitations, the authors evaluated theoretically using a transport model [232] the effect of the relevant for industrial application high pressure of around 1000 kPa and stated that the *p*-xylene production enhancement could be obtained by operation in CMR despite the selectivity decrease of the membrane at higher pressure. However, experimental evaluation would be still interesting for the verification of the theoretical observations.

Recently, Yeong [164] studied theoretically and experimentally the isomerization of *m*-xylene in acid-functionalized silicalite-1 catalytic membrane reactors. Propylsulfonic acid sites or arenesulfonic acid sites were provided to the inert silicalite-1 membranes via post-synthesis modifications. Higher isomerization activity was obtained with the arenesulfonic acid-functionalized membrane mainly ascribed to its higher acidity and more effective continuous removal of *p*-xylene. According to the results gained in this study, the acid-modified membranes turned out to be more effective in terms of *m*-xylene conversion and *p*-xylene productivity improvement compared with the membranes reported in early studies [158–161]. Moreover, the kinetic parameters reported in this study offer useful platform for further optimization of the catalytic membrane reactor design. Zhang *et al.* [165] prepared H⁺ ion-exchanged MFI zeolite membranes on $\alpha\text{-Al}_2\text{O}_3$ disc support. In earlier works of the same working group [161], the use of that very catalytic active zeolite membrane was proposed as an effective tool for achieving high permeation flux. The catalytic MFI zeolite membrane exhibited notable *p*-xylene selectivity of nearly 92%, however, at a significantly low *m*-xylene conversion of 6.5%, which was mainly ascribed to the limited number of active sites on disk-shaped membrane. Further on, the benefit of membrane reactor combining catalytic active and permselective boron substituted MFI zeolite membrane was demonstrated in the 1-butene double-bond isomerization [166]. Thereby, the incorporated boron in the framework generated Brønsted sites with low acid strength providing the catalytic selectivity. On the other side, the MFI membrane displayed selective permeation for *trans*-2 butene, giving rise to enhanced *trans/cis* ratio. So, in the retentate a *trans/cis* ratio between 1.4 and 1.5 being the same as the equilibrium ratio was found while in the permeate it was increased to a value of 2.2.

Bernal *et al.* [167] was the first who proposed the use of H-ZSM-5 zeolite membrane reactors in the continuous esterification. The idea behind was the lower diffusion resistance offered by a reactor configuration integrating the reaction and separation in once, which could assure the immediate removal of the formed products, thus displacing the equilibrium and giving rise to higher turnover. The catalytic

zeolite membrane reactor outperformed both the conventional fixed-bed reactor and the inert zeolite membrane reactor in the conversion of acetic acid with ethanol. The improved performance over the latter was mainly attributed to the absence of a diffusion step from the catalyst bed to the membrane surface. In this way, de la Iglesia *et al.* [231] coupled the catalytic activity of H-ZSM-5 and the selective water separation properties of modernite membranes in two-layered mordenite-ZSM-5 bi-functional membranes thus improving further the performance of the zeolite membrane reactor in the esterification of acetic acid with ethanol. In fact, much more advanced improvement could be reached by simultaneous control of the membrane thickness and the zeolite membrane composition.

Using composite catalytically active H-USY zeolite membranes Peters *et al.* [230] managed to couple reaction and separation for continuous esterification of acetic acid and butanol. Again, the authors pointed that optimization of the catalytic layer will contribute to further enhancement of the reactor performance.

6. Zeolite Membrane Coatings on Catalyst Particles

The potential of combining macroscopic units of zeolite membranes and catalysts in chemical reactors was described for diverse applications in the previous chapters. However, the desired improvements in reaction selectivity and productivity are not all of the important reaction parameters to be optimized. Relatively often zeolite membranes suffer from low permeation flux. To overcome this issue a sufficiently larger membrane area (related to the catalyst volume) is demanded which would lead to space velocities compatible to conventional reactors. The shape selectivity, often being the main property of zeolites membranes, could be used to design novel catalyst materials by adding this feature to conventional catalysts. In this regard, coating permselective zeolite membranes (shell) on particular catalysts (core) may provide selectivity and possible additional catalytic sites. Importantly, such encapsulated catalysts will offer a much larger membrane area per unit reactor volume than conventional membrane reactors. Figure 9 displays a scheme of a catalyst bed filled with such core-shell particles, whereas each of them can be understood as a kind of zeolite membrane microreactor.

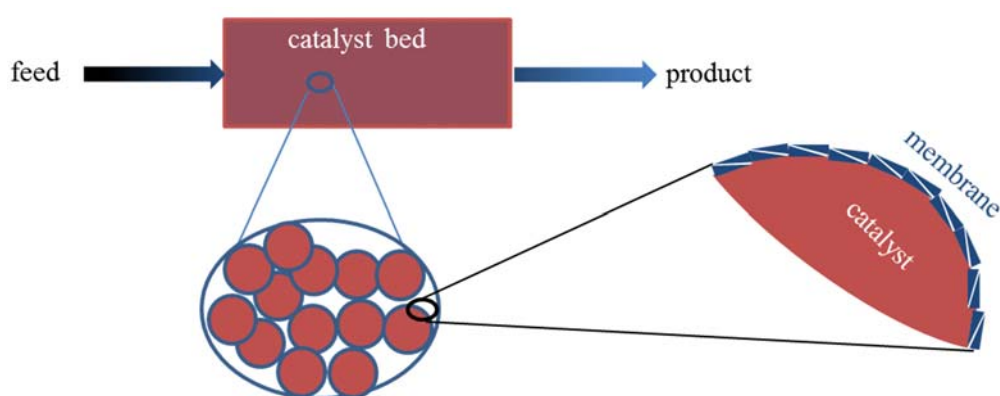


Figure 9. Catalyst bed filled with core-shell particles whereas each of them can be understood as zeolite membrane microreactor.

The application of core-shell catalysts as particle level membrane reactors follows the concept of the traditional membrane reactor so that they could be applied in either reactant-selective or product-selective reactions based on the diffusivities of the reaction components/products within the membrane. In the first case, the controlled supply of reactants could prevent undesirable reaction, due to the selective permeation through the zeolite membrane to the catalyst core. Additionally, the zeolite shell could act as protective barrier against impurities or poisons, e.g., in a direct internal reforming-molten carbonate fuel cell [233]. In the second case, the selective removal of the desired product could shift the equilibrium in thermodynamically limited reactions and enhance the selectivity. Alternatively, the zeolite shell can provide catalytic properties and so encapsulated catalyst can be applied as catalytic membrane e.g., in Fischer-Tropsch synthesis reactions [234]. The reaction selectivity is predetermined to some extent by the membrane synthesis conditions since they affect the membrane thickness and quality. The concept of zeolite membrane coatings on particles was inspired mostly by the pioneering work of Puil *et al.* describing the coating of TiO₂-supported platinum catalyst particles by a silicalite layer for hydrogenation reactions [235] as well as the preparation procedure of MFI and BEA type coatings on preshaped α -alumina supports applied in alkylation reactions [236].

So far, different synthesis techniques have been reported for the preparation of zeolite coated catalyst. Generally, hydrothermal synthesis is applied for the preparation of the zeolite membrane enwrapping the core catalyst. Bouizi *et al.* evaluated the factors governing the formation of core-shell zeolite-zeolite composites by reversing the negative charge of the crystals with 0.5 wt. % aqueous solution of a polycation agent prior to seeding and secondary growth technique [237]. The authors concluded that successful synthesis could be observed for materials displaying compatible framework compositions and close crystallization conditions. Moreover, in order to induce the zeolite matrix seeding turned out to be a crucial step in the preparation technique. On the contrary, a H- β zeolite was coated directly on the surface of Co/Al₂O₃ by one-step hydrothermal synthesis [238,239]. Alternatively, liquid membrane crystallization being a modified vapor transport method was proposed as economic, environmental and highly effective method for synthesis of zeolite-encapsulated catalysts [240]. Furthermore, physical coating was suggested for easy scalable synthesis where the required high temperature and alkaline conditions during hydrothermal synthesis were excluded [241–243]. Recently, steam-assisted crystallization process was recommended as an efficient method for capsuled catalysts preparation [244].

A brief overview of recent publications dealing with zeolite capsuled catalysts is given in Table 2.

Table 2. Overview of the application of packed bed reactor consisting of permselective membrane coated catalyst particles reported in the literature.

Reaction	Reactor Type	Feed	Operating Conditions	Core-Shell Catalyst	X_{mixed} (%)	X_{MR} (%)	References	
					S_{mixed} (%)	S_{MR} (%)		
					Y_{mixed} (%)	Y_{MR} (%)		
Disproportionation of toluene	PLMR product selective	toluene	723–823 K $p = 101.3$ kPa WHSV = 0.1 h ⁻¹	silicalite coated on silica-alumina catalyst	$S_{p\text{-xylene}} = 22$	$S_{p\text{-xylene}} > 91$	[245]	
Alkylation of toluene	PLMR product selective	toluene, methanol	673 K	silicalite coated on H-ZSM-5 crystals with different Si/Al ratios	$X_{\text{toluene}} = 63$ $S_{p\text{-xylene}} = 40$	$X_{\text{toluene}} = 42$ $S_{p\text{-xylene}} > 99.9$	[246,247]	
Hydro-formylation of 1-hexene	batch type reactor product selective	1-hexene, carbon monoxide, hydrogen	130 °C $H_2/CO = 1$	silicalite-1 coated on Pd-Co/activated carbon	$X = 75.7$ $S_{\text{hexan}} = 13.3$ $S_{\text{isomer}} = 15.4$ $S_{i\text{-hept.}} = 37.1$ $S_{n\text{-nept.}} = 33.1$	$X = 54$ $S_{\text{hexan}} = 28.3$ $S_{\text{isomer}} = 21.9$ $S_{i\text{-hept.}} = 13.9$ $S_{n\text{-nept.}} = 35.9$	[248]	
Hydrogenation of linear and branched alkenes	PLMR reactant selective	1-hexene, 3,3-dimethyl-but-1-ene	323–373 K $p = 101.3$ kPa	silicalite-1 coated on Pt/TiO ₂ particles	$X_{1\text{-hex}} > 90$ $X_{3,3\text{-DMB}} > 90$ $S = 1\text{--}1.2$	$X_{1\text{-hex}} > 90$ $X_{3,3\text{-DMB}} < 10$ $S = 12\text{--}20$	[249,250]	
Oxidation of CO and <i>n</i> -butane	PLMR reactant selective	air, carbon monoxide and <i>n</i> -butane	483 K $p = 101.3$ kPa	zeolite-4A coated on spherical Pt/ γ -Al ₂ O ₃ particles (two-steps hydrothermal synthesis)	$X_{n\text{-butane}} = 95$ $X_{CO} = 93$	$X_{n\text{-butane}} = 0$ $X_{CO} > 90$	[251]	
Shape-selective hydrogenation of xylene isomers	PLMR reactant selective	<i>p</i> -/ <i>o</i> -xylene or <i>p</i> -/ <i>m</i> - xylene	473 K $p = 1.0$ MPa WHSV = 1.0 h ⁻¹	silicalite-1 coated on Pt/Al ₂ O ₃ pellets	-	$S_{p/o} = 17$ $S_{p/m} = 13.6$	[252]	

Table 2. Cont.

Reaction	Reactor Type	Feed	Operating Conditions	Core-Shell Catalyst	X_{mixed} (%)	X_{MR} (%)	References	
					S_{mixed} (%)	S_{MR} (%)		
					Y_{mixed} (%)	Y_{MR} (%)		
Steam reforming of methane and toluene	PLMR reactant selective	methane or toluene, steam, helium	780–840 °C $p = 1$ bar $\text{CH}_4/\text{H}_2\text{O} = 1$ $\text{H}_2\text{O}/\text{C}_7\text{H}_8 = 7$	H β zeolite coated on Ni/Mg/Ce _{0.6} Zr _{0.4} O ₂ pellets	X_{CH_4} increases with temperature up to ~20 $X_{\text{C}_7\text{H}_8} \sim 58$	X_{CH_4} increases with temperature up to ~30 $X_{\text{C}_7\text{H}_8} \sim 22$	[242]	
Direct synthesis of middle <i>i</i> -paraffins	PLMR catalytic	hydrogen and carbon monoxide	533 K $p = 1.0$ MPa $\text{H}_2/\text{CO} = 2$	H-ZSM-5 coated on Co/SiO ₂ pellets with different size	$X_{\text{CO}} = 93.6$ $S_{\text{CH}_4} = 16.9$ $S_{\text{CO}_2} = 8$ $C_i/C_n = 0.49$	$X_{\text{CO}} = 89.1$ $S_{\text{CH}_4} = 22.4$ $S_{\text{CO}_2} = 6.9$ $C_i/C_n = 0.74$	[234,253,254]	
Direct synthesis of <i>i</i> -paraffins	PLMR catalytic	hydrogen and carbon monoxide	533 K $p = 1$ MPa $\text{H}_2/\text{CO} = 2$	H- β zeolite coated on Co/Al ₂ O ₃ catalyst pellets with different size	$X_{\text{CO}} = 80.8$ $S_{\text{CH}_4} = 16.6$ $S_{\text{CO}_2} = 3.9$ $C_i/C_n = 1.4$	$X_{\text{CO}} = 74.3$ $S_{\text{CH}_4} = 13.6$ $S_{\text{CO}_2} = 2.7$ $C_i/C_n = 2.3$	[239]	
Direct synthesis of <i>i</i> -paraffins	PLMR catalytic	hydrogen and carbon monoxide	533 K $p = 1$ MPa $\text{H}_2/\text{CO} = 2$	H-ZSM-5 coated on Ru/SiO ₂ catalyst pellets with different size	$X_{\text{CO}} = 82.1$ $S_{\text{CH}_4} = 17.1$ $S_{\text{CO}_2} = 5$ $C_i/C_n = 0.42$	$X_{\text{CO}} = 81.7$ $S_{\text{CH}_4} = 20.5$ $S_{\text{CO}_2} = 6.1$ $C_i/C_n = 1.5$	[255]	
Direct synthesis of <i>i</i> -paraffins	PLMR catalytic	hydrogen and carbon monoxide	533 K $p = 1$ MPa $\text{H}_2/\text{CO} = 2$	H-ZSM-5 coated on Pd/SiO ₂	-	$X_{\text{CO}} = 86.1$ $S_{\text{CH}_4} = 37.4$ $S_{\text{CO}_2} = 7.0$ $C_i/C_n = 1.88$	[256]	
Direct synthesis of middle <i>i</i> -paraffins	PLMR catalytic	hydrogen and carbon monoxide	573 K $p = 1.0$ MPa $\text{H}_2/\text{CO} = 1$	H-ZSM-5 crystalized on fused-iron catalyst pellet	$X_{\text{CO}} = 96.7$ $S_{\text{CH}_4} = 12.8$ $S_{\text{CO}_2} = 44.7$ $C_i/C_n = 2.31$	$X_{\text{CO}} = 96.9$ $S_{\text{CH}_4} = 8.7$ $S_{\text{CO}_2} = 33.9$ $C_i/C_n = 4.17$	[257]	

Table 2. Cont.

Reaction	Reactor Type	Feed	Operating Conditions	Core-Shell Catalyst	X_{mixed} (%)	X_{MR} (%)	References	
					S_{mixed} (%)	S_{MR} (%)		
					Y_{mixed} (%)	Y_{MR} (%)		
Synthesis of gasoline-range <i>i</i> -paraffins	PLMR catalytic	hydrogen and carbon monoxide	483–533 K $p = 2.0$ MPa $H_2/CO = 2$ GHSV = 1000 h ⁻¹	H-ZSM-5 coated on CoZr catalyst particles	$X_{CO} = 97.4$	$X_{CO} = 82.3$	[258]	
					$S_{CH_4} = 16$	$S_{CH_4} = 14.8$		
					$S_{18+} = 5.6$	$S_{18+} = 0.3$		
					$S_{i-C_5-11} = 16.7$	$S_{i-C_5-11} = 24.7$		
Direct synthesis of light <i>i</i> -paraffins	PLMR catalytic	hydrogen and carbon monoxide	553 K $p = 1$ MPa $H_2/CO = 2$	H-ZSM-5 zeolite coated on Co/SiO ₂	$X_{CO} = 98.5$	$X_{CO} = 99.1$	[259]	
					$S_{CH_4} = 23.7$	$S_{CH_4} = 20.1$		
					$S_{CO_2} = 16$	$S_{CO_2} = 18.2$		
					$S_n = 53.4$	$S_n = 47.6$		
					$S_i = 36.2$	$S_i = 43.8$		
Direct synthesis of middle <i>i</i> -paraffins	PLMR catalytic	hydrogen and carbon monoxide	300 °C $p = 1$ MPa $H_2/CO = 1$	H-ZSM-5 coated on Fe/SBA-15	$X_{CO} = 63.9$	$X_{CO} = 57.6$	[244]	
					$S_{CO_2} = 43.8$	$S_{CO_2} = 37.3$		
					$S_{CH_4} = 19.2$	$S_{CH_4} = 15.3$		
					$S_n = 56$	$S_n = 36.7$		
					$S_i = 33.9$	$S_i = 46.5$		
Direct synthesis of <i>i</i> -paraffins	PMLR catalytic	carbon monoxide, hydrogen	280 °C $p = 1$ MPa $H_2/CO = 1$	Silicalite-1 and H-ZSM-5 coated on Fe/SiO ₂ dual-membrane coated catalyst	$X_{CO} = 60$	$X_{CO} = 54.8$	[260]	
					$S_{CO_2} = 29.9$	$S_{CO_2} = 33.8$		
					$S_{CH_4} = 7$	$S_{CH_4} = 14.9$		
					$S_i = 12.9$	$S_i = 29.8$		
Dimethyl ether direct synthesis	PLMR catalytic	hydrogen, carbon monoxide, carbon dioxide and argon	523 K $p = 5.0$ MPa	H-ZSM-5 coated on Cu/ZnO/Al ₂ O ₃	$X_{CO} = 58.07$	$X_{CO} = 30.4$	[261]	
					$S_{MeOH} = 57.29$	$S_{MeOH} = 21.43$		
					$S_{DME} = 40.51$	$S_{DME} = 78.57$		
Dimethyl ether direct synthesis	PLMR catalytic	hydrogen, carbon monoxide, carbon dioxide and argon	573-623 K $p = 5.0$ MPa	Double layer H-ZSM-5/Silicalite-1 membrane coated on Cr/ZnO core catalyst	$X_{CO} = 45.16$	$X_{CO} = 9.53$	[262]	
					$S_{MeOH} = 12.12$	$S_{MeOH} = 21.23$		
					$S_{DME} = 0.47$	$S_{DME} = 50.84$		

Table 2. Cont.

Reaction	Reactor Type	Feed	Operating Conditions	Core-Shell Catalyst	X_{mixed} (%)	X_{MR} (%)	References
					S_{mixed} (%)	S_{MR} (%)	
					Y_{mixed} (%)	Y_{MR} (%)	
Dimethyl ether direct synthesis	PLMR catalytic	hydrogen, carbon monoxide, carbon dioxide, argon	523 K $p = 5.0$ MPa	Double layer H-ZSM-5/Silicalite-1 membrane coated on Pd/SiO ₂ core catalyst	$X_{\text{CO}} = 12.84$	$X_{\text{CO}} = 9.48$	[263]
					$S_{\text{CH}_4} = 1.47$	$S_{\text{CH}_4} = 16.8$	
					$S_{\text{MeOH}} = 16.51$	$S_{\text{MeOH}} = 4.76$	
					$S_{\text{DME}} = 48.40$	$S_{\text{DME}} = 68.70$	
Dimethyl ether direct synthesis	PLMR catalytic	hydrogen, carbon monoxide, carbon dioxide, argon	350 °C $p = 5$ MPa	SAPO-46 zeolite shell encapsulated Cr/ZnO catalyst	$X_{\text{CO}} = 4.7$	$X_{\text{CO}} = 6.9$	[243]
					$S_{\text{CH}_4} = 3.7$	$S_{\text{CH}_4} = 4.7$	
					$S_{\text{MeOH}} = 71.7$	$S_{\text{MeOH}} = 52.2$	
					$S_{\text{DME}} = 16.5$	$S_{\text{DME}} = 37.0$	
Dimethyl ether direct synthesis	PLMR catalytic	hydrogen, carbon monoxide, carbon dioxide, argon	250 °C $p = 5$ MPa	SAPO11 coated on Cu/ZnO/Al ₂ O ₃	$X_{\text{CO}} = 64.9$	$X_{\text{CO}} = 92$	[241]
					$S_{\text{MeOH}} = 51.4$	$S_{\text{MeOH}} = 9.2$	
					$S_{\text{DME}} = 46.6$	$S_{\text{DME}} = 90.3$	
					$Y_{\text{DME}} = 30.2$	$Y_{\text{DME}} = 83.1$	
Carbon dioxide hydrogenation to dimethyl ether	PLMR	carbon dioxide and hydrogen	270 °C $p = 3.0$ MPa SV = 1800 mL·g ⁻¹ ·cat ⁻¹ ·h ⁻¹ H ₂ /CO = 3	H-ZSM-5 coated on CuO-ZnO-Al ₂ O ₃ nanoparticles	$X_{\text{CO}_2} = \sim 24$	$X_{\text{CO}_2} = 48.3$	[264]
					$S_{\text{DME}} = \sim 26$	$S_{\text{DME}} = 48.5$	
					$Y_{\text{DME}} = \sim 6$	$Y_{\text{DME}} = 23.4$	

6.1. Application in Reactant-Selective or Product-Selective Reactions (Non-Catalytic Membranes)

Nishiyama *et al.* [249] coated a silicalite-1 membrane on spherical Pt/TiO₂ particles applying a hydrothermal synthesis and obtained core-shell catalysts displaying reactant selectivity due to the adsorption-based permselective properties of the zeolite membrane. The authors impregnated the beforehand prepared Pt/TiO₂ with a solution of 0.4 wt. % cationic polyethyleneimine in order to charge its surface positively and thus facilitate the adsorption of the silicalite-1 seeds by subsequent immersing in 1.0 wt. % silicalite-1 seed solution. The final membrane zeolite coating crystallization was performed in a closed vessel at 180 °C for 24 h. Figure 10 depicts the SEM images revealing the dense uniformly formed silicalite-1 shell with a thickness of approximately 40 μm on the surface of the core Pt/TiO₂ spheres.

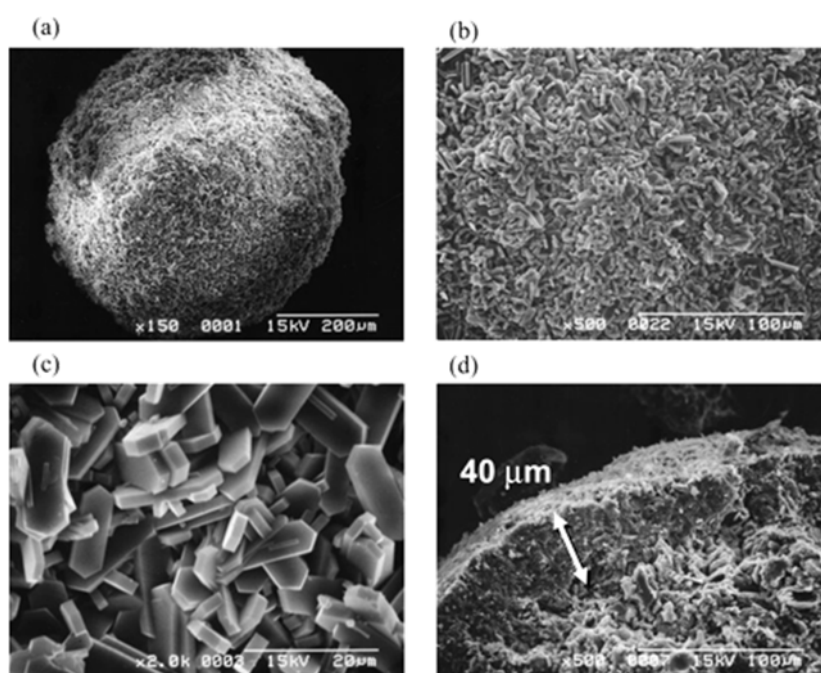


Figure 10. SEM images of Pt/TiO₂ particles coated with silicalite-1. Reprinted with permission from [249]. Copyright (2004) American Chemical Society.

The thereby prepared silicate-1 membrane layer permeated preferentially the reactant 1-hexene from a mixture comprising 1-hexene and dibranched 3,3-dimethylbut-1-ene towards the Pt/TiO₂ catalyst leading to improved hydrogenation selectivities for 1-hexene. At a reaction temperature of 323 K the ratio of hydrogenation selectivities for the linear/branched alkene mixture was between 12 and 20. At 373 K the selectivity range was increased to 18–30 revealing the positive impact of the selective permeation of 1-hexene across the silicalite-1 membrane towards the Pt/TiO₂ particles in principle and the temperature influence in addition. By applying a hydrothermal synthesis including two crystallization steps, the same working group prepared thinner silicate-1 membranes with improved quality. In that case, the authors adopted first a short crystallization step under rotation in order to increase the number density of crystal nuclei at the particle surface responsible for the small crystal size. Then, a thinner membrane was crystallized in a second synthesis at 453 K for 48 h without rotation. The so prepared core-shell catalyst exhibited even higher hydrogenation selectivities (selectivity of 1-hexene/3,3-dimethylbut-1-ene at

323 K of 35 and 80 at 373 K) due to higher permselectivity of the linear/branched alkene mixture through the membrane revealing the enormous impact of the membrane quality in terms of the thickness on the reaction rate [250]. Moreover, it was shown that due to the coating procedure the reaction rate of the process was changed from kinetic-controlled to diffusion-controlled, pointing once again that the permeation of 1-hexene and 3,3-dimethylbut-1-ene is the rate controlling step in the hydrogenation reaction. In addition, reduced catalyst deactivation ascribed to the catalyst protection against poisoning impurities from the feed by the zeolite membrane was reported.

The concept of reactant selectivity was further demonstrated by Zhong *et al.* [251] by applying defect-free zeolite-4A coated on Pt/ γ -Al₂O₃ particles prepared via two-step hydrothermal synthesis in a model oxidation reaction of CO and *n*-butane mixture. The permeation of *n*-butane was obviously restrained due to sieving effects, so that only CO and O₂ were able to pass the zeolite membrane and react in the catalyst core. The authors pointed out that the membrane coated catalyst might be attractive for applications where the hydrocarbon feed streams contain a trace amount of CO and it should be removed in order to prevent the catalyst poisoning. Ren *et al.* [265] suggested the encapsulation of noble metal particles with protective, size-selective zeolite shells as an effective strategy to overcome deactivation problems [266,267] occurring during liquid phase reactions, e.g., for targeted production of fine or intermediate chemicals. As an example the selective oxidation of alcohols was chosen. The significantly improved selectivity and the core catalyst protection (Ag and Pt nanoparticles) by a silicalite-1 membrane coating compared to commercial catalysts was attributed to selective permeation through the zeolite membrane. Under those circumstances, the diffusion of large reactants and poison molecules in the reaction environment was restricted due to the shape selectivity of the membrane resulting respectively in retention of the catalytic activity. Moreover, as the ICP-AES analysis revealed, almost no Pd leaching from the core-shell catalyst after 6 cycles of recycling was observed, pointing out the benefit of coating on the reusability of the catalyst.

The application of zeolite membranes being quite lucrative for shape-selective hydrogenation of xylene isomers was also reported. As discussed in Section 4.2., MFI zeolites are considered as appropriate candidates for the preparation of membranes, since their pore diameters approximates the size of *p*-xylene, while the bulkier *m*- and *o*-xylene isomer molecules cannot pass the material due to sterical hindrance resulting in significant permselectivity of *p*-xylene over the other isomers. Coming back, the combination of molecular sieving and hydrogenation of xylene isomers was demonstrated over silicalite-1 coated Pt/Al₂O₃ catalysts [252]. An excellent para-selectivity was achieved, whereas the hydrogenation of the *o*- and *m*-xylene isomers to 1,3-dimethylcyclohexane and 1,2-dimethylcyclohexane was suppressed since almost exclusively *p*-xylene was passing the membrane to reach the catalytic active sites in the core in order to hydrogenate and produce 1,4-dimethylcyclohexane which diffused across the membrane to the product site.

More recently, Zhang *et al.* [268] has chosen a porous metal-organic framework (MOF), namely zeolitic imidazolate framework-8 (ZIF-8), as a shell enwrapping the Pd/ZSM-5 core. A layer by layer self-assembly of polyelectrolyte was used to overcome the incompatibility between the materials prior to the two-step temperature synthesis employing ice bath for the initial nucleation and temperature of 30 °C for further crystallization. The catalytic performance and molecular-size-selectivity of the core-shell structure was evaluated in hydrogenation of 1-hexene and cyclohexene. By applying 1-hexene as a reactant, full conversion was achieved with *n*-hexane being the only product displaying

similar performance as the not enshrouded Pd/ZSM-5 catalyst. On the other hand, the diffusion of cyclohexane into the core catalyst was significantly restrained since its molecular size exceeded the aperture size of ZIF-8 resulting in decreased conversion compared to the Pd/ZSM-5 catalyst. However, the observed conversion of 25.1% was obviously the result of cracks in the ZIF-8 shell.

The controlled traffic of reactants providing improved reforming selectivity was demonstrated very recently by Cimenler [242] in the steam reforming of CH_4 and C_7H_8 where the latter represents a model for tar impurity in feed. Applying H- β zeolite membrane shell on the steam reforming Ni/Mg/Ce_{0.6}Zr_{0.4}O₂ catalyst led to decreased C_7H_8 conversion compared to the uncoated catalyst exemplifying the molecular-size selective properties of the membrane. The authors suggested that the shape selective effect could be boosted either by preparing thicker shell membranes or by using dealuminated zeolite.

The concept of selective product removal was illustrated for the selective formation of *p*-xylene in the disproportionation of toluene [245]. Thereby, high *p*-xylene selectivity was obtained due to the selective permeation of the produced *p*-xylene through the silicalite membrane coated on the silica-alumina catalyst causing an equilibrium shift. Even so, the activity of the coated catalyst was lower than that of the non-coated catalyst as a direct result of the relatively thick membrane which was limiting the products diffusion.

Another interesting approach described in the literature is the enwrapping of active zeolite crystals with zeolite membranes. The proposed model for the formation of the silicalite-1 layer on ZSM-5 crystals is illustrated in Figure 11 [269]. Silicalite-1 crystals grow on the ZSM-5 crystal surface perpendicular to the *a* and *c* axes under hydrothermal conditions at 453 K for 24 h without agitation. In this context, the benefit of silicalite zeolite membrane coated on H-ZSM-5 crystals was evidenced for the selective *p*-xylene formation in alkylation of toluene with methanol [246,247,269]. The obtained para-selectivity of up to 99.9% was attributed to the suppressed further isomerization of *p*-xylene since the silicalite coating reduced the acid sites on the external surface of the H-ZSM-5 catalyst.

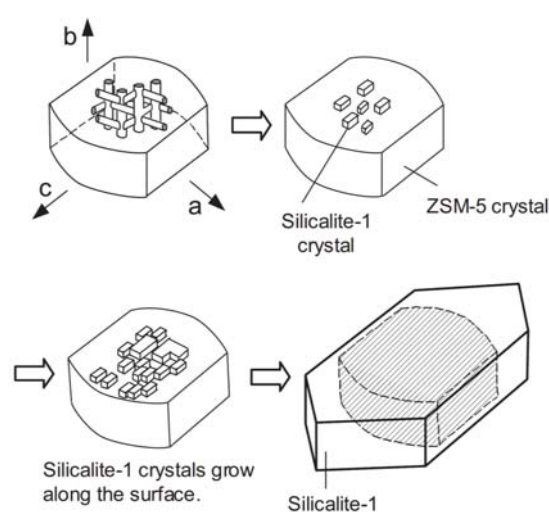


Figure 11. Graphical illustration of the proposed model for the formation of a silicalite-1 layer on a ZSM-5 crystal. Reprinted with permission from [269]. Copyright (2005) John Wiley and Sons.

The toluene conversion remained high even after the coating suggesting catalyst protection against coke formation on the one side and evidencing the positive effect of the thin membrane layer over the crystals on the other side if compared to the relatively thick membrane reported early by Nishiyama *et al.* [245]. Moreover, FE-SEM and TEM screening indicated that the pores of silicalite-1 were directly connected to the pores of H-ZSM-5 considered as the main reason for the obtained high selectivity and activity [247]. Additionally, the effect of the H-ZSM-5 crystal size was studied revealing a slight decline in the *para*-selectivity with increasing crystal size, thus pointing out the severity of silicalite layer defect-free growth on larger crystals. Recently, MFI-type zeolite containing aluminum and gallium within its framework (GaAlMFI) was coated with silicalite-1 and applied in propane aromatization reaction [270]. Thereby, the *para*-selectivity was increased to 80% in comparison to *para*-selectivity of 57% for the GaAlMFI catalyst without the silicalite-1 coating, remaining however lower than the respective *para*-selectivity in toluene alkylation over silicalite-1/H-ZSM-5 reported above. Going one step further, the same working group evaluated the effect of the synthesis conditions in terms of alkali concentration in the synthesis solution and proton-exchange procedure on the preparation of silicalite-1 coated GaAlMFI [271]. In this context, low TPAOH concentration was reported to improve the *para*-selectivity due to decreased number of acid sites on the external surface of the catalyst. On the other hand, the *para*-selectivity was significantly decreased by repeating the proton-exchanged procedure since Ga and Al species were removed from the framework leading to the formation of non-selective sites on the catalyst surface. Interestingly, during *n*-butane and propane aromatization, the silicalite-1/GaAlMFI performed better in the former case attributed by the authors to the higher formation of naphthalene and its derivatives during the propane aromatization.

Very recently, Zhou *et al.* [272] examined the oriented growth of MFI zeolite shells on ZSM-5 crystals. Ammonia as surface modifier was applied for the pretreatment of the catalyst core in order to facilitate the formation of *b*-oriented MFI film. The shape-selective core-shell catalyst was evaluated in toluene methylation experiments, demonstrating optimized selectivity and stability against the common ZSM-5 zeolite. However, due to incorporation of small amount of aluminum in the framework near the external surface of the shell, the obtained *para*-selectivity was lower than that in the previous reports [245,246].

Silicalite zeolite membrane was also employed as membrane coating over Pd-Co/activated carbon catalysts for the hydroformylation of 1-hexene with syngas [248]. The silicalite membrane decreased the 1-hexene conversion, while higher *n*- to *i*-heptanal ratios were reported due to the spatial confinement of the zeolite membrane pore channels limiting the diffusion of the *i*-heptanal out of the core. By increasing the membrane thickness via second hydrothermal synthesis, and thus complicating the diffusion of the reactants into the core catalyst, a further decrease in the 1-hexene conversion was observed. However, the ratio of the aldehyde products experienced sharp increase due to the rise in the *n*-heptanal selectivity predominated by the membrane thickness.

6.2. Application as Catalytic Membranes

A further extensively studied area for application of encapsulated catalysts with zeolite membrane as a shell possessing catalytic properties represent the Fischer-Tropsch synthesis reactions. The Fischer-Tropsch synthesis converts syngas (mixture of CO and H₂) to aliphatic hydrocarbons. Typical

mixtures of linear, branched and oxygenated hydrocarbons, linear paraffins and α -olefins are the main products [273]. As fuel, they are appropriate only as diesel, while for the use as synthetic gasoline, they must be further hydrocracked and isomerized to branched, light hydrocarbons. In industrial term, the direct production of *i*-paraffins from syngas is of great interest. Physical mixture of Fischer-Tropsch catalyst and zeolite catalyst providing active site for the two reactions was proposed in the literature for the direct synthesis of *i*-paraffins rich hydrocarbons [274–277]. The Fischer-Tropsch catalyst offers thereby the active sites for the conversion of syngas to linear hydrocarbons which then undergo hydrocracking and isomerization to the desired branched hydrocarbons on the acidic sites of zeolites. Even so, a major problem by applying catalyst mixtures is the random distribution of the active sites. The linear hydrocarbons formed on the active sites of the Fischer-Tropsch catalyst can leave the reaction zone without reaching the active sites of the zeolite for further reforming resulting in low selectivity.

In order to improve the migration of the linear hydrocarbons to the active sites of the zeolite, catalysts with core-shell structure have been proposed as a more efficient alternative and extensively studied by the working group of Tsubaki. Accordingly, the selectivity could be significantly improved since the intermediate products are enforced to pass a zeolite membrane in order to desorb from the Fischer-Tropsch catalyst experiencing a higher possibility for further conversion so as to yield the desired product. In detail, the working group of Tsubaki [234,253,254] coated H-ZSM-5 membranes on preshaped Co/SiO₂ pellets and evaluated their performances in *i*-paraffins synthesis from syngas. Thereby, syngas permeated through the membrane to the core catalyst and reacted to straight-chain hydrocarbons which were then hydrocracked and isomerized while passing the zeolite channels as show schematically in Figure 12.

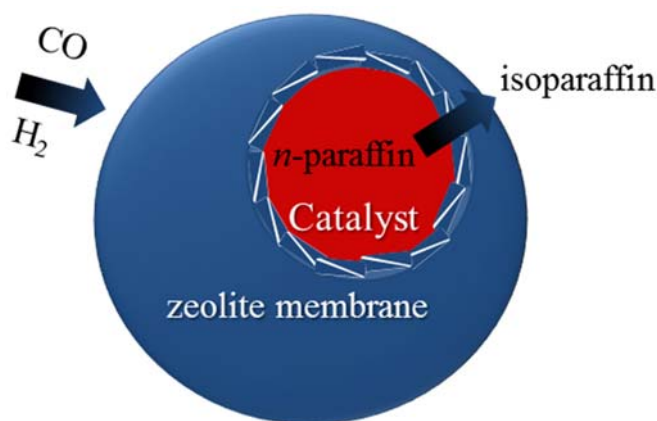


Figure 12. Schematic drawing of a core/shell catalyst in the synthesis of *i*-paraffins from syngas, where the core catalyst is responsible for the Fischer-Tropsch synthesis and the zeolite membrane for the further hydrocracking and isomerization of *n*-paraffins to *i*-paraffins.

The formation of C₁₀₊ hydrocarbons was completely suppressed. Moreover, an indication was given that the size of the pellets affects the properties of the capsule catalyst since coating smaller pellets of Co/SiO₂ resulted in a higher *i*-paraffin/*n*-paraffin ratio. However, the prepared core-shell catalysts showed higher methane selectivity compared to the mechanical mixture of Co/SiO₂ and H-ZSM-5 due to the lower diffusion efficiency for CO caused by the different diffusion rates of CO and H₂ in the zeolite pores. The same working group managed to coat H-beta membranes onto the surface of Co/Al₂O₃

pellets and observed excellent performance for the direct synthesis of *i*-paraffins [239]. Not only the formation of C₁₂₊ hydrocarbons was completely suppressed, but also lower methane selectivity was recorded due to the hydrophilicity provided by the zeolite coating. The presence of water favors higher CO concentrations passing the membrane leading to decreased H₂/CO ratios in the catalyst core and thus to lower CH₄ selectivity.

Based on early literature reports revealing the improved selectivity of C₅₊ hydrocarbons due to addition of Zr as promotor to Co-based Fischer-Tropsch catalysts [278–280], Huang *et al.* [258] prepared H-ZSM-5 enwrapped CoZr catalyst particles and evaluated their activity for the direct synthesis of gasoline-ranged *i*-paraffins. The authors employed aluminum isopropoxide as Al source during membrane synthesis and confirmed its beneficial impact with respect to the minimized coke deposition. The core-shell catalyst exhibited lower activity compared to the solo CoZr catalyst or the physical mixture of CoZr and zeolite powder. Nevertheless, lower methane selectivity and facilitated selectivity towards *n*- and *i*-C_{5–11} hydrocarbons were reported.

Significantly decreased methane selectivity compared to Co-based core catalysts was observed on Fe-based catalyst pellets coated with H-ZSM-5 zeolite membranes [257]. Fused iron-based capsule catalyst covered with H-modernite zeolite-shell, synthesized without organic template exhibited increased CO conversion and nearly 8 times higher *i*-paraffin/*n*-paraffin ratio compared to the core catalyst [281]. However, since the fused iron (FI) catalyst is lacking in surface hydroxyl groups, its surface was modified by initial treatment with a solution of an organic adhesive, 3-aminopropyltrimethoxysilane (APTES), and ethanol as shown in Figure 13. In the next step, the pretreated catalyst was immersed in a silicalite-1/ethanol solution so that the surface could adsorb silicalite-1 since this layer provides Si-OH groups for sticking the zeolite shell. In the final step, modernite (MOR) shell was crystallized without the use of template at 180 °C for 48 h under rotation. The obtained HMOR/FI core/shell catalyst exhibited increased CO conversion and higher selectivity to middle *i*-paraffins than the other catalyst as compared in Figure 13. Despite its remarkable performance, the necessity of product diffusion improvement was pointed out.

Very recently, Xing *et al.* [244] applied SBA-15 as support for iron-based catalyst cores which were micro-capsuled by H-ZSM-5 with sizes of about 1–2 μm. The mesoporous silica enables high activity and stability of the catalyst cores thanks to confinement effects already discussed in the literature for Fischer-Tropsch synthesis reactions [282–284]. The achieved high *i*-paraffin selectivity of 46.5% was attributed to the improved diffusion rate of reactants and products provided by the mesopore channels of the catalyst core as well as to the micro-pores of the zeolite membrane combined with acidic sites responsible for further hydrocracking and isomerization of the heavy hydrocarbons. However, experience has shown that zeolite membrane synthesis onto Fischer-Tropsch catalyst might be difficult to control since it requires alkaline conditions which could lead to catalyst damage or badly coating [255,257,281]. Another weakness is the already discussed increased methane selectivity. Larger metal particle size or larger amount of metal loading over the used supports in the design of Fischer-Tropsch catalysts is suggested in the literature as a possible route to overcome these drawbacks [284–287].

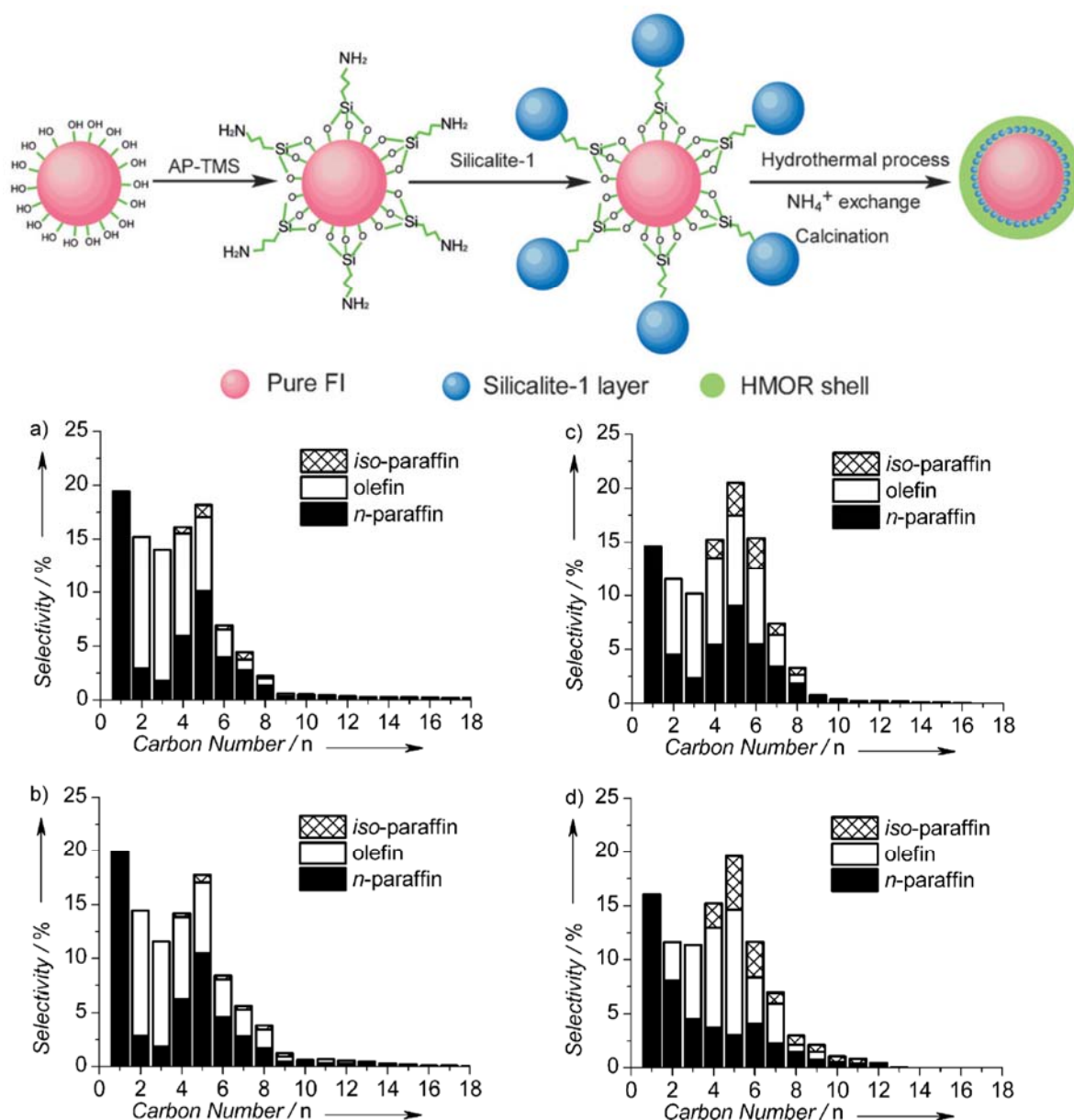


Figure 13. Scheme of the synthesis procedure of HMOR/FI capsule catalysts (FI = Fused Iron) without template and product distributions during Fischer-Tropsch synthesis (operating conditions: $\text{H}_2/\text{CO} = 1/1$, 1.0 MPa, 300 °C, $10 \text{ g}_{\text{FI}} \cdot \text{h}^{-1} \cdot \text{mol}^{-1}$) obtained using (a) pure FI; (b) Silicalite-1/FI; (c) HMOR + FI; and (d) HMOR/FI. Reprinted with permission from [281]. Copyright (2013) John Wiley and Sons.

Very recently, Jin *et al.* [260] developed a novel dual-membrane coating Fe/SiO₂ catalyst core with silicalite-1 and H-ZSM-5 zeolite membranes following a previously reported synthesis procedure for double-shell capsule catalyst [262]. The silicalite-1 synthesized under close-to-neutral condition was acting as catalyst protective membrane for the core with high iron loading, whereas the H-ZSM-5 was the active membrane for the synthesis of *i*-paraffins. The authors stressed that attempts to coat H-ZSM-5 directly over high iron loading Fe/SiO₂ core failed due to the strong alkaline conditions required for its synthesis. The *i*-paraffin selectivity of 29.8% being higher than that of Fe/SiO₂ catalyst (12.9%) and the physical mixture (16.6%) was attributed to the combination

of the hydrogenation and isomerization of the formed olefins at the core and the hydrocracking and isomerization of the heavy hydrocarbons in the dual-membrane catalyst. Moreover, relatively low methane selectivity (14.9%) compared to the other reported core-shell catalysts was obtained [234,256,281], indeed being still higher than that of the core catalyst and the physical mixture. Additionally, Yang *et al.* reported the benefit of controlling the pellet size for the preparation of H-ZSM-5 zeolite capsule catalysts on small Ru/SiO₂ pellets [255]. It was demonstrated that catalyst with smaller pellet size promoted the growth of the zeolite capsule while increasing the zeolite membrane thickness led to high activity and remarkable *i*-paraffin selectivity.

Another research incentive comes from the request to design appropriate catalysts for the direct production of dimethyl ether (DME) being considered as a basic feedstock and a clean fuel [288]. Beside the dehydration of methanol (produced from syngas) to DME, a more desired and thermodynamically favorable alternative is the direct conversion of syngas to DME over hybrid catalysts [289–293]. Generally, the hybrid catalysts usually utilized in such consecutive reactions comprise two types of active sites, namely for the methanol synthesis and acid sites for the dehydration of methanol to DME. Nevertheless, the core-shell catalysts were proposed as a better alternative to the conventional hybrid catalysts [261]. The main advantage of the capsule catalysts, pointed by the authors, is the feasibility to better control the sequential reactions. In detail, the syngas conversion to methanol takes place on the active sites in the core and the further methanol dehydrogenation to produce DME occurs in the zeolite shell. Therefore, zeolite membranes were coated on Cu/Zn/Al₂O₃ applying two different hydrothermal techniques, namely H-ZSM-5 zeolite synthesis containing aluminum sources in the precursor solution and close-to-neutral silicalite-1 zeolite synthesis where the core catalyst was used as aluminum source. The so prepared zeolite capsuled catalysts exhibited extraordinary dimethyl ether selectivity compared to the physical mixture of core catalyst and zeolite powder. Moreover, no further dehydrogenation of the desired product to alkane or alkene occurred on the capsule catalysts. It should be noted that the hybrid catalyst experienced significantly higher conversion than the capsule catalyst. However, the hybrid catalyst provides random contact between methanol and the active sites of zeolite catalyst so that the two consecutive reactions occur independently resulting in moderate selectivity for the desired dimethyl ether. On the other hand, the zeolite shell offers better control of the reaction order since it affords unavoidable contact for methanol formed in the core while passing the membrane and as a result enhances the probability for its further conversion into dimethyl ether leading to the desired high selectivity. Although the H-ZSM-5 coated catalyst exhibited excellent dimethyl ether selectivity, indication was given that the core catalyst structure was damaged during the acidic hydrothermal synthesis resulting in much lower CO conversion. In this context, Yang *et al.* [262,263] discussed the challenges and strategies for preparation of H-ZSM-5 zeolite shells on either bimetallic or silica-based catalyst. It has been demonstrated that the dual-layer method is an effective tool for the preparation of defect-free and compact zeolite shells. A silicalite-1 membrane was first synthesized as intermediate layer acting as core catalyst protection, further facilitating the growth of the H-ZSM-5 under the stronger alkaline conditions. The double-layer capsule catalysts with Cr/ZnO or Pd/SiO₂ core achieved a sharply controlled reaction with excellent DME selectivity and no formation of C₄₊ hydrocarbons.

Next to H-ZSM-5, silico-aluminophosphate molecular sieves (SAPO) are considered as attractive catalysts for the dehydration of methanol to DME [294,295]. Respectively, Pinkaew *et al.* [243] proposed a physical coating procedure using SiO₂ as an adhesive for the preparation of a defect-free SAPO-46 shell

over Cr/ZnO catalyst core. According to the authors, the developed method, performed under normal ambient conditions, is an effective way to overcome the disadvantages of the conventional hydrothermal synthesis e.g., high temperature and alkaline conditions. Accordingly, the capsuled catalyst employed exhibited slightly higher activity than the mixed catalyst which can be ascribed to the enhanced syngas diffusion rate through the SAPO zeolite shell.

Very recently, Phienluphon *et al.* [241] applied the physical coating technique and synthesized silicoaluminophosphate-11 (SAPO-11) shell over Cu/ZnO/Al₂O₃ core catalyst. The so created defect-free, uniform and compact tandem catalyst outperformed the mixture catalyst giving rise to CO conversion of 92.0% and DME selectivity of 90.3%, accompanied by extremely low by-product formation.

The promising results achieved with the core-shell catalysts, where core catalyst and zeolite membrane as shell are combined according to the desired reaction as well as the improvement of the synthesis techniques are good prerequisites for meeting the requirements for wide range of application in particle level membrane reactors.

7. Conclusions

We reviewed literature on the application of zeolite membranes enhancing catalytic reactions in terms of conversion, selectivity or yield. The main advantage of zeolite membranes is based on their property to displace equilibria of thermodynamic difficult reactions. But also shape selectivity or simply separation and purification problems can be solved by using zeolite membranes. Thus, it appears that permselective zeolite membranes can be located (i) spatially decoupled; (ii) in a direct contact to a catalyst packed bed; (iii) as membrane and catalyst all in one, or (iv) as a capsule around a catalyst core. The preferred way how to use a zeolite membrane in catalytic reactions is dependent on numerous factors where membrane and catalyst properties should be carefully evaluated.

From macroscopic zeolite membrane reactors a lot of knowledge has been gained over the last decades. However, may be due to two serious drawbacks such arrays had never got entry into the industrial level in the past. First of all it is the difficulty in producing zeolite membranes on a large scale what makes them still economically unattractive. Secondly, the permeation per membrane area does often not meet the requirements of the volume ratio of the catalytic reactor. Since zeolite capsuled catalysts are able to overcome both the issues it is believed these are the most promising candidates to reach the high criteria of industrial standards. Nevertheless, recent developments on membrane synthesis promise better permeation characteristics as well as easier and cheaper upscaling. Hence, supported zeolite membranes could still also be noticeable candidates for intensified industrial processes in the future.

Author Contributions

R.D. wrote the first draft of the review. R.D. and S.W. iteratively brought it to its final state.

Conflicts of Interest

The authors declare no conflict of interest.

References

1. Corma, A. Inorganic Solid Acids and Their Use in Acid-Catalyzed Hydrocarbon Reactions. *Chem. Rev.* **1995**, *95*, 559–614.
2. Corma, A. From Microporous to Mesoporous Molecular Sieve Materials and Their Use in Catalysis. *Chem. Rev.* **1997**, *97*, 2373–2420.
3. Kulprathipanja, S. *Zeolites in Industrial Separation and Catalysis*; Wiley-VCH: Weinheim, Germany, 2010.
4. Ackley, M.W.; Rege, S.U.; Saxena, H. Application of natural zeolites in the purification and separation of gases. *Microporous Mesoporous Mater.* **2003**, *61*, 25–42.
5. Jasra, R.V.; Choudary, N.V.; Bhat, S.G.T. Separation of Gases by Pressure Swin. *Sep. Sci. Technol.* **1991**, *26*, 885–930.
6. Reiß, G. Status and development of oxygen generation processes on molecular sieve zeolites. *Gas Sep. Purif.* **1994**, *8*, 95–99.
7. Tagliabue, M.; Farrusseng, D.; Valencia, S.; Aguado, S.; Ravon, U.; Rizzo, C.; Corma, A.; Mirodatos, C. Natural gas treating by selective adsorption: Material science and chemical engineering interplay. *Chem. Eng. J.* **2009**, *155*, 553–566.
8. Wang, S.; Peng, Y. Natural zeolites as effective adsorbents in water and wastewater treatment. *Chem. Eng. J.* **2010**, *156*, 11–24.
9. Hedström, A. Ion Exchange of Ammonium in Zeolites: A Literature Review. *J. Environ. Eng.* **2001**, *127*, 673–681.
10. Bein, T. Synthesis and Applications of Molecular Sieve Layers and Membranes. *Chem. Mater.* **1996**, *8*, 1636–1653.
11. Tavolaro, A.; Drioli, E. Zeolite membranes. *Adv. Mater.* **1999**, *11*, 975–996.
12. Caro, J.; Noack, M.; Kölsch, P.; Schäfer, R. Zeolite membranes—State of their development and perspective. *Microporous Mesoporous Mater.* **2000**, *38*, 3–24.
13. Bowen, T.C.; Noble, R.D.; Falconer, J.L. Fundamentals and applications of pervaporation through zeolite membranes. *J. Membr. Sci.* **2004**, *245*, 1–33.
14. Caro, J.; Noack, M.; Kölsch, P. Zeolite Membranes: From the Laboratory Scale to Technical Applications. *Adsorption* **2005**, *11*, 215–227.
15. Snyder, M.A.; Tsapatsis, M. Hierarchical Nanomanufacturing: From Shaped Zeolite Nanoparticles to High-Performance Separation Membranes. *Angew. Chem. Int. Ed.* **2007**, *46*, 7560–7573.
16. Caro, J.; Noack, M. Zeolite membranes—Recent developments and progress. *Microporous Mesoporous Mater.* **2008**, *115*, 215–233.
17. Aroon, M.A.; Ismail, A.F.; Matsuura, T.; Montazer-Rahmati, M.M. Performance studies of mixed matrix membranes for gas separation: A review. *Sep. Purif. Technol.* **2010**, *75*, 229–242.
18. Yu, M.; Noble, R.D.; Falconer, J.L. Zeolite Membranes: Microstructure Characterization and Permeation Mechanisms. *Acc. Chem. Res.* **2011**, *44*, 1196–1206.
19. Gascon, J.; Kapteijn, F.; Zornoza, B.; Sebastian, V.; Casado, C.; Coronas, J. Practical Approach to Zeolitic Membranes and Coatings: State of the Art, Opportunities, Barriers, and Future Perspectives. *Chem. Mater.* **2012**, *24*, 2829–2844.

20. Nasir, R.; Mukhtar, H.; Man, Z.; Mohshim, D.F. Material Advancements in Fabrication of Mixed-Matrix Membranes. *Chem. Eng. Technol.* **2013**, *36*, 717–727.
21. Miachon, S.; Dalmon, J.-A. Catalysis in Membrane Reactors: What About the Catalyst? *Top. Catal.* **2004**, *29*, 59–65.
22. Caro, J. 3.01—Basic Aspects of Membrane Reactors. In *Comprehensive Membrane Science and Engineering*; Drioli, E., Giorno, L., Eds.; Elsevier: Oxford, UK, 2010; pp. 1–24.
23. McLeary, E.E.; Jansen, J.C.; Kapteijn, F. Zeolite based films, membranes and membrane reactors: Progress and prospects. *Microporous Mesoporous Mater.* **2006**, *90*, 198–220.
24. Gascon, J.; van Ommen, J.R.; Moulijn, J.A.; Kapteijn, F. Structuring catalyst and reactor—An inviting avenue to process intensification. *Catal. Sci. Technol.* **2015**, *5*, 807–817.
25. Drioli, E.; Romano, M. Progress and New Perspectives on Integrated Membrane Operations for Sustainable Industrial Growth. *Ind. Eng. Chem. Res.* **2001**, *40*, 1277–1300.
26. Coronas, J.; Santamaría, J. Catalytic reactors based on porous ceramic membranes. *Catal. Today* **1999**, *51*, 377–389.
27. Armor, J.N. Membrane catalysis: Where is it now, what needs to be done? *Catal. Today* **1995**, *25*, 199–207.
28. Daramola, M.O.; Aransiola, E.F.; Ojumu, T.V. Potential applications of zeolite membranes in reaction coupling separation processes. *Materials* **2012**, *5*, 2101–2136.
29. Coronas, J.; Santamaria, J. State-of-the-art in zeolite membrane reactors. *Top. Catal.* **2004**, *29*, 29–44.
30. Saracco, G.; Specchia, V. Catalytic Inorganic-Membrane Reactors: Present Experience and Future Opportunities. *Catal. Rev.* **1994**, *36*, 305–384.
31. Michalkiewicz, B.; Koren, Z. Zeolite membranes for hydrogen production from natural gas: State of the art. *J. Porous Mater.* **2015**, *22*, 635–646.
32. Van den Bergh, J.; Nishiyama, N.; Kapteijn, F. Zeolite Membranes in Catalysis: What Is New and How Bright Is the Future? In *Novel Concepts in Catalysis and Chemical Reactors*; Wiley-VCH Verlag GmbH & Co. KGaA: Weinheim, Germany, 2010; pp. 211–237.
33. Tsapatsis, M. Toward High-Throughput Zeolite Membranes. *Science* **2011**, *334*, 767–768.
34. Agrawal, K.V.; Topuz, B.; Pham, T.C.T.; Nguyen, T.H.; Sauer, N.; Rangnekar, N.; Zhang, H.; Narasimharao, K.; Basahel, S.N.; Francis, L.F.; *et al.* Oriented MFI Membranes by Gel-Less Secondary Growth of Sub-100 nm MFI-Nanosheet Seed Layers. *Adv. Mater.* **2015**, *27*, 3243–3249.
35. Pham, T.C.T.; Nguyen, T.H.; Yoon, K.B. Gel-Free Secondary Growth of Uniformly Oriented Silica MFI Zeolite Films and Application for Xylene Separation. *Angew. Chem. Int. Ed.* **2013**, *52*, 8693–8698.
36. Wang, Z.; Yu, T.; Nian, P.; Zhang, Q.; Yao, J.; Li, S.; Gao, Z.; Yue, X. Fabrication of a Highly *b*-Oriented MFI-Type Zeolite Film by the Langmuir-Blodgett Method. *Langmuir* **2014**, *30*, 4531–4534.
37. Sjöberg, E.; Sandström, L.; Öhrman, O.G.W.; Hedlund, J. Separation of CO₂ from black liquor derived syngas using an MFI membrane. *J. Membr. Sci.* **2013**, *443*, 131–137.
38. Zhou, M.; Korelskiy, D.; Ye, P.; Grahn, M.; Hedlund, J. A Uniformly Oriented MFI Membrane for Improved CO₂ Separation. *Angew. Chem. Int. Ed.* **2014**, *53*, 3492–3495.

39. Davis, M.E. Zeolites from a Materials Chemistry Perspective. *Chem. Mater.* **2014**, *26*, 239–245.
40. Peng, Y.; Lu, H.; Wang, Z.; Yan, Y. Microstructural optimization of MFI-type zeolite membranes for ethanol-water separation. *J. Mater. Chem. A* **2014**, *2*, 16093–16100.
41. Iyoki, K.; Itabashi, K.; Okubo, T. Progress in seed-assisted synthesis of zeolites without using organic structure-directing agents. *Microporous Mesoporous Mater.* **2014**, *189*, 22–30.
42. Kosinov, N.; Gascon, J.; Kapteijn, F.; Hensen, E.J.M. Recent developments in zeolite membranes for gas separation. *J. Membr. Sci.* **2016**, *499*, 65–79.
43. Morigami, Y.; Kondo, M.; Abe, J.; Kita, H.; Okamoto, K. The first large-scale pervaporation plant using tubular-type module with zeolite NaA membrane. *Sep. Purif. Technol.* **2001**, *25*, 251–260.
44. Gallego-Lizon, T.; Edwards, E.; Lobiundo, G.; Freitas dos Santos, L. Dehydration of water/*t*-butanol mixtures by pervaporation: Comparative study of commercially available polymeric, microporous silica and zeolite membranes. *J. Membr. Sci.* **2002**, *197*, 309–319.
45. Urtiaga, A.; Gorri, E.D.; Casado, C.; Ortiz, I. Pervaporative dehydration of industrial solvents using a zeolite NaA commercial membrane. *Sep. Purif. Technol.* **2003**, *32*, 207–213.
46. Richter, H.; Voigt, I.; Kühnert, J.-T. Dewatering of ethanol by pervaporation and vapour permeation with industrial scale NaA-membranes. *Desalination* **2006**, *199*, 92–93.
47. Sato, K.; Aoki, K.; Sugimoto, K.; Izumi, K.; Inoue, S.; Saito, J.; Ikeda, S.; Nakane, T. Dehydrating performance of commercial LTA zeolite membranes and application to fuel grade bio-ethanol production by hybrid distillation/vapor permeation process. *Microporous Mesoporous Mater.* **2008**, *115*, 184–188.
48. Rangnekar, N.; Mittal, N.; Elyassi, B.; Caro, J.; Tsapatsis, M. Zeolite membranes—A review and comparison with MOFs. *Chem. Soc. Rev.* **2015**, *44*, 7128–7154.
49. Bai, C.; Jia, M.-D.; Falconer, J.L.; Noble, R.D. Preparation and separation properties of silicalite composite membranes. *J. Membr. Sci.* **1995**, *105*, 79–87.
50. Dong, J.; Lin, Y.S. *In Situ* Synthesis of P-Type Zeolite Membranes on Porous α -Alumina Supports. *Ind. Eng. Chem. Res.* **1998**, *37*, 2404–2409.
51. Yan, Y.; Davis, M.E.; Gavalas, G.R. Preparation of Zeolite ZSM-5 Membranes by *In-situ* Crystallization on Porous α -Al₂O₃. *Ind. Eng. Chem. Res.* **1995**, *34*, 1652–1661.
52. Tuan, V.A.; Li, S.; Falconer, J.L.; Noble, R.D. *In situ* Crystallization of Beta Zeolite Membranes and Their Permeation and Separation Properties. *Chem. Mater.* **2002**, *14*, 489–492.
53. Lin, X.; Chen, X.; Kita, H.; Okamoto, K. Synthesis of silicalite tubular membranes by *in situ* crystallization. *AIChE J.* **2003**, *49*, 237–247.
54. Vilaseca, M.; Mateo, E.; Palacio, L.; Prádanos, P.; Hernández, A.; Paniagua, A.; Coronas, J.N.; Santamaría, J. AFM characterization of the growth of MFI-type zeolite films on alumina substrates. *Microporous Mesoporous Mater.* **2004**, *71*, 33–37.
55. Guillou, F.; Rouleau, L.; Pirngruber, G.; Valtchev, V. Synthesis of FAU-type zeolite membrane: An original *in situ* process focusing on the rheological control of gel-like precursor species. *Microporous Mesoporous Mater.* **2009**, *119*, 1–8.
56. Huang, A.; Liang, F.; Steinbach, F.; Caro, J. Preparation and separation properties of LTA membranes by using 3-aminopropyltriethoxysilane as covalent linker. *J. Membr. Sci.* **2010**, *350*, 5–9.

57. Huang, A.; Wang, N.; Caro, J. Seeding-free synthesis of dense zeolite FAU membranes on 3-aminopropyltriethoxysilane-functionalized alumina supports. *J. Membr. Sci.* **2012**, *389*, 272–279.
58. Wang, Z.; Yan, Y. Controlling crystal orientation in zeolite MFI thin films by direct *in situ* crystallization. *Chem. Mater.* **2001**, *13*, 1101–1107.
59. Zhang, F.-Z.; Fuji, M.; Takahashi, M. *In situ* growth of continuous *b*-oriented MFI zeolite membranes on porous α -alumina substrates precoated with a mesoporous silica sublayer. *Chem. Mater.* **2005**, *17*, 1167–1173.
60. Wang, Z.; Yan, Y. Oriented zeolite MFI monolayer films on metal substrates by *in situ* crystallization. *Microporous Mesoporous Mater.* **2001**, *48*, 229–238.
61. Li, S.; Demmelmaier, C.; Itkis, M.; Liu, Z.; Haddon, R.C.; Yan, Y. Micropatterned oriented zeolite monolayer films by direct *in situ* crystallization. *Chem. Mater.* **2003**, *15*, 2687–2689.
62. Xomeritakis, G.; Gouzinis, A.; Nair, S.; Okubo, T.; He, M.; Overney, R.M.; Tsapatsis, M. Growth, microstructure, and permeation properties of supported zeolite (MFI) films and membranes prepared by secondary growth. *Chem. Eng. Sci.* **1999**, *54*, 3521–3531.
63. Bernal, M.A.P.; Xomeritakis, G.; Tsapatsis, M. Tubular MFI zeolite membranes made by secondary (seeded) growth. *Catal. Today* **2001**, *67*, 101–107.
64. Nair, S.; Lai, Z.; Nikolakis, V.; Xomeritakis, G.; Bonilla, G.; Tsapatsis, M. Separation of close-boiling hydrocarbon mixtures by MFI and FAU membranes made by secondary growth. *Microporous Mesoporous Mater.* **2001**, *48*, 219–228.
65. Tomita, T.; Nakayama, K.; Sakai, H. Gas separation characteristics of DDR type zeolite membrane. *Microporous Mesoporous Mater.* **2004**, *68*, 71–75.
66. Liu, Y.; Yang, Z.; Yu, C.; Gu, X.; Xu, N. Effect of seeding methods on growth of NaA zeolite membranes. *Microporous Mesoporous Mater.* **2011**, *143*, 348–356.
67. Wohlrab, S.; Meyer, T.; Stöhr, M.; Hecker, C.; Lubenau, U.; Oßmann, A. On the performance of customized MFI membranes for the separation of *n*-butane from methane. *J. Membr. Sci.* **2011**, *369*, 96–104.
68. Fan, W.; Snyder, M.A.; Kumar, S.; Lee, P.-S.; Yoo, W.C.; McCormick, A.V.; Lee Penn, R.; Stein, A.; Tsapatsis, M. Hierarchical nanofabrication of microporous crystals with ordered mesoporosity. *Nat. Mater.* **2008**, *7*, 984–991.
69. Chen, H.; Wydra, J.; Zhang, X.; Lee, P.-S.; Wang, Z.; Fan, W.; Tsapatsis, M. Hydrothermal Synthesis of Zeolites with Three-Dimensionally Ordered Mesoporous-Imprinted Structure. *J. Am. Chem. Soc.* **2011**, *133*, 12390–12393.
70. Roth, W.J.; Nachtigall, P.; Morris, R.E.; Čejka, J. Two-Dimensional Zeolites: Current Status and Perspectives. *Chem. Rev.* **2014**, *114*, 4807–4837.
71. Diaz, U.; Corma, A. Layered zeolitic materials: An approach to designing versatile functional solids. *Dalton Trans.* **2014**, *43*, 10292–10316.
72. Morawetz, K.; Reiche, J.; Kamusewitz, H.; Kosmella, H.; Ries, R.; Noack, M.; Brehmer, L. Zeolite films prepared via the Langmuir-Blodgett technique. *Colloids Surf. A* **2002**, *198–200*, 409–414.
73. Pan, M.; Lin, Y.S. Template-free secondary growth synthesis of MFI type zeolite membranes. *Microporous Mesoporous Mater.* **2001**, *43*, 319–327.
74. Huang, A.; Lin, Y.S.; Yang, W. Synthesis and properties of A-type zeolite membranes by secondary growth method with vacuum seeding. *J. Membr. Sci.* **2004**, *245*, 41–51.

75. Li, G.; Kikuchi, E.; Matsukata, M. The control of phase and orientation in zeolite membranes by the secondary growth method. *Microporous Mesoporous Mater.* **2003**, *62*, 211–220.
76. Lovallo, M.C.; Gouzinis, A.; Tsapatsis, M. Synthesis and characterization of oriented MFI membranes prepared by secondary growth. *AIChE J.* **1998**, *44*, 1903–1913.
77. Choi, J.; Ghosh, S.; Lai, Z.; Tsapatsis, M. Uniformly a-oriented MFI zeolite films by secondary growth. *Angew. Chem.* **2006**, *118*, 1172–1176.
78. Gouzinis, A.; Tsapatsis, M. On the preferred orientation and microstructural manipulation of molecular sieve films prepared by secondary growth. *Chem. Mater.* **1998**, *10*, 2497–2504.
79. Lai, Z.; Tsapatsis, M.; Nicolich, J.P. Siliceous ZSM-5 Membranes by Secondary Growth of b-Oriented Seed Layers. *Adv. Funct. Mater.* **2004**, *14*, 716–729.
80. Liu, Y.; Li, Y.; Yang, W. Fabrication of Highly b-Oriented MFI Film with Molecular Sieving Properties by Controlled in-Plane Secondary Growth. *J. Am. Chem. Soc.* **2010**, *132*, 1768–1769.
81. Hedlund, J.; Schoeman, B.; Sterte, J. Ultrathin oriented zeolite LTA films. *Chem. Commun.* **1997**, doi:10.1039/A702616A.
82. Pham, T.C.T.; Kim, H.S.; Yoon, K.B. Growth of Uniformly Oriented Silica MFI and BEA Zeolite Films on Substrates. *Science* **2011**, *334*, 1533–1538.
83. Xu, W.; Dong, J.; Li, J.; Li, J.; Wu, F. A novel method for the preparation of zeolite ZSM-5. *Chem. Commun.* **1990**, 755–756.
84. Nishiyama, N.; Ueyama, K.; Matsukata, M. Synthesis of defect-free zeolite-alumina composite membranes by a vapor-phase transport method. *Microporous Mater.* **1996**, *7*, 299–308.
85. Matsufuji, T.; Nishiyama, N.; Matsukata, M.; Ueyama, K. Separation of butane and xylene isomers with MFI-type zeolitic membrane synthesized by a vapor-phase transport method. *J. Membr. Sci.* **2000**, *178*, 25–34.
86. Kikuchi, E.; Yamashita, K.; Hiromoto, S.; Ueyama, K.; Matsukata, M. Synthesis of a zeolitic thin layer by a vapor-phase transport method: Appearance of a preferential orientation of MFI zeolite. *Microporous Mater.* **1997**, *11*, 107–116.
87. Matsufuji, T.; Nishiyama, N.; Ueyama, K.; Matsukata, M. Crystallization of ferrierite (FER) on a porous alumina support by a vapor-phase transport method. *Microporous Mesoporous Mater.* **1999**, *32*, 159–168.
88. Nishiyama, N.; Matsufuji, T.; Ueyama, K.; Matsukata, M. FER membrane synthesized by a vapor-phase transport method: Its structure and separation characteristics. *Microporous Mater.* **1997**, *12*, 293–303.
89. Li, Y.; Yang, W. Microwave synthesis of zeolite membranes: A review. *J. Membr. Sci.* **2008**, *316*, 3–17.
90. Weisz, P.B. The Science of the Possible. *Chemtech* **1982**, *12*, 689–690.
91. Boudart, M. Surface Time Yields of Membrane Reactors. In *CaITech*; Springer Science & Business: Berlin, Germany, 1997.
92. Yan, S.; Maeda, H.; Kusakabe, K.; Morooka, S. Thin Palladium Membrane Formed in Support Pores by Metal-Organic Chemical Vapor Deposition Method and Application to Hydrogen Separation. *Ind. Eng. Chem. Res.* **1994**, *33*, 616–622.
93. Graaf, J.M.V.; Zwiép, M.; Kapteijn, F.; Moulijn, J.A. Application of a silicalite-1 membrane reactor in metathesis reactions. *Appl. Catal. A* **1999**, *178*, 225–241.

94. Graaf, J.M.V.D.; Zwiep, M.; Kapteijn, F.; Moulijn, J.A. Application of a zeolite membrane reactor in the metathesis of propene. *Chem. Eng. Sci.* **1999**, *54*, 1441–1445.
95. Moon, W.S.; Park, S.B. Design guide of a membrane for a membrane reactor in terms of permeability and selectivity. *J. Membr. Sci.* **2000**, *170*, 43–51.
96. Battersby, S.; Teixeira, P.W.; Beltramini, J.; Duke, M.C.; Rudolph, V.; Diniz da Costa, J.C. An analysis of the Peclet and Damkohler numbers for dehydrogenation reactions using molecular sieve silica (MSS) membrane reactors. *Catal. Today* **2006**, *116*, 12–17.
97. Choi, S.-W.; Jones, C.W.; Nair, S.; Sholl, D.S.; Moore, J.S.; Liu, Y.; Dixit, R.S.; Pendergast, J.G. Material properties and operating configurations of membrane reactors for propane dehydrogenation. *AIChE J.* **2015**, *61*, 922–935.
98. Baker, R.W. *Membrane Technologies and Applications*; John Wiley & Sons Ltd.: Chichester, UK, 2004.
99. Krishna, R.; van den Broeke, L.J.P. The Maxwell-Stefan description of mass transport across zeolite membranes. *Chem. Eng. J. Biochem. Eng. J.* **1995**, *57*, 155–162.
100. Krishna, R.; Wesselingh, J.A. The Maxwell-Stefan approach to mass transfer. *Chem. Eng. Sci.* **1997**, *52*, 861–911.
101. Kapteijn, F.; Moulijn, J.A.; Krishna, R. The generalized Maxwell-Stefan model for diffusion in zeolites: Sorbate molecules with different saturation loadings. *Chem. Eng. Sci.* **2000**, *55*, 2923–2930.
102. Krishna, R.; Baur, R. Modelling issues in zeolite based separation processes. *Sep. Purif. Technol.* **2003**, *33*, 213–254.
103. Krishna, R. The Maxwell-Stefan description of mixture diffusion in nanoporous crystalline materials. *Microporous Mesoporous Mater.* **2014**, *185*, 30–50.
104. Yuan, W.; Lin, Y.S.; Yang, W. Molecular Sieving MFI-Type Zeolite Membranes for Pervaporation Separation of Xylene Isomers. *J. Am. Chem. Soc.* **2004**, *126*, 4776–4777.
105. Aoki, K.; Kusakabe, K.; Morooka, S. Gas permeation properties of A-type zeolite membrane formed on porous substrate by hydrothermal synthesis. *J. Membr. Sci.* **1998**, *141*, 197–205.
106. Xu, X.; Bao, Y.; Song, C.; Yang, W.; Liu, J.; Lin, L. Synthesis, characterization and single gas permeation properties of NaA zeolite membrane. *J. Membr. Sci.* **2005**, *249*, 51–64.
107. Van de Graaf, J.M.; van der Bijl, E.; Stol, A.; Kapteijn, F.; Moulijn, J.A. Effect of Operating Conditions and Membrane Quality on the Separation Performance of Composite Silicalite-1 Membranes. *Ind. Eng. Chem. Res.* **1998**, *37*, 4071–4083.
108. Vroon, Z.A.E.P.; Keizer, K.; Burggraaf, A.J.; Verweij, H. Preparation and characterization of thin zeolite MFI membranes on porous supports. *J. Membr. Sci.* **1998**, *144*, 65–76.
109. Keizer, K.; Burggraaf, A.J.; Vroon, Z.A.E.P.; Verweij, H. Two component permeation through thin zeolite MFI membranes. *J. Membr. Sci.* **1998**, *147*, 159–172.
110. Coronas, J.; Falconer, J.L.; Noble, R.D. Characterization and permeation properties of ZSM-5 tubular membranes. *AIChE J.* **1997**, *43*, 1797–1812.
111. Jiang, M.; Eic, M.; Miachon, S.; Dalmon, J.-A.; Kocirik, M. Diffusion of *n*-butane, isobutane and ethane in a MFI-zeolite membrane investigated by gas permeation and ZLC measurements. *Sep. Purif. Technol.* **2001**, *25*, 287–295.
112. Barrer, R.M. Porous crystal membranes. *J. Chem. Soc. Faraday Trans.* **1990**, *86*, 1123–1130.

113. Bakker, W.J.W.; Kapteijn, F.; Poppe, J.; Moulijn, J.A. Permeation characteristics of a metal-supported silicalite-1 zeolite membrane. *J. Membr. Sci.* **1996**, *117*, 57–78.
114. Neubauer, K.; Lubenau, U.; Hecker, C.; Lücke, B.; Paschek, D.; Wohlrab, S. Abreicherung von Flüssiggas aus Erdgas mittels Zeolithmembranen; Depletion of Liquefied Petroleum Gas from Natural Gas by Zeolite Membranes. *Chem. Ing. Tech.* **2013**, *85*, 713–722.
115. Dragomirova, R.; Stohr, M.; Hecker, C.; Lubenau, U.; Paschek, D.; Wohlrab, S. Desorption-controlled separation of natural gas alkanes by zeolite membranes. *RSC Adv.* **2014**, *4*, 59831–59834.
116. Neubauer, K.; Dragomirova, R.; Stöhr, M.; Mothes, R.; Lubenau, U.; Paschek, D.; Wohlrab, S. Combination of membrane separation and gas condensation for advanced natural gas conditioning. *J. Membr. Sci.* **2014**, *453*, 100–107.
117. Baker, R.W.; Lokhandwala, K. Natural Gas Processing with Membranes: An Overview. *Ind. Eng. Chem. Res.* **2008**, *47*, 2109–2121.
118. Arruebo, M.; Coronas, J.; Menéndez, M.; Santamaría, J. Separation of hydrocarbons from natural gas using silicalite membranes. *Sep. Purif. Technol.* **2001**, *25*, 275–286.
119. Dragomirova, R.; Kreft, S.; Georgi, G.; Seeburg, D.; Wohlrab, S. Liquefied Petroleum Gas Enrichment by Zeolite Membranes for Low-Temperature Steam Reforming of Natural Gas. In Proceedings of Synthesis Gas Chemistry, 2015-2, DGMK International Conference, Dresden, Germany, 7–9 October 2015; pp. 273–280.
120. Ockwig, N.W.; Nenoff, T.M. Membranes for Hydrogen Separation. *Chem. Rev.* **2007**, *107*, 4078–4110.
121. Varela-Gandía, F.J.; Berenguer-Murcia, Á.; Lozano-Castelló, D.; Cazorla-Amorós, D. Zeolite A/carbon membranes for H₂ purification from a simulated gas reformer mixture. *J. Membr. Sci.* **2011**, *378*, 407–414.
122. Gallo, M.; Nenoff, T.M.; Mitchell, M.C. Selectivities for binary mixtures of hydrogen/methane and hydrogen/carbon dioxide in silicalite and ETS-10 by Grand Canonical Monte Carlo techniques. *Fluid Phase Equilibria* **2006**, *247*, 135–142.
123. Mitchell, M.C.; Autry, J.D.; Nenoff, T.M. Molecular dynamics simulations of binary mixtures of methane and hydrogen in zeolite A and a novel zinc phosphate. *Mol. Phys.* **2001**, *99*, 1831–1837.
124. Tang, Z.; Dong, J.; Nenoff, T.M. Internal Surface Modification of MFI-Type Zeolite Membranes for High Selectivity and High Flux for Hydrogen. *Langmuir* **2009**, *25*, 4848–4852.
125. Wee, S.-L.; Tye, C.-T.; Bhatia, S. Membrane separation process—Pervaporation through zeolite membrane. *Sep. Purif. Technol.* **2008**, *63*, 500–516.
126. Lima, S.Y.; Parkb, B.; Hunga, F.; Sahimia, M.; Tsotsisa, T.T. Design issues of pervaporation membrane reactors for esterification. *Chem. Eng. Sci.* **2002**, *57*, 4933–4946.
127. Jafar, J.J.; Budd, P.M.; Hughes, R. Enhancement of esterification reaction yield using zeolite—A vapour permeation membrane. *J. Membr. Sci.* **2002**, *199*, 117–123.
128. Khajavi, S.; Jansen, J.C.; Kapteijn, F. Application of a sodalite membrane reactor in esterification—Coupling reaction and separation. *Catal. Today* **2010**, *156*, 132–139.
129. Hasegawa, Y.; Abe, C.; Mizukami, F.; Kowata, Y.; Hanaoka, T. Application of a CHA-type zeolite membrane to the esterification of adipic acid with isopropyl alcohol using sulfuric acid catalyst. *J. Membr. Sci.* **2012**, *415*, 368–374.

130. Okamoto, K.-I.; Kita, H.; Horii, K. Zeolite NaA Membrane: Preparation, Single-Gas Permeation, and Pervaporation and Vapor Permeation of Water/Organic Liquid Mixtures. *Ind. Eng. Chem. Res.* **2001**, *40*, 163–175.
131. Kita, H.; Horii, K.; Ohtoshi, Y.; Tanaka, K.; Okamoto, K.-I. Synthesis of a zeolite NaA membrane for pervaporation of water/organic liquid mixtures. *J. Mater. Sci. Lett.* **1995**, *14*, 206–208.
132. Hasegawa, Y.; Nagase, T.; Kiyozumi, Y.; Hanaoka, T.; Mizukami, F. Influence of acid on the permeation properties of NaA-type zeolite membranes. *J. Membr. Sci.* **2010**, *349*, 189–194.
133. Inoue, T.; Nagase, T.; Hasegawa, Y.; Kiyozumi, Y.; Sato, K.; Nishioka, M.; Hamakawa, S.; Mizukami, F. Stoichiometric ester condensation reaction processes by pervaporative water removal via acid-tolerant zeolite membranes. *Ind. Eng. Chem. Res.* **2007**, *46*, 3743–3750.
134. Khajavi, S.; Jansen, J.C.; Kapteijn, F. Application of hydroxy sodalite films as novel water selective membranes. *J. Membr. Sci.* **2009**, *326*, 153–160.
135. Zhang, W.; Na, S.; Li, W.; Xing, W. Kinetic Modeling of Pervaporation Aided Esterification of Propionic Acid and Ethanol Using T-Type Zeolite Membrane. *Ind. Eng. Chem. Res.* **2015**, *54*, 4940–4946.
136. Aiouache, F.; Goto, S. Reactive distillation-pervaporation hybrid column for tert-amyl alcohol etherification with ethanol. *Chem. Eng. Sci.* **2003**, *58*, 2465–2477.
137. Thomas, S.; Hamel, C.; Seidel-Morgenstern, A. Basic Problems of Chemical Reaction Engineering and Potential of Membrane Reactors. In *Membrane Reactors*; Wiley-VCH Verlag GmbH & Co. KGaA: Weinheim, Germany, 2010; pp. 1–27.
138. Gallucci, F.; Fernandez, E.; Corengia, P.; van Sint Annaland, M. Recent advances on membranes and membrane reactors for hydrogen production. *Chem. Eng. Sci.* **2013**, *92*, 40–66.
139. Gallucci, F.; Basile, A.; Hai, F.I. Introduction—A Review of Membrane Reactors. In *Membranes for Membrane Reactors*; John Wiley & Sons, Ltd.: Chichester, UK, 2011; pp. 1–61.
140. Téllez, C.; Menéndez, M. Zeolite Membrane Reactors. In *Membranes for Membrane Reactors*; John Wiley & Sons, Ltd.: Chichester, UK, 2011; pp. 243–273.
141. Koros, W.J.; Ma, Y.H.; Shimidzu, T. Terminology for membranes and membrane processes. *Pure Appl. Chem.* **1999**, *68*, 1479–1489.
142. Dittmeyer, R.; Hollein, V.; Daub, K. Membrane reactors for hydrogenation and dehydrogenation processes based on supported palladium. *J. Mol. Catal. A* **2001**, *173*, 135–184.
143. Dittmeyer, R.; Caro, J. Catalytic Membrane Reactors. In *Handbook of Heterogeneous Catalysis*; Wiley-VCH Verlag GmbH & Co. KGaA: Weinheim, Germany, 2008.
144. Xiongfū, Z.; Yongsheng, L.; Jinqū, W.; Huairong, T.; Changhou, L. Synthesis and characterization of Fe-MFI zeolite membrane on a porous g-Al₂O₃ tube. *Sep. Purif. Technol.* **2001**, *25*, 269–274.
145. Ciavarella, P.; Casanave, D.; Moueddeb, H.; Miachon, S.; Fiaty, K.; Dalmon, J.A. Isobutane dehydrogenation in a membrane reactor—Influence of the operating conditions on the performance. *Catal. Today* **2001**, *67*, 177–184.
146. Illgen, U.; Schäfer, R.; Noack, M.; Kölsch, P.; Kühnle, A.; Caro, J. Membrane supported catalytic dehydrogenation of iso-butane using an MFI zeolite membrane reactor. *Catal. Commun.* **2001**, *2*, 339–345.
147. Bergh, J.V.D.; Gücüyener, C.; Gascon, J.; Kapteijn, F. Isobutane dehydrogenation in a DD₃R zeolite membrane reactor. *Chem. Eng. J.* **2011**, *166*, 368–377.

148. Jeong, B.H.; Sotowa, K.I.; Kusakabe, K. Catalytic dehydrogenation of cyclohexane in an FAU-type zeolite membrane reactor. *J. Membr. Sci.* **2003**, *224*, 151–158.
149. Jeong, B.H.; Sotowa, K.I.; Kusakabe, K. Modeling of an FAU-type zeolite membrane reactor for the catalytic dehydrogenation of cyclohexane. *Chem. Eng. J.* **2004**, *103*, 69–75.
150. Kong, C.L.; Lu, J.M.; Yang, H.H.; Wang, J.Q. Catalytic dehydrogenation of ethylbenzene to styrene in a zeolite silicalite-1 membrane reactor. *J. Membr. Sci.* **2007**, *306*, 29–35.
151. Avila, A.M.; Yu, Z.; Fazli, S.; Sawada, J.A.; Kuznicki, S.M. Hydrogen-selective natural mordenite in a membrane reactor for ethane dehydrogenation. *Microporous Mesoporous Mater.* **2014**, *190*, 301–308.
152. Tang, Z.; Kim, S.J.; Reddy, G.K.; Dong, J.H.; Smirniotis, P. Modified zeolite membrane reactor for high temperature water gas shift reaction. *J. Membr. Sci.* **2010**, *354*, 114–122.
153. Zhang, Y.T.; Wu, Z.J.; Hong, Z.; Gu, X.H.; Xu, N.P. Hydrogen-selective zeolite membrane reactor for low temperature water gas shift reaction. *Chem. Eng. J.* **2012**, *197*, 314–321.
154. Kim, S.J.; Xu, Z.; Reddy, G.K.; Smirniotis, P.; Dong, J.H. Effect of Pressure on High-Temperature Water Gas Shift Reaction in Microporous Zeolite Membrane Reactor. *Ind. Eng. Chem. Res.* **2012**, *51*, 1364–1375.
155. Kim, S.J.; Yang, S.W.; Reddy, G.K.; Smirniotis, P.; Dong, J.H. Zeolite Membrane Reactor for High-Temperature Water-Gas Shift Reaction: Effects of Membrane Properties and Operating Conditions. *Energy Fuels* **2013**, *27*, 4471–4480.
156. Dong, X.L.; Wang, H.B.; Rui, Z.B.; Lin, Y.S. Tubular dual-layer MFI zeolite membrane reactor for hydrogen production via the WGS reaction: Experimental and modeling studies. *Chem. Eng. J.* **2015**, *268*, 219–229.
157. Zhang, Y.; Sun, Q.; Gu, X. Pure H₂ production through hollow fiber hydrogen-selective MFI zeolite membranes using steam as sweep gas. *AIChE J.* **2015**, doi:10.1002/aic.14924.
158. Dyk, L.V.; Lorenzen, L.; Miachon, S.; Dalmon, J.-A. Xylene isomerization in an extractor type catalytic membrane reactor. *Catal. Today* **2005**, *104*, 274–280.
159. Haag, S.; Hanebuth, M.; Mabande, G.T.P.; Avhale, A.; Schwieger, W.; Dittmeyer, R. On the use of a catalytic H-ZSM-5 membrane for xylene isomerization. *Microporous Mesoporous Mater.* **2006**, *96*, 168–176.
160. Tarditi, A.M.; Horowitz, G.I.; Lombardo, E.A. Xylene isomerization in a ZSM-5/SS membrane reactor. *Catal. Lett.* **2008**, *123*, 7–15.
161. Zhang, C.; Hong, Z.; Gu, X.H.; Zhong, Z.X.; Jin, W.Q.; Xu, N.P. Silicalite-1 Zeolite Membrane Reactor Packed with HZSM-5 Catalyst for *meta*-Xylene Isomerization. *Ind. Eng. Chem. Res.* **2009**, *48*, 4293–4299.
162. Daramola, M.O.; Deng, Z.; Pera-Titus, M.; Giroir-Fendler, A.; Miachon, S.; Burger, A.J.; Lorenzen, L.; Guo, Y. Nanocomposite MFI-alumina membranes prepared via pore-pugging synthesis: Application as packed-bed membrane reactors for *m*-xylene isomerization over a Pt-HZSM-5 catalyst. *Catal. Today* **2010**, 261–267.
163. Daramola, M.O.; Burger, A.J.; Giroir-Fendler, A.; Miachon, S.; Lorenzen, L. Extractor-type catalytic membrane reactor with nanocomposite MFI-alumina membrane tube as separation unit: Prospect for ultra-pure *para*-Xylene production from *m*-Xylene isomerization over Pt-HZSM-5 catalyst. *Appl. Catal. A* **2010**, *386*, 109–115.

164. Yeong, Y.F.; Abdullah, A.Z.; Ahmad, A.L.; Bhatia, S. Xylene isomerization kinetic over acid-functionalized silicalite-1 catalytic membranes: Experimental and modeling studies. *Chem. Eng. J.* **2010**, *157*, 579–589.
165. Zhang, C.; Hong, Z.; Chen, J.; Gu, X.H.; Jin, W.; Xu, N. Catalytic MFI zeolite membranes supported on Al₂O₃ substrates for *m*-xylene isomerization. *J. Membr. Sci.* **2012**, *389*, 451–458.
166. Mihályi, R.M.; Patis, A.; Nikolakis, V.; Kollár, M.; Valyon, J. [B]MFI membrane: Synthesis, physico-chemical properties and catalytic behavior in the double-bond isomerization of 1-butene. *Sep. Purif. Technol.* **2013**, *118*, 135–143.
167. Bernal, M.P.; Coronas, J.; Menendez, M.; Santamaria, J. Coupling of reaction and separation at the microscopic level: Esterification processes in a H-ZSM-5 membrane reactor. *Chem. Eng. Sci.* **2002**, *57*, 1557–1562.
168. De la Iglesia, Ó.; Mallada, R.; Menéndez, M.; Coronas, J. Continuous zeolite membrane reactor for esterification of ethanol and acetic acid. *Chem. Eng. J.* **2007**, *131*, 35–39.
169. Fedosov, D.A.; Smirnov, A.V.; Shkirskiy, V.V.; Voskoboynikov, T.; Ivanova, I.I. Methanol dehydration in NaA zeolite membrane reactor. *J. Membr. Sci.* **2015**, *486*, 189–194.
170. Gallucci, F.; Paturzo, L.; Basile, A. An experimental study of CO₂ hydrogenation into methanol involving a zeolite membrane reactor. *Chem. Eng. Process.* **2004**, *43*, 1029–1036.
171. Gora, L.; Jansen, J.C. Hydroisomerization of C₆ with a zeolite membrane reactor. *J. Catal.* **2005**, *230*, 269–281.
172. Mota, S.; Miachon, S.; Volta, J.C.; Dalmon, J.A. Membrane reactor for selective oxidation of butane to maleic anhydride. *Catal. Today* **2001**, *67*, 169–176.
173. Abon, M.; Volta, J.-C. Vanadium phosphorus oxides for *n*-butane oxidation to maleic anhydride. *Appl. Catal. A* **1997**, *157*, 173–193.
174. Mallada, R.; Menéndez, M.; Santamaría, J. Use of membrane reactors for the oxidation of butane to maleic anhydride under high butane concentrations. *Catal. Today* **2000**, *56*, 191–197.
175. Xue, E.; Ross, J. The use of membrane reactors for catalytic *n*-butane oxidation to maleic anhydride with a butane-rich feed. *Catal. Today* **2000**, *61*, 3–8.
176. Cruz-López, A.M.; Guilhaume, N.; Miachon, S.; Dalmon, J.-A. Selective oxidation of butane to maleic anhydride in a catalytic membrane reactor adapted to rich butane feed. *Catal. Today* **2005**, *2005*, 949–956.
177. Pantazidis, A.; Dalmon, J.A.; Mirodatos, C. Oxidative Dehydrogenation of Propane on Catalytic Membrane Reactors. *Catal. Today* **1995**, *25*, 403–408.
178. Julbe, A.; Farrusseng, D.; Jalibert, J.C.; Mirodatos, C.; Guizard, C. Characteristics and performance in the oxidative dehydrogenation of propane of MFI and V-MFI zeolite membranes. *Catal. Today* **2000**, *56*, 199–209.
179. Diakov, V.; Blackwell, B.; Varma, A. Methanol oxidative dehydrogenation in a catalytic packed-bed membrane reactor: Experiments and model. *Chem. Eng. Sci.* **2002**, *57*, 1563–1569.
180. Diakov, V.; Varma, A. Optimal Feed Distribution in a Packed-Bed Membrane Reactor: The Case of Methanol Oxidative Dehydrogenation. *Ind. Eng. Chem. Res.* **2004**, *43*, 309–314.
181. Chommeloux, B.; Cimaomo, S.; Jolimaitre, E.; Uzio, D.; Magnoux, P.; Sanchez, J. New membrane for use as hydrogen distributor for hydrocarbon selective hydrogenation. *Microporous Mesoporous Mater.* **2008**, *109*, 28–37.

182. Torres, M.; López, L.; Domínguez, J.M.; Mantilla, A.; Ferrat, G.; Gutierrez, M.; Maubert, M. Olefins catalytic oligomerization on new composites of beta-zeolite films supported on α -Al₂O₃ membranes. *Chem. Eng. J.* **2003**, *92*, 1–6.
183. Torres, M.; Gutiérrez, M.; Mugica, V.; Romero, M.; López, L. Oligomerization of isobutene with α , β -zeolite membrane: Effect of the acid properties of the catalytic membrane. *Catal. Today* **2011**, *166*, 205–208.
184. Aguado, S.; Coronas, J.; Santamaría, J. Use of Zeolite Membrane Reactors for the Combustion of VOCs Present in Air at Low Concentrations. *Chem. Eng. Res. Des.* **2005**, *83*, 295–301.
185. Tanaka, K.; Yoshikawa, R.; Ying, C.; Kita, H.; Okamoto, K. Application of zeolite membranes to esterification reactions. *Catal. Today* **2001**, *67*, 121–125.
186. Tanaka, K.; Yoshikawa, R.; Ying, C.; Kita, H.; Okamoto, K. Application of zeolite T membrane to vapor-permeation-aided esterification of lactic acid with ethanol. *Chem. Eng. Sci.* **2002**, *57*, 1577–1584.
187. Salomón, M.A.; Coronas, J.; Menéndez, M.; Santamaría, J. Synthesis of MTBE in zeolite membrane reactors. *Appl. Catal. A* **2000**, *200*, 201–210.
188. Pera-Titus, M.; Llorens, J.; Cunill, F. Technical and economical feasibility of zeolite NaA membrane-based reactors in liquid-phase etherification reactions. *Chem. Eng. Process. Process Intensif.* **2009**, *48*, 1072–1079.
189. Aresta, M.; Galatola, M. Life cycle analysis applied to the assessment of the environmental impact of alternative synthetic processes. The dimethylcarbonate case: Part 1. *J. Clean Prod.* **1999**, *7*, 181–193.
190. Aresta, M.; Dibenedetto, A.; Tommasi, I. Developing Innovative Synthetic Technologies of Industrial Relevance Based on Carbon Dioxide as Raw Material. *Energy Fuels* **2001**, *15*, 269–273.
191. Diban, N.; Urriaga, A.M.; Ortiz, I.; Ereña, J.; Bilbao, J.; Aguayo, A.T. Influence of the membrane properties on the catalytic production of dimethyl ether with *in situ* water removal for the successful capture of CO₂. *Chem. Eng. J.* **2013**, *234*, 140–148.
192. Olah, G.A.; Goepfert, A.; Prakash, G.K.S. Chemical Recycling of Carbon Dioxide to Methanol and Dimethyl Ether: From Greenhouse Gas to Renewable, Environmentally Carbon Neutral Fuels and Synthetic Hydrocarbons. *J. Org. Chem.* **2009**, *74*, 487–498.
193. Aguayo, A.T.; Ereña, J.; Sierra, I.; Olazar, M.; Bilbao, J. Deactivation and regeneration of hybrid catalysts in the single-step synthesis of dimethyl ether from syngas and CO₂. *Catal. Today* **2005**, *106*, 265–270.
194. Diban, N.; Urriaga, A.M.; Ortiz, I.; Ereña, J.; Bilbao, J.; Aguayo, A.T. Improved Performance of a PBM Reactor for Simultaneous CO₂ Capture and DME Synthesis. *Ind. Eng. Chem. Res.* **2014**, *53*, 19479–19487.
195. Rohde, M.P.; Unruh, D.; Schaub, G. Membrane application in Fischer-Tropsch synthesis reactors—Overview of concepts. *Catal. Today* **2005**, *106*, 143–148.
196. Rohde, M.P.; Schaub, G.; Khajavi, S.; Jansen, J.C.; Kapteijn, F. Fischer-Tropsch synthesis with *in situ* H₂O removal—Directions of membrane development. *Microporous Mesoporous Mater.* **2008**, *115*, 123–136.

197. Espinoza, R.L.; du Toit, E.; Santamaria, J.; Menendez, M.; Coronas, J.; Irusta, S. Use of membranes in Fischer-Tropsch reactors. In *Studies in Surface Science and Catalysis*; Avelino Corma, F.V.M.S.M., José Luis, G.F., Eds.; Elsevier: Amsterdam, The Netherlands, 2000; Volume 130, pp. 389–394.
198. Khajavi, S.; Kapteijn, F.; Jansen, J.C. Synthesis of thin defect-free hydroxy sodalite membranes: New candidate for activated water permeation. *J. Membr. Sci.* **2007**, *299*, 63–72.
199. Rahimpour, M.R.; Mirvakili, A.; Paymooni, K. A novel water perm-selective membrane dual-type reactor concept for Fischer-Tropsch synthesis of GTL (gas to liquid) technology. *Energy* **2011**, *36*, 1223–1235.
200. Rahimpour, M.R.; Mirvakili, A.; Paymooni, K.; Moghtaderi, B. A comparative study between a fluidized-bed and a fixed-bed water perm-selective membrane reactor with *in situ* H₂O removal for Fischer-Tropsch synthesis of GTL technology. *J. Nat. Gas Sci. Eng.* **2011**, *3*, 484–495.
201. Cavani, F.; Trifiro, F. Classification of industrial catalysts and catalysis for the petrochemical industry. *Catal. Today* **1997**, *34*, 269–279.
202. Casanave, D.; Giroirfendler, A.; Sanchez, J.; Loutaty, R.; Dalmon, J.A. Control of Transport-Properties with a Microporous Membrane Reactor to Enhance Yields in Dehydrogenation Reactions. *Catal. Today* **1995**, *25*, 309–314.
203. Casanave, D.; Ciavarella, P.; Fiaty, K.; Dalmon, J.A. Zeolite membrane reactor for isobutane dehydrogenation: Experimental results and theoretical modelling. *Chem. Eng. Sci.* **1999**, *54*, 2807–2815.
204. Dyk, L.V.; Miachon, S.; Lorenzen, L.; Torres, M.; Fiaty, K.; Dalmon, J.-A. Comparison of microporous MFI and dense Pd membrane performances in an extractor-type CMR. *Catal. Today* **2003**, *82*, 167–177.
205. Gokhale, Y.V.; Noble, R.D.; Falconer, J.L. Effects of reactant loss and membrane selectivity on a dehydrogenation reaction in a membrane-enclosed catalytic reactor. *J. Membr. Sci.* **1995**, *103*, 235–242.
206. Vaezi, M.J.; Babaluo, A.A.; Shafiei, S. Modeling of ethylbenzene dehydrogenation membrane reactor to investigate the potential application of a microporous hydroxy sodalite membrane. *J. Chem. Pet. Eng.* **2015**, *49*, 51–62.
207. Rhodes, C.; Hutchings, G.J.; Ward, A.M. Water-gas shift reaction: Finding the mechanistic boundary. *Catal. Today* **1995**, *23*, 43–58.
208. Tosti, S.; Basile, A.; Chiappetta, G.; Rizzello, C.; Violante, V. Pd-Ag membrane reactors for water gas shift reaction. *Chem. Eng. J.* **2003**, *93*, 23–30.
209. Basile, A.; Chiappetta, G.; Tosti, S.; Violante, V. Experimental and simulation of both Pd and Pd/Ag for a water gas shift membrane reactor. *Sep. Purif. Technol.* **2001**, *25*, 549–571.
210. Peters, T.A.; Stange, M.; Klette, H.; Bredesen, R. High pressure performance of thin Pd-23%Ag/stainless steel composite membranes in water gas shift gas mixtures; influence of dilution, mass transfer and surface effects on the hydrogen flux. *J. Membr. Sci.* **2008**, *316*, 119–127.
211. Augustine, A.S.; Ma, Y.H.; Kazantzis, N.K. High pressure palladium membrane reactor for the high temperature water-gas shift reaction. *Int. J. Hydrogen Energy* **2011**, *36*, 5350–5360.

212. Giessler, S.; Jordan, L.; Diniz da Costa, J.C.; Lu, G.Q. Performance of hydrophobic and hydrophilic silica membrane reactors for the water gas shift reaction. *Sep. Purif. Technol.* **2003**, *32*, 255–264.
213. Battersby, S.; Duke, M.C.; Liu, S.; Rudolph, V.; Costa, J.C.D.D. Metal doped silica membrane reactor: Operational effects of reaction and permeation for the water gas shift reaction. *J. Membr. Sci.* **2008**, *316*, 46–52.
214. Gu, X.; Tang, Z.; Dong, J. On-stream modification of MFI zeolite membranes for enhancing hydrogen separation at high temperature. *Microporous Mesoporous Mater.* **2008**, *111*, 441–448.
215. Liu, B.S.; Au, C.T. A La₂NiO₄-Zeolite Membrane Reactor for the CO₂ Reforming of Methane to Syngas. *Catal. Lett.* **2001**, *77*, 67–74.
216. Liu, B.S.; Gao, L.Z.; Au, C.T. Preparation, characterization and application of a catalytic NaA membrane for CH₄/CO₂ reforming to syngas. *Appl. Catal. A* **2002**, *235*, 193–206.
217. Barbieri, G.; Marigliano, G.; Golemme, G.; Drioli, E. Simulation of CO₂ hydrogenation with CH₃OH removal in a zeolite membrane reactor. *Chem. Eng. J.* **2002**, *85*, 53–59.
218. Lee, G.-S.; McCain, J.; Bhasin, M. Synthetic Organic Chemicals. In *Kent and Riegel's Handbook of Industrial Chemistry and Biotechnology*; Kent, J., Ed.; Springer US: New York, NY, USA, 2007; pp. 345–403.
219. Yan, T.Y. Separation of *p*-xylene and ethylbenzene from C₈ aromatics using medium-pore zeolites. *Ind. Eng. Chem. Res.* **1989**, *28*, 572–576.
220. Daramola, M.O.; Burger, A.J.; Pera-Titus, M.; Giroir-Fendler, A.; Miachon, S.; Dalmon, J.A.; Lorenzen, L. Separation and isomerization of xylenes using zeolite membranes: A short overview. *Asia-Pac. J. Chem. Eng.* **2010**, *5*, 815–837.
221. Xomeritakis, G.; Lai, Z.; Tsapatsis, M. Separation of Xylene Isomer Vapors with Oriented MFI Membranes Made by Seeded Growth. *Ind. Eng. Chem. Res.* **2001**, *40*, 544–552.
222. Baerlocher, C.; McCusker, L.B.; Olson, D.H. MFI-Pnma. In *Atlas of Zeolite Framework Types*, 6th ed.; Baerlocher, C., Olson, L.B.M.H., Eds.; Elsevier Science B.V.: Amsterdam, The Netherlands, 2007; pp. 212–213.
223. Sakai, H.; Tomita, T.; Takahashi, T. *p*-Xylene separation with MFI-type zeolite membrane. *Sep. Purif. Technol.* **2001**, *25*, 297–306.
224. Gu, X.; Dong, J.; Nenoff, T.M.; Ozokwelu, D.E. Separation of *p*-xylene from multicomponent vapor mixtures using tubular MFI zeolite membranes. *J. Membr. Sci.* **2006**, *280*, 624–633.
225. Gump, C.J.; Tuan, V.A.; Noble, R.D.; Falconer, J.L. Aromatic Permeation through Crystalline Molecular Sieve Membranes. *Ind. Eng. Chem. Res.* **2001**, *40*, 565–577.
226. Lai, Z.; Bonilla, G.; Diaz, I.; Nery, J.G.; Sujaoti, K.; Amat, M.A.; Kokkoli, E.; Terasaki, O.; Thompson, R.W.; Tsapatsis, M.; *et al.* Microstructural optimization of a zeolite membrane for organic vapor separation. *Science* **2003**, *300*, 456–460.
227. Daramola, M.O.; Burger, A.J.; Pera-Titus, M.; Giroir-Fendler, A.; Miachon, S.; Lorenzen, L.; Dalmon, J.A. Nanocomposite MFI-ceramic hollow fibre membranes via pore-plugging synthesis: Prospects for xylene isomer separation. *J. Membr. Sci.* **2009**, *337*, 106–112.
228. Maloney, M.L.; Maschmeyer, T.; Jansen, J.C. Technical and economical evaluation of a zeolite membrane based heptane hydroisomerization process. *Chem. Eng. J.* **2005**, *106*, 187–195.

229. Piera, E.; Tellez, C.; Coronas, J.; Menendez, M.; SaIntamaria, J. Use of zeolite membrane reactors for selectivity enhancement: Application to the liquid-phase oligomerization of *i*-butene. *Catal. Today* **2001**, *67*, 127–138.
230. Peters, T.A.; Benes, N.E.; Keurentjes, J.T.F. Zeolite-Coated Ceramic Pervaporation Membranes; Pervaporation-Esterification Coupling and Reactor Evaluation. *Ind. Eng. Chem. Res.* **2005**, *44*, 9490–9496.
231. De la Iglesia, Ó.; Irusta, S.; Mallada, R.; Menéndez, M.; Coronas, J.; Santamaría, J. Preparation and characterization of two-layered mordenite-ZSM-5 bi-functional membranes. *Microporous Mesoporous Mater.* **2006**, *93*, 318–324.
232. Tarditi, A.M.; Lombardo, E.A.; Avila, A.M. Xylene Permeation Transport through Composite Ba-ZSM-5/SS Tubular Membranes: Modeling the Steady-State Permeation. *Ind. Eng. Chem. Res.* **2008**, *47*, 2377–2385.
233. Zhou, J.L.; Zhang, X.F.; Zhang, J.; Liu, H.O.; Zhou, L.; Yeung, K.L. Preparation of alkali-resistant, Sil-1 encapsulated nickel catalysts for direct internal reforming-molten carbonate fuel cell. *Catal. Commun.* **2009**, *10*, 1804–1807.
234. He, J.; Yoneyama, Y.; Xu, B.; Nishiyama, N.; Tsubaki, N. Designing a Capsule Catalyst and Its Application for Direct Synthesis of Middle Isoparaffins. *Langmuir* **2005**, *21*, 1699–1702.
235. Puil, N.V.D.; Creighton, E.J.; Rodenburg, E.C.; Sie, T.S.; Bekkum, H.v.; Jansen, J.C. Catalytic testing of TiO₂/platinum/silicalite-1 composites. *Faraday Trans.* **1996**, *96*, 4609–4615.
236. Van der Puil, N.; Dautzenberg, F.M.; van Bekkum, H.; Jansen, J.C. Preparation and catalytic testing of zeolite coatings on preshaped alumina supports. *Microporous Mesoporous Mater.* **1999**, *27*, 95–106.
237. Bouzidi, Y.; Rouleau, L.; Valtchev, V.P. Factors Controlling the Formation of Core-Shell Zeolite-Zeolite Composites. *Chem. Mater.* **2006**, *18*, 4959–4966.
238. Li, X.; He, J.; Meng, M.; Yoneyama, Y.; Tsubaki, N. One-step synthesis of H-β zeolite-enwrapped Co/Al₂O₃ Fischer-Tropsch catalyst with high spatial selectivity. *J. Catal.* **2009**, *265*, 26–34.
239. Bao, J.; He, J.; Zhang, Y.; Yoneyama, Y.; Tsubaki, N. A Core/Shell Catalyst Produces a Spatially Confined Effect and Shape Selectivity in a Consecutive Reaction. *Angew. Chem. Int. Ed.* **2008**, *47*, 353–356.
240. Li, C.; Xu, H.; Kido, Y.; Yoneyama, Y.; Suehiro, Y.; Tsubaki, N. A capsule catalyst with a zeolite membrane prepared by direct liquid membrane crystallization. *ChemSusChem* **2012**, *5*, 862–866.
241. Phienluphon, R.; Pinkaew, K.; Yang, G.H.; Li, J.; Wei, Q.H.; Yoneyama, Y.; Vitidsant, T.; Tsubaki, N. Designing core (Cu/ZnO/Al₂O₃)-shell (SAPO-11) zeolite capsule catalyst with a facile physical way for dimethyl ether direct synthesis from syngas. *Chem. Eng. J.* **2015**, *270*, 605–611.
242. Cimenler, U.; Joseph, B.; Kuhn, J.N. Molecular-size selective H-β zeolite-encapsulated Ce-Zr/Ni-Mg catalysts for steam reforming. *Appl. Catal. A* **2015**, *505*, 494–500.
243. Pinkaew, K.; Yang, G.; Vitidsant, T.; Jin, Y.; Zeng, C.; Yoneyama, Y.; Tsubaki, N. A new core-shell-like capsule catalyst with SAPO-46 zeolite shell encapsulated Cr/ZnO for the controlled tandem synthesis of dimethyl ether from syngas. *Fuel* **2013**, *111*, 727–732.
244. Xing, C.; Sun, J.; Chen, Q.; Yang, G.; Muranaka, N.; Lu, P.; Shen, W.; Zhu, P.; Wei, Q.; Li, J.; *et al.* Tunable isoparaffin and olefin yields in Fischer-Tropsch synthesis achieved by a novel iron-based micro-capsule catalyst. *Catal. Today* **2015**, *251*, 41–46.

245. Nishiyama, N.; Miyamoto, M.; Egashira, Y.; Ueyama, K. Zeolite membrane on catalyst particles for selective formation of *p*-xylene in the disproportionation of toluene. *Chem. Commun.* **2001**, 1746–1747.
246. Vu, D.V.; Miyamoto, M.; Nishiyama, N.; Egashira, Y.; Ueyama, K. Selective formation of para-xylene over H-ZSM-5 coated with polycrystalline silicalite crystals. *J. Catal.* **2006**, *243*, 389–394.
247. Vu, D.V.; Miyamoto, M.; Nishiyama, N.; Ichikawa, S.; Egashira, Y.; Ueyama, K. Catalytic activities and structures of silicalite-1/H-ZSM-5 zeolite composites. *Microporous Mesoporous Mater.* **2008**, *115*, 106–112.
248. Li, X.; Zhang, Y.; Meng, F.; San, X.; Yang, G.; Meng, M.; Takahashi, M.; Tsubaki, N. Hydroformylation of 1-Hexene on Silicalite-1 Zeolite Membrane Coated Pd-Co/AC Catalyst. *Top Catal.* **2010**, *53*, 608–614.
249. Nishiyama, N.; Ichioka, K.; Park, D.-H.; Egashira, Y.; Ueyama, K.; Gora, L.; Zhu, W.; Kapteijn, F.; Moulijn, J.A. Reactant-Selective Hydrogenation over Composite Silicalite-1-Coated Pt/TiO₂ Particles. *Ind. Eng. Chem. Res.* **2004**, *43*, 1211–1215.
250. Nishiyama, N.; Ichioka, K.; Miyamoto, M.; Egashira, Y.; Ueyama, K.; Gora, L.; Zhu, W.D.; Kapteijn, F.; Moulijn, J.A. Silicalite-1 coating on Pt/TiO₂ particles by a two-step hydrothermal synthesis. *Microporous Mesoporous Mater.* **2005**, *83*, 244–250.
251. Zhong, Y.; Chen, L.; Luo, M.; Xie, Y.; Zhu, W. Fabrication of zeolite-4A membranes on a catalyst particle level. *Chem. Commun.* **2006**, 2911–2912.
252. Wu, Y.; Chai, Y.; Li, J.; Guo, H.; Wena, L.; Liu, C. Preparation of silicalite-1@Pt/alumina core-shell catalyst for shape-selective hydrogenation of xylene isomers. *Catal. Commun.* **2015**, *64*, 110–113.
253. He, J.; Liu, Z.; Yoneyama, Y.; Nishiyama, N.; Tsubaki, N. Multiple-Functional Capsule Catalysts: A Tailor-Made Confined Reaction Environment for the Direct Synthesis of Middle Isoparaffins from Syngas. *Chemistry* **2006**, *12*, 8296–8304.
254. Yang, G.H.; He, J.J.; Yoneyama, Y.; Tan, Y.S.; Han, Y.Z.; Tsubaki, N. Preparation, characterization and reaction performance of H-ZSM-5/cobalt/silica capsule catalysts with different sizes for direct synthesis of isoparaffins. *Appl. Catal. A* **2007**, *329*, 99–105.
255. Yang, G.H.; Tan, Y.S.; Han, Y.Z.; Qiu, J.S.; Tsubaki, N. Increasing the shell thickness by controlling the core size of zeolite capsule catalyst: Application in iso-paraffin direct synthesis. *Catal. Commun.* **2008**, *9*, 2520–2524.
256. Yang, G.H.; He, J.J.; Zhang, Y.; Yoneyama, Y.; Tan, Y.S.; Han, Y.Z.; Vitidsant, T.; Tsubaki, N. Design and modification of zeolite capsule catalyst, a confined reaction field, and its application in one-step isoparaffin synthesis from syngas. *Energy Fuels* **2008**, *22*, 1463–1468.
257. Bao, J.; Yang, G.H.; Okada, C.; Yoneyama, Y.; Tsubaki, N. H-type zeolite coated iron-based multiple-functional catalyst for direct synthesis of middle isoparaffins from syngas. *Appl. Catal. A* **2011**, *394*, 195–200.
258. Huang, X.; Hou, B.; Wang, J.G.; Li, D.B.; Jia, L.T.; Chen, J.G.; Sun, Y.H. CoZr/H-ZSM-5 hybrid catalysts for synthesis of gasoline-range isoparaffins from syngas. *Appl. Catal. A* **2011**, *408*, 38–46.

259. Yang, G.; Xing, C.; Hirohama, W.; Jin, Y.; Zeng, C.; Suehiro, Y.; Wang, T.; Yoneyama, Y.; Tsubaki, N. Tandem catalytic synthesis of light isoparaffin from syngas via Fischer-Tropsch synthesis by newly developed core-shell-like zeolite capsule catalysts. *Catal. Today* **2013**, *215*, 29–35.
260. Jin, Y.; Yang, G.; Chen, Q.; Niu, W.; Lu, P.; Yoneyama, Y.; Tsubaki, N. Development of dual-membrane coated Fe/SiO₂ catalyst for efficient synthesis of isoparaffins directly from syngas. *J. Membr. Sci.* **2015**, *475*, 22–29.
261. Yang, G.; Tsubaki, N.; Shamoto, J.; Yoneyama, Y.; Zhang, Y. Confinement effect and synergistic function of H-ZSM-5/Cu-ZnO-Al₂O₃ capsule catalyst for one-step controlled synthesis. *J. Am. Chem. Soc.* **2010**, *132*, 8129–8136.
262. Yang, G.; Thongkam, M.; Vitidsant, T.; Yoneyama, Y.; Tan, Y.; Tsubaki, N. A double-shell capsule catalyst with core-shell-like structure for one-step exactly controlled synthesis of dimethyl ether from CO₂ containing syngas. *Catal. Today* **2011**, *171*, 229–235.
263. Yang, G.; Wang, D.; Yoneyama, Y.; Tan, Y.; Tsubaki, N. Facile synthesis of H-type zeolite shell on a silica substrate for tandem catalysis. *Chem. Commun.* **2012**, *48*, 1263–1265.
264. Liu, R.; Tian, H.; Yang, A.; Zha, F.; Ding, J.; Chang, Y. Preparation of HZSM-5 membrane packed CuO-ZnO-Al₂O₃ nanoparticles for catalysing carbon dioxide hydrogenation to dimethyl ether. *Appl. Surf. Sci.* **2015**, *345*, 1–9.
265. Ren, N.; Yang, Y.H.; Shen, J.; Zhang, Y.H.; Xu, H.L.; Gao, Z.; Tang, Y. Novel, efficient hollow zeolitically microcapsulized noble metal catalysts. *J. Catal.* **2007**, *251*, 182–188.
266. Besson, M.; Gallezot, P. Deactivation of metal catalysts in liquid phase organic reactions. *Catal. Today* **2003**, *81*, 547–559.
267. Papp, A.; Miklos, K.; Forgo, M.; Molnar, A. Heck coupling by Pd deposited onto organic-inorganic hybrid supports. *J. Mol. Catal. A* **2005**, *229*, 107–116.
268. Zhang, T.; Zhang, X.; Yan, X.; Lin, L.; Liu, H.; Qiu, J.; Yeung, K.L. Core-shell Pd/ZSM-5@ZIF-8 membrane micro-reactors with size selectivity properties for alkene hydrogenation. *Catal. Today* **2014**, *236*, 41–48.
269. Miyamoto, M.; Kamei, T.; Nishiyama, N.; Egashira, Y.; Ueyama, K. Single crystals of ZSM-5/silicalite composites. *Adv. Mater.* **2005**, *17*, 1985–1988.
270. Mabuchi, K.; Miyamoto, M.; Oumi, Y.; Uemiya, S. Selective formation of *p*-xylene in aromatization of propane over silicalite-1-coated GaAlMFI. *J. Jpn. Pet. Inst.* **2011**, *54*, 275–276.
271. Miyamoto, M.; Mabuchi, K.; Kamada, J.; Hirota, Y.; Oumi, Y.; Nishiyama, N.; Uemiya, S. para-Selectivity of silicalite-1 coated MFI type galloaluminosilicate in aromatization of light alkanes. *J. Porous Mater.* **2015**, *22*, 769–778.
272. Zhou, Y.X.; Tong, W.Y.; Zou, W.; Qi, X.L.; Kong, D.J. Manufacture of *b*-Oriented ZSM-5/Silicalite-1 Core/Shell Structured Zeolite Catalyst. *Synth. React. Inorg. Met.-Org. Nano-Met. Chem.* **2015**, *45*, 1356–1362.
273. Van der Laan, G.P.; Beenackers, A.A.C.M. Kinetics and Selectivity of the Fischer-Tropsch Synthesis: A Literature Review. *Catal. Rev.* **1999**, *41*, 255–318.
274. Li, X.H.; Asami, K.; Luo, M.F.; Michiki, K.; Tsubaki, N.; Fujimoto, K. Direct synthesis of middle iso-paraffins from synthesis gas. *Catal. Today* **2003**, *84*, 59–65.

275. Li, X.H.; Luo, M.F.; Asami, K. Direct synthesis of middle iso-paraffins from synthesis gas on hybrid catalysts. *Catal. Today* **2004**, *89*, 439–446.
276. Botes, F.G.; Böhringer, W. The addition of HZSM-5 to the Fischer-Tropsch process for improved gasoline production. *Appl. Catal. A* **2004**, *267*, 217–225.
277. Yoneyama, Y.; He, J.; Morii, Y.; Azuma, S.; Tsubaki, N. Direct synthesis of isoparaffin by modified Fischer-Tropsch synthesis using hybrid catalyst of iron catalyst and zeolite. *Catal. Today* **2005**, *104*, 37–40.
278. Moradi, G.R.; Basir, M.M.; Taeb, A.; Kiennemann, A. Promotion of Co/SiO₂ Fischer-Tropsch catalysts with zirconium. *Catal. Commun.* **2003**, *4*, 37–32.
279. Xiong, H.; Zhang, Y.; Liew, K.; Li, J. Catalytic performance of zirconium-modified Co/Al₂O₃ for Fischer-Tropsch synthesis. *J. Mol. Catal. A* **2005**, *231*, 145–151.
280. Koizumi, N.; Seki, H.; Hayasaka, Y.; Oda, Y.; Shindo, T.; Yamada, M. Application of liquid phase deposition method for preparation of Co/ZrO_x/SiO₂ catalyst with enhanced Fischer-Tropsch synthesis activity: Importance of Co-Zr interaction. *Appl. Catal. A* **2011**, *398*, 168–178.
281. Lin, Q.; Yang, G.; Li, X.; Yoneyama, Y.; Wan, H.; Tsubaki, N. A Catalyst for One-step Isoparaffin Production via Fischer-Tropsch Synthesis: Growth of a H-Mordenite Shell Encapsulating a Fused Iron Core. *ChemCatChem* **2013**, *5*, 3101–3106.
282. Panpranot, J.; Goodwin, J.G.; Sayari, A. CO hydrogenation on Ru-promoted Co/MCM-41 catalysts. *J. Catal.* **2002**, *211*, 530–539.
283. Panpranot, J.; Goodwin, J.G.; Sayari, A. Effect of H₂ partial pressure on surface reaction parameters during CO hydrogenation on Ru-promoted silica-supported Co catalysts. *J. Catal.* **2003**, *213*, 78–85.
284. Cano, L.A.; Cagnoli, M.V.; Fellenz, N.A.; Bengoa, J.F.; Gallegos, N.G.; Alvarez, A.M.; Marchetti, S.G. Fischer-Tropsch synthesis. Influence of the crystal size of iron active species on the activity and selectivity. *Appl. Catal. A* **2010**, *379*, 105–110.
285. Bezemer, G.L.; Bitter, J.H.; Kuipers, H.P.; Oosterbeek, H.; Holewijn, J.E.; Xu, X.; Kapteijn, F.; van Dillen, A.J.; de Jong, K.P. Cobalt particle size effects in the Fischer-Tropsch reaction studied with carbon nanofiber supported catalysts. *J. Am. Chem. Soc.* **2006**, *128*, 3956–3964.
286. Khodakov, A.Y. Fischer-Tropsch synthesis: Relations between structure of cobalt catalysts and their catalytic performance. *Catal. Today* **2009**, *144*, 251–257.
287. Zhang, Q.H.; Deng, W.P.; Wang, Y. Recent advances in understanding the key catalyst factors for Fischer-Tropsch synthesis. *J. Energy Chem.* **2013**, *22*, 27–38.
288. Arcoumanis, C.; Bae, C.; Crookes, R.; Kinoshita, E. The potential of di-methyl ether (DME) as an alternative fuel for compression-ignition engines: A review. *Fuel* **2008**, *87*, 1014–1030.
289. Mao, D.S.; Yang, W.M.; Xia, J.C.; Zhang, B.; Song, Q.Y.; Chen, Q.L. Highly effective hybrid catalyst for the direct synthesis of dimethyl ether from syngas with magnesium oxide-modified HZSM-5 as a dehydration component. *J. Catal.* **2005**, *230*, 140–149.
290. Ramos, F.S.; de Farias, A.M.D.; Borges, L.E.P.; Monteiro, J.L.; Fraga, M.A.; Sousa-Aguiar, E.F.; Appel, L.G. Role of dehydration catalyst acid properties on one-step DME synthesis over physical mixtures. *Catal. Today* **2005**, *101*, 39–44.
291. Moradi, G.R.; Nosrati, S.; Yaripor, F. Effect of the hybrid catalysts preparation method upon direct synthesis of dimethyl ether from synthesis gas. *Catal. Commun.* **2007**, *8*, 598–606.

292. Jin, D.; Zhu, B.; Hou, Z.; Fei, J.; Lou, H.; Zheng, X. Dimethyl ether synthesis via methanol and syngas over rare earth metals modified zeolite Y and dual Cu-Mn-Zn catalysts. *Fuel* **2007**, *86*, 2707–2713.
293. Mao, D.; Xia, J.; Zhang, B.; Lu, G. Highly efficient synthesis of dimethyl ether from syngas over the admixed catalyst of CuO-ZnO-Al₂O₃ and antimony oxide modified HZSM-5 zeolite. *Energy Convers. Manag.* **2010**, *51*, 1134–1139.
294. Pop, G.; Bozga, G.; Ganea, R.; Natu, N. Methanol Conversion to Dimethyl Ether over H-SAPO-34 Catalyst. *Ind. Eng. Chem. Res.* **2009**, *48*, 7065–7071.
295. Dai, W.L.; Kong, W.B.; Wu, G.J.; Li, N.; Li, L.D.; Guan, N.J. Catalytic dehydration of methanol to dimethyl ether over aluminophosphate and silico-aluminophosphate molecular sieves. *Catal. Commun.* **2011**, *12*, 535–538.

© 2015 by the authors; licensee MDPI, Basel, Switzerland. This article is an open access article distributed under the terms and conditions of the Creative Commons Attribution license (<http://creativecommons.org/licenses/by/4.0/>).